WÍLERSON VENCESLAU CALIL

Methodology for specification of generator step-up transformers in photovoltaic power plants based on real loading profile

São Paulo
2021

WÍLERSON VENCESLAU CALIL

Methodology for specification of generator step-up transformers in photovoltaic power plants based on real loading profile

Doctoral thesis submitted to the Polytechnic School of the University of São Paulo in fulfillment of the requirements of the Ph.D. degree in Doctor Science

São Paulo
2021

WÍLERSON VENCESLAU CALIL

Metodologia para Especificação de Transformadores Elevadores de Tensão em Usinas Fotovoltáicas Baseado em Perfil de Carga Real

Versão Corrigida

Doctoral thesis submitted to the Polytechnic School of the University of São Paulo in fulfillment of the requirements of the Ph.D. degree in Doctor Science

Concentration Area: Power System

Advisor: Prof. Dr. Eduardo Coelho Marques da Costa
Coadvisor: Prof. Dr. Maurício Barbosa de Camargo Salles

São Paulo
2021

Este exemplar foi revisado e corrigido em relação à versão original, sob responsabilidade única do autor e com a anuência de seu orientador.

São Paulo, 08 de Janeiro de 2021

Assinatura do autor: ____________________

Assinatura do orientador: ____________________

Catalogação-na-publicação

Calil, Wilerson Venceslau Calil
Methodology for specification of generator step-up transformers in photovoltaic power plants based on real loading profile / W. V. C. Calil -- versão corr. -- São Paulo, 2021.
118 p.

Tese (Doutorado) - Escola Politécnica da Universidade de São Paulo. Departamento de Engenharia de Energia e Automação Elétricas.

1.Transformer 2.Dynamic Loading 3.Aging 4.End-of-Life 5.Efficiency I.Universidade de São Paulo. Escola Politécnica. Departamento de Engenharia de Energia e Automação Elétricas II.t.

To my parents, my brothers, my wife, and my son, for encouragement, comprehension, and support.

ACKNOWLEDGMENT

First and foremost, Thanks to **God Almighty**, for the wisdom he bestowed upon me, the strength, peace, amazing family, and good health in order to finish this research.

My deepest gratitude goes to my parents, **Fátima** and **Wilerson**, for their unflagging love and support throughout my life. Parents who from an early age, went to great lengths to provide me the greatest legacy anyone can receive: the study.

I would like to thank my supervisor Professor **Dr. Eduardo Costa** for his valuable guidance and advice, and for inspiring and motivating me in this project. Moreover, I would like to offer my special thanks to him for very careful reviews of my thesis and papers. I would like to thank my co-supervisor Professor **Dr. Mauricio Salles** for his direction in this research since 2012 when this idea of the thesis was very embryonic, for trusting me and giving the opportunity.

I would like to gratefully acknowledge the ABB Company, now **Hitachi ABB Power Grid**, and colleagues from this company who gave me the industrial insight and enlightened my way in this work: **André Souza, Luiz Yamazaki, Hitochi Taninaga, Joachim Zacharias, Leandro Tamura, Tor Laneryd, Vinicius Rubio, Jorge Inhasz, Jorge Tsukahara, Daniel Bahcivanji, Thomas Matsumoto, Francisco Bloise, Dr. José Carlos Mendes, Paulo Avelino** and others my co-workers by of timely discussions.

To my wife **Paola** for the love, affection, partnership, and many moments of happiness and motivation, for always being present in the crucial moments of this thesis and for making my life more fulfilling and fruits that are yet to come. To my son **Leonardo**, for showing me how my life is complete when he looks into my eyes.

To my sister **Adriana** and my brother **Wendel** who always raise my self-esteem and support me. I would like to express my gratitude towards professors **Dr. Alfeu Sguarezi** and **Dr. Rogerio Flauzino** which attended the qualification board of this thesis and gave good ideas and contributions to finalize this work. I am also thankful to the labmate, **Luis Loureço**, for valuable high-level technical support and Professor **Dr. José Roberto Cardoso** for the motivation of this project and the **Department of Energy and Automation of the Polytechnic School USP**.

Last but not least, my gratitude to the other people who, directly or indirectly, contributed to the execution of this work.

The scientific man does not aim at an immediate result. He does not expect that his advances ideas will be readily taken up. His work is like that of a planter - for the future. His duty is to lay foundation of those who are to come and point the way.

Nikola Tesla

ABSTRACT

Calil, W. V. (2020). *Methodology for Specification of Generator Step-Up Transformers in Photovoltaic Power Plants Based on Real Loading Profile.* Tese (Doutorado) – Escola Politécnica, Universidade de São Paulo, São Paulo, 2020.

This research presents a methodology for dimensioning the top-rated for the collected step-up power transformer applied in the large photovoltaic power plant through many technical and financial variables. The power transformer equipment is an expensive asset that often is used well below its power rating on a photovoltaic farm. A precise estimation of this cost is in the interest of the photovoltaic farm owners, in order to evaluate the initial investment economic feasibility. The proposed method allows correcting the value of total losses utilizing the concept of the Dynamic Loading Model without neglecting the aging of the solid insulation neither reducing the reliability of the operation of the transformer, providing the best-in-class cost-benefit for the procurement engineer. This novel methodology has been based, especially, in the well-established loading guide model by IEEE standard. All techniques and procedures to be evaluated in this research were obtained using a real loading and temperature profile of the solar plant and a probabilist curves.

Keywords: Transformers, Dynamic Loading, Aging, End-of-Life, Efficiency.

RESUMO

Calil, W. V. (2020). *Metodologia para Especificação de Transformadores Elevadores de Tensão em Usinas Fotovoltáicas Baseado em Perfil de Carga Real.* Tese (Doutorado) – Escola Politécnica, Universidade de São Paulo, São Paulo, 2020.

Esta pesquisa apresenta uma metodologia para dimensionar a potência máxima de um transformador elevador coletor aplicado em grandes usinas fotovoltaicas através de diversas variáveis técnicas e financeiras. O transformador de potência é um ativo de alto valor agregado e costuma ser dimensionado para utilização abaixo da potência máxima quando aplicado em uma fazenda fotovoltaica. Uma estimativa precisa desse custo é de interesse para os proprietários de fazendas fotovoltaicas poderem avaliar a viabilidade econômica do investimento inicial. O método proposto permite corrigir o valor das perdas totais utilizando o conceito do Modelo de Carregamento Dinâmico sem descuidar do envelhecimento da isolação sólida e tampouco reduzir a confiabilidade do funcionamento do transformador, proporcionando o melhor custo-benefício durante o processo de aquisição do equipamento. Esta nova metodologia foi baseada, especialmente, no modelo de guia de carregamento bem estabelecido pela norma IEEE. Todas as técnicas e procedimentos a serem abordados nesta pesquisa foram obtidos utilizando um perfil real de carga e temperatura da planta solar e curvas de probabilidades.

Palavras-Chave: Transformadores, Carregamento Dinâmico em Transformadores, Envelhecimento, Fim de Vida, Eficiência.

SUMMARY

Chapter 1 – INTRODUCTION

The increasing permeability of renewable energy in power systems around the world requires more economic and efficient methods as well as operation and integrated technologies that support all specific characteristics from these emerging energy sources (ZAREI et al., 2019). The profiles of this type of energy are different from traditional sources like gas, coal, and hydroelectric, which generates higher complexity of integration and control of the power flow. Furthermore, eventual irregularities in power generation and consumption require more dynamic solutions for rating of power system equipment.

Power transformers are one of the most critical and expensive component in a substation systems due to the raw material for manufacturing (MELO and CALIL, 2014) (e.g. silicon steel, carbon steel, mineral oil, copper and cellulose) and project customization, which depends on the application and characteristics of the electric grid. The manufacture of large power transformers, generally above 100 MVA, represents a meticulous and handcrafted process since the first drafts to the last electrical tests. This way, the technical and financial cost analyses require a great experience and know-how from the manufacturer.

Generator Step-Up – GSU power transformers are designed according to the customer specifications requirements and standards. The process of transformer supply is an "engineering to order", i.e., for each project the manufacture has to design accordingly with technical specification and variables such as altitude, ambient temperature, the seismic level, and others will change the design of this equipment.

In this sense, a huge number of variables must be considered in the technical and economic analyses during power transformers concept, which means each transformer represents a customized and laborious process. Although a few cost evaluation methods were previously proposed in the technical literature, most of them is limited to distribution power transformers (OLIVARES et al., 2003; GEORGILAKIS & AMOIRALIS, 2010; AMOIRALIS et al., 2012), there is not a consensus or standard procedure to evaluate technical and economic issues, considering both manufacturing and material costs, which makes the technical/economic correlation an even more complex process (IEEE, 1991; CARALAMBOUS, 2013; 2013a).

Furthermore, the increasing integration of renewable energy sources imposes on manufacturers an additional challenge, given the intermittent behavior in the electric energy generation provided from these energy sources. For example, a photovoltaic power plant is characterized by generation peaks around noon, during great incidence of solar radiation (*generating state* – GS), while the electric power generation is null throughout the night time (*non-generating state* – NGS), as illustrated in figure 1.1 (LAZARI & CARALAMBOUS, 2015). In this context, the GSU transformer operates in the nominal power only a few hours during the day whereas at nighttime it operates without any load, *consuming* only the active power dissipated in the magnetization core. From this example, it is evident that the power transformer design for a photovoltaic power plant must be different from a GSU transformer in a hydroelectric plant, which operates close to the nominal maximum power throughout the entire lifetime to increase its efficiency, however, the rated power of the equipment is near from the maximum. The same statement is true for any other renewable energy source, which are characterized by an intermittent electric power generation along the day.

The technical literature presents a few documents and researches on loss evaluation of power transformers in renewable energy power plants and describes the life-cycle as the sum of the present cost for each kilowatt of loss in a power transformer throughout its lifetime (BOICE et al., 1988). For example, an interesting method was recently proposed for life-cycle loss evaluation of the total ownership cost of power transformers connected to large wind farms, which are represented as an intermittent energy source with varying operational and financial characteristics. This method differs from those previously proposed because takes into account the probabilistic total ownership costs, electricity market issues, and uncertainties of wind energy generation. Finally, the loss evaluation method proved to be reliable when compared to empiric data obtained from different manufacturers (LAZARI & CHARALAMBOS, 2015a).

Another loss evaluation method was previously proposed for power transformers designed to serve independent photovoltaic power producers or regulated utilities. In these two cases, the capitalization of losses is an important issue for the adequate capital and future operating costs of the power transformer over its lifetime brought back into a present-day cost. This method simultaneously attends the concept of loss evaluation in both vertically integrated and decentralized energy systems with a high penetration of renewable energy (LAZARI & CARALAMBOUS, 2015).

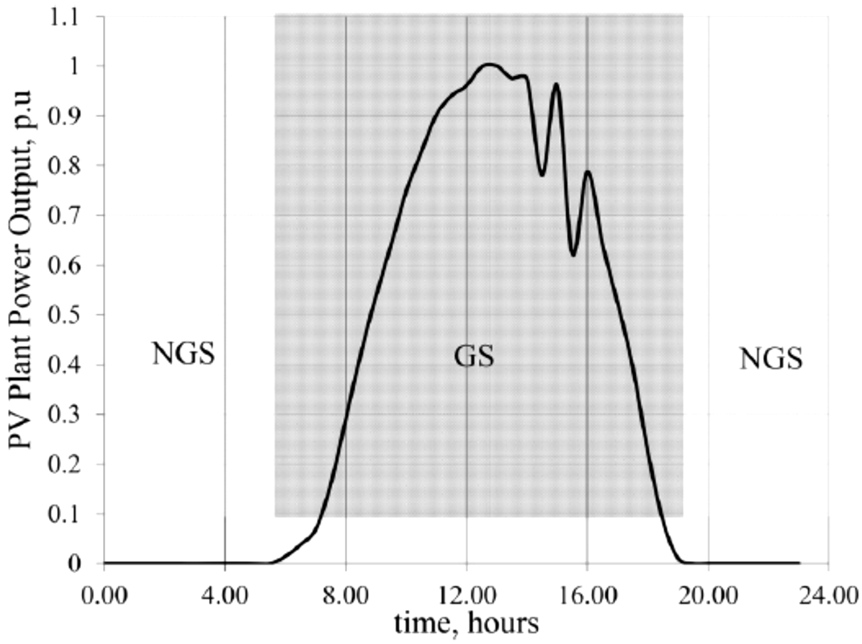

Figure 1.1 – Electric power generation of a photovoltaic plant during a day.
Source: LAZARI & CARALAMBOUS, 2015.

It is common some generation and power transmission companies evaluate economic issues on new power transformers based solely on the initial investments, without concern the life-cycle losses and dynamic degradation process in which the equipment is subjected throughout its lifetime. A simplified analytic formulation was previously proposed as a reliable technical-economic method for evaluation of power transformers designed to serve large photovoltaic plants. Various factors are considered in this analytic method in terms of initial investment (manufacturing, tests and installation costs) and operational costs (insurance, maintenance, taxes and required energy to cover the transformer power losses). In general, this simplified formulation takes into account some relevant issues in power transformers with intermittent loading, such as (CALIL et al., 2016):

- ❖ Power transformer cost;
- ❖ Energy losses in the power transformer operating with load;
- ❖ Energy losses in the power transformer operating no-load;
- ❖ Specified lifetime;
- ❖ Power factor (energization time).

In these terms, a well-established evaluation method in the electric power market is based on the *loss capitalization*, in which a currency cost per power losses ($/kW) is determined for power transformers with and without load. From this information, the manufacturer is able to optimize the power transformer design in order to attend technical and cost requirements from the clients (TOBAR et al., 2016).

The loss capitalization without load, as known no-load losses (NLL), is given in currency cost per energy ($/kWh). This index is a function of the currency investment to reduce one kW loss ($/kW), energy cost ($/kWh), total energization time per year (hours) and percentage average increase in the energy cost. The loss capitalization with load, as known load losses (LL), differs from the capitalization without loss because depends on the loading percentage and period in which the power transformer operates. This loss capitalization indicates the currency investment to reduce one kW loss in a power transformer with load (CALIL et al., 2016).

The energy cost in kWh is dependent on several factors, such as the supply and demand of electricity, taxes, monetary inflation, politic and environmental issues. In this sense, the energy cost forecast represents a critical variable in the loss capitalization method. Nevertheless, this method is able to calculate different cases, with different variables, in order to evaluate variations in the final results, which include the capitalization of the energy consumed in the cooling system of the power transformer.

Among all technical and economic issues to be considered in the loss capitalization, the electric power generation profile of the photovoltaic plant should be carefully analyzed. Figure 1.2 shows the power generation in 24 hours during a day per month in a northeast Brazilian region with high incidence of solar radiation.

Figure 1.2 shows that the power transformer operates with some load profile around 50% throughout a year. The average loading of the power transformer is approximately 35% during the entire lifetime, since it is designed to operate with 1 p.u. and solar radiation incidence of 66% per day. From these technical characteristics and others in association with economic indexes, e.g. interest rate and monetary inflation, the return on investment in years and the loss capitalization in currency unit can be calculated.

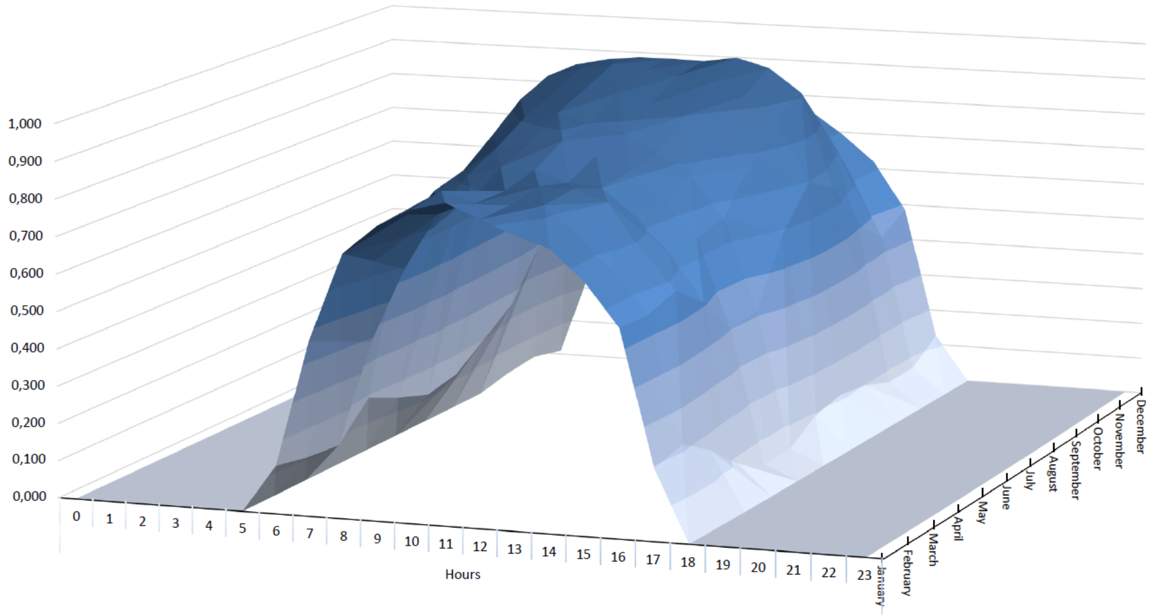

Figure 1.2 – Power generation profile per day during a year of a photovoltaic plant.

Source: Adapted from CALIL et al., 2016

Although the loss capitalization method shows to be useful in many applications, some important issues are not considered, such as risk analysis and environmental characteristics where the power transformer is installed (e.g. ambient temperature). The risk analysis consists basically in correlate the hours per year in which the transformer operates in total power capacity to its currency cost *versus* lifetime, i.e. to determine the optimum point of power capacity and cost *versus* the expected lifetime. For example, considering a photovoltaic power plant with a total power capacity of 100 MVA with a 60 MVA power transformer, which operates a few hours per year over its nominal power, the risk analysis can estimate cost issues and lifetime based on the technical characteristics and operation conditions of this power transformer. In this sense, if the total capacity of the power plant and power profile per year are previously known, such as in figure 1.2, the risk analysis can determine the optimum cost and nominal power of the power transformer based on a pre-defined life cycle for this equipment. Thus, the risk analysis represents a very useful tool to correlate technical *versus* economic issues during power transformer design and manufacturing.

1.1. BRIEF BACKGROUND ON SOLAR PHOTOVOLTAIC POWER IN BRAZIL

The increasing electric power demand in the past few years shows to be higher than its historical trend. The share of renewable sources, including hydropower, is almost 26% of the total energy installed in the world. Nowadays, most of the growth comes from new wind and solar capacity, which is supported by ambitious climate policies imposed by the European Union, USA, China, India, Japan and Australia. In addition, the continuous decrease in photovoltaic and wind turbines costs through the last decade enables the developing countries to expand their renewable energy installed capacity (ENERDATA, 2019).

Global renewable-based power capacity will grow by 50% between 2019 and 2024. This increase of 1200 gigawatts, which is equivalent to the current total power capacity of the United States that is driven by cost reductions and concerted government policy efforts. Solar PV accounts to 60% of the rise. The share of renewables in global power generation is set to rise to 30% in 2024. (IEA, 2019)

The renewable energy sector has employed around 11 million people since 2018, in which solar photovoltaic is the largest employer, with approximately 3.6 million job positions. In Brazil these numbers are discrete and the workforce in solar energy sector are around 15 thousand against 2.2 million in China and 225 thousand in United States.

In the Stated Policies Scenario, solar becomes the largest source of installed capacity around 2035, surpassing coal and gas. Global coal-fired capacity plateaus, with the project pipeline of 710 GW, mainly in Asia, just exceeding coal plant retirements, mainly in advanced economies. As an example, The Pavagada solar park in located in Kartanataka's Tumakuru district, southern India is expected to generate 2000 MW of electricity, making it the world's largest solar station. The park span across 52.2 square kilometers over five villages. (BENGALI, 2018).

Figure 1.3 – Aerial photography of “The Pavagada” solar park. Karnataka Solar Power Development Corp. (LOS ANGELES TIMES, 2018)

Renewables make up two-thirds of all capacity additions to 2040 globally. Wind power capacity triples, with offshore wind taking off in Europe, China and the United States. Gas-fired capacity grows in most markets for reliability purposes and battery storage skyrockets.

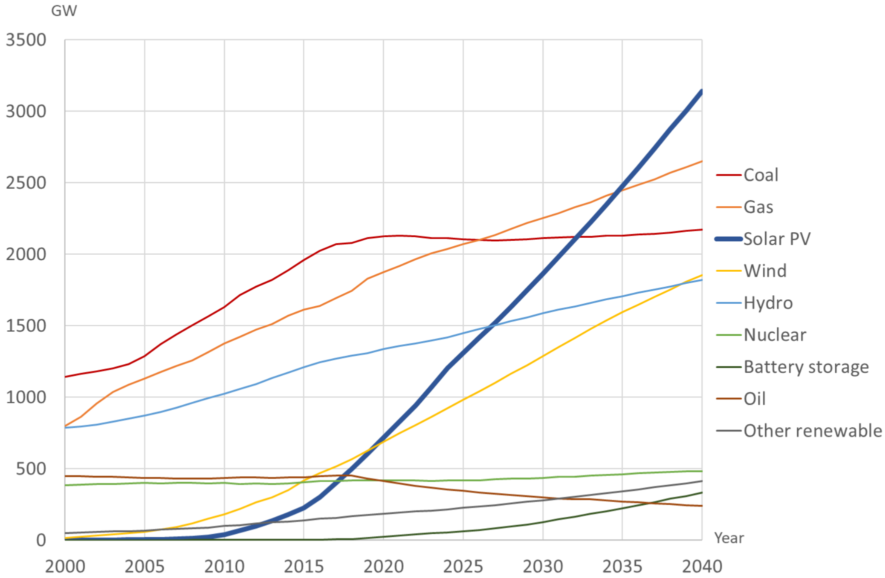

Figure 1.4 – Installed power generation capacity by source in new policies scenario, 2000-2040.

Source: Adapted from IEA, 2020

Figure 1.4 shows the yaw of the solar PV sources from 2015. As an example, in 2018 the solar capacity addictions were more than 100 GW and cumulative reached 505 GW as shown in the Figure 1.5.

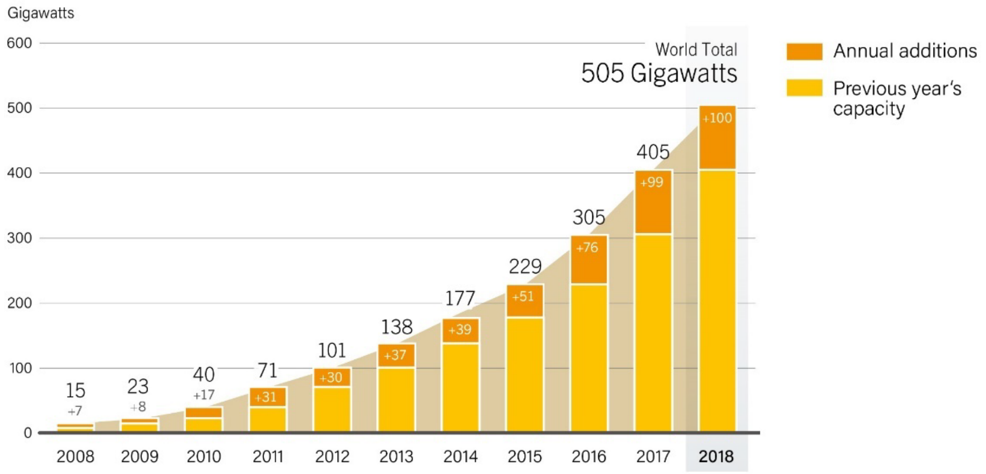

Figure 1.5 – Solar photovoltaic global capacity and annual addition, 2008-2018.

Source: Adapted from REN21. 2019

Since 2008 a Solar photovoltaic is the fastest growing energy technology, and in an increasing number of countries. In 2018, 11 countries have added more than 1GW and 32 countries had cumulative capacity of at least 1GW. China remains leader in solar photovoltaic with cumulative capacity reached 176.1GW, followed by United States and Japan. In terms of annual addition, China accounted for about 74% of global additions, followed by Turkey, India, Brazil and United States. (REN21, 2019).

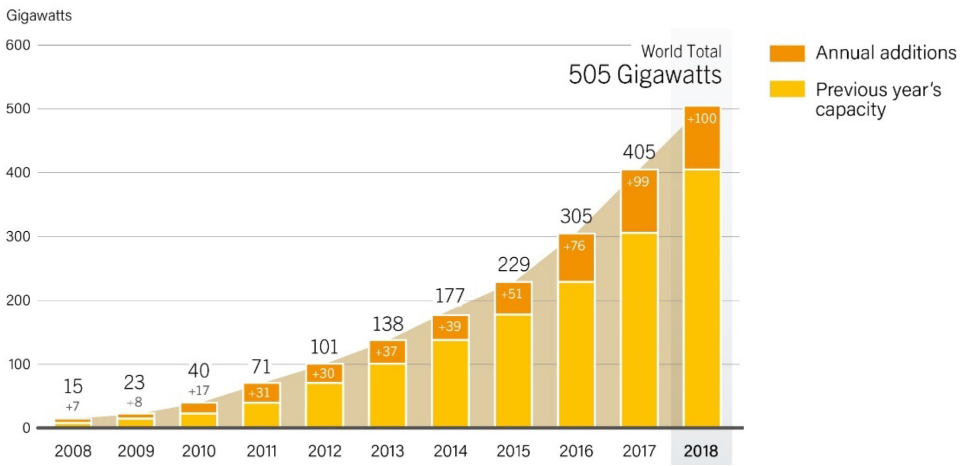

Figure 1.6 – Solar photovoltaic capacity and additions, top 10 countries, 2018

Source: Adapted from REN21. 2019

Brazil added more than 1.2 GW in 2018, doubling its capacity to nearly 2.4 GW, contributing with 1.4% of the energetic matrix, because the extension of Brazil's national net metering programmed as well as to a rising number of state-level incentives, falling module prices, rising electricity tariffs and increased environmental awareness (REN21, 2019).

Figure 1.7 illustrates the primary sources used for electricity conversion in Brazil in January 2019. Despite the changes, more than 60% of the electrical energy came from hydro source, however solar sources are increasing in recent years. (ANEEL, 2020).

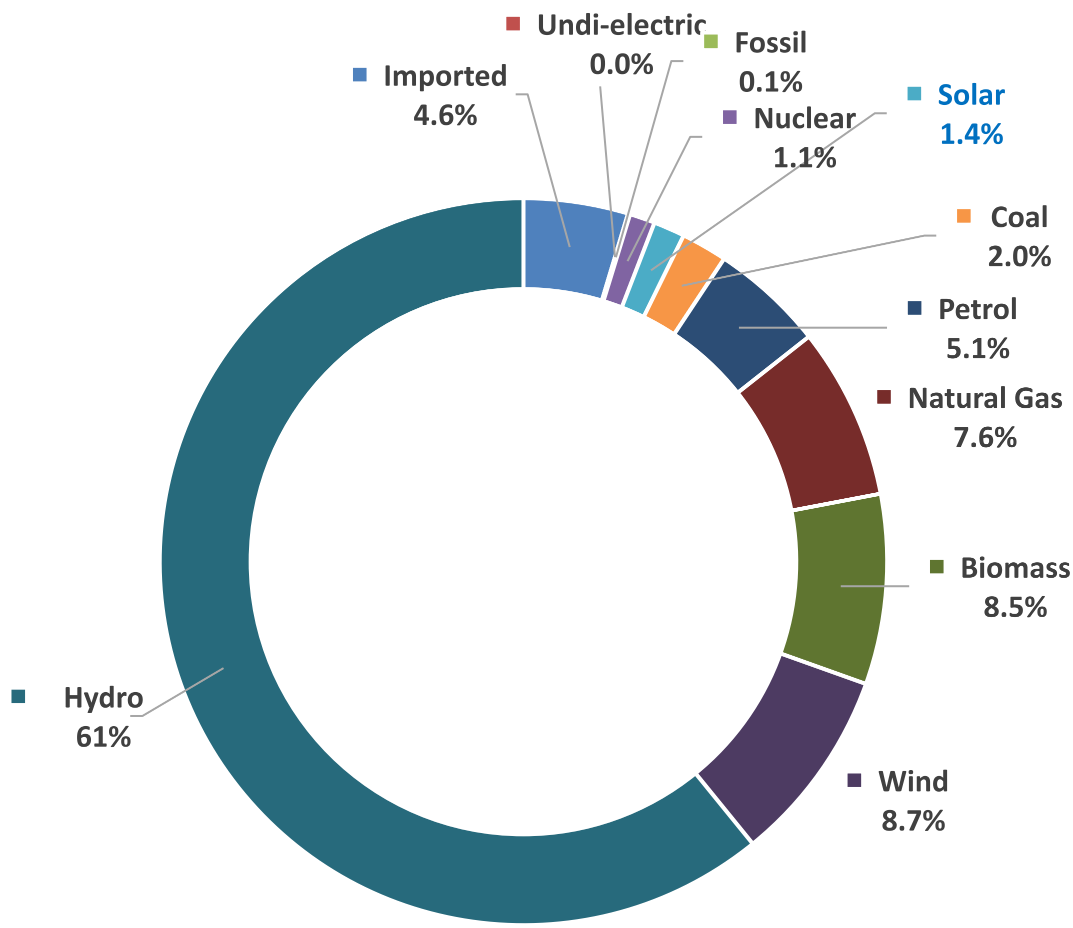

Figure 1.7 – Primary sources used in Brazil, 2020

Source: Adapted from ABSOLAR, 2019 and ANEEL, 2020.

Photovoltaic generation is a highly modular technology with almost no emission of pollutants and noise during the operation and with low maintenance requirements. The photovoltaic generation has been developed and refined since 1970s and currently represents a viable option for electrical energy production, aiming supplement and/or replacing energy from conventional sources. (GAMA et al., 2013).

Brazil has been constructing a large solar power plant like Parque Solar Nova Olinda, in Piauí State, as shown in figure 1.8. The installation covers an area of 690 hectares, with a total installed capacity of 290 MW and will generate approximately 600 GWh per year. (BRANDÃO, 2018). This solar power plant has 2 power transformers of 140 MVA rated capacity which will raise the voltage level from 34.5 kV to 500 kV and is directly connected in the Brazilian National Electrical Grid System. (BRANDÃO, 2018)

Figure 1.8 – Nova Olinda solar park, aerial view, 2018

Also, in Piauí State, the city of São Gonçalo do Gurguéia, was chosen to house one of the most significant solar parks in the world, with a power of 475 MW. This solar park will contribute to the diversification and resilience of the country energy matrix, supporting a virtuous economic cycle through the supply of sustainable energy in the long term. (PORTAL SOLAR, 2019).

Figure 1.9 – São Gonçalo solar park, aerial view - photo: Rafael Souza/Planner Tozzolatam, (CIDADE VERDE, 2020)

This project is the largest photovoltaic solar plant in South America and in 2020 starts the operation in January 13th. São Gonçalo plant uses bifacial solar modules, which capture energy from both sides of the panel, with an increase of up to 18% in power generation. (MORAES, 2019). This solar power plant has transformers with 500kV voltage level to directly connected in the Brazilian National Electrical Grid System.

Auction results and continued technical innovation suggest that costs will fall further in the future. Recent auctions results suggest that some future projects will significantly undercut. The price evolution of the solar photovoltaic sources during last auctions in the regulated market in Brazil has been present a similarity with the global trend in the reduction energy prices as shown in the Figure 1.8.

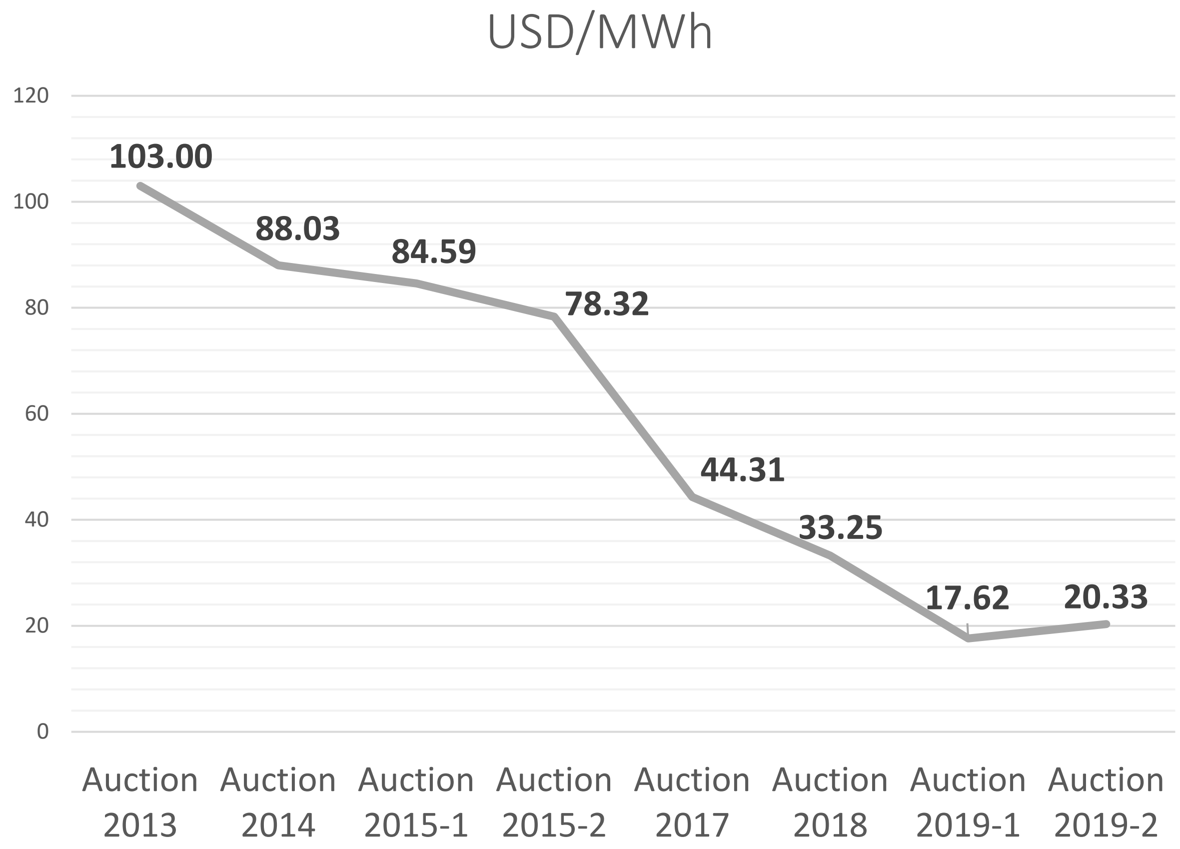

Figure 1.10 – Prices evolution during auction in Brazilian regulated market

Source: Adapted from ABSOLAR, 2019.

Figure 1.10 shows a depreciation of 80% between the first action in 2013 to the last auction which occurred in 2019, reducing the prices from 103 USD/MWh to 20.33 USD/MWh. Solar sources, diversify the energic matrix as a new renewable source, increasing the feasibility of the energy supply; reducing losses and postpose investment in transmissions and distribution besides to relieve the electrical demand during day light, decreasing customer costs.

Step-up power transformer has a significant weight in the total cost of installation of a large photovoltaic farm. Optimizing this equipment will financially beneficial and decrease investment cost, while providing equal operating performance as specified without compromising the availability and safety and life expectance.

1.2. OBJECTIVE AND STRUCTURE OF THE THESIS

The main objective of this thesis is to define a methodology to quantify the optimum power transformer in terms of cost-benefit to be installed in a solar power plant. This methodology aimed to explore the mix between the dynamic rating based on a real solar loading curve and ambient temperature, aging and economic analysis capitalization, since these variables are not taken into account in previous optimization method for power transformers.

Dimensioning the transformer according to the loading profile it is possible to reduce the quantity of raw material used. The benefits are the reduction of the total cost of the equipment which will impact the reduction of the freight cost, the base of the installation, the quantity of oil usage, and the overall carbon footprint necessary to manufacture the transformer. Another important benefit is the reduction of no-load losses that will increase asset profitability.

Such methodology is essential for an adequate analysis and design of GSU power transformers for large solar photovoltaic power plant, since this renewable energy source is characterized by an intermittent behavior. Only this issue makes the project of large power transformers for such application a great challenge in electrical engineering, without counting many other economic and technical issues which will be discussed in this thesis. Furthermore, a better understanding on GSU transformers, in the context of photovoltaic power generation, represents a significant technical and scientific knowledge about this emerging renewable energy technology.

In the Chapter 2 are described some technical and economic characteristics that must be taken into account during the concept design of the transformers as: no-load losses, load losses and its components and, how it impacts in the energy efficiency and indexes. Still in this chapter important understanding of the capitalization financial analysis is detailed. Chapter 3 are presented others important feature of the transformer design such as solid insulation materials and its behavior under temperature *versus* time. Equations used in the literature to determine the aging of the transformer are discussed in this chapter as well as the methods present currently in the international standards and its methods. Finally, Chapter 4 is presented the background of the dynamic model and brings proposed method which merges all information presented until here like efficiency, aging, loading, losses capitalization are joint in the method and an example with a real loading curve and temperature profile is tested and in Chapter 5, followed by discussions and conclusions.

Chapter 2 – CAPITALIZATION OF POWER TRANSFORMER LOSSES

Large power transformer, usually with more than 100 MVA, are devices with great added value in substations. Even with continuous improving of material and constructive techniques, power transformers present losses in the magnetization core and windings, which result in thousands of TWh during operation with and without load demand (BAGGINI & BUA, 2015). Nevertheless, power transformers are one of the most efficient electrical devices, which are designed to operate for many decades, and even minor improvements in some constructive characteristics may result in significant reduction in power losses.

Modern power transformers consist of a tank with oil fill in it and an active part which are formed by 2 main components: core and winding. There are at least two winding, low voltage winding, and high voltage winding. In some cases, are applied regulation winding and/or tertiary winding. Figure 2.1 presents three figures which from left to right shows a complete assembly transformer, the active part which is the heat source, and detailed windings and core. (JIAO, 2012).

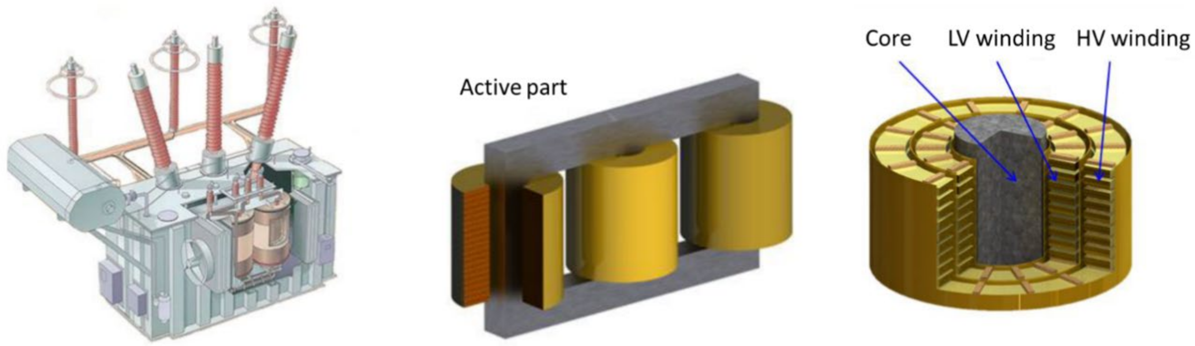

Figure 2.1 – Complete transformer, active part and detail of the active part.
Source: Adapted from JIAO, 2012.

The total losses in GSU transformers are characterized mainly by three components: *no-load losses*, *load losses* and *auxiliary losses*. During transformer design, these three types of losses are balanced in order to attend specific operation conditions of the electric grid in which the device will be installed. For example, a GSU transformer usually operates in nominal load through its entire lifetime in a hydroelectric power plant. On the other hand, a power transformer installed in a photovoltaic solar plant operates with full load only during a few hours during the day and operating without load at nighttime. Thus, the load losses are an important issue in the first case whereas in the second case, both load and no-load losses should be considered.

No-load losses are concentrated in the transformer magnetic circuit without load demand. Basically, these losses occur when the secondary circuit is open (without load) and the primary terminal operates with nominal voltage. In that case there is only a small primary current and thermal Joule losses are negligible. These losses are incurred from the very first moment that the transformer is energized and are not depend on the transformer load level. The technical literature describes the no-losses into three components: *hysteresis losses*, *Foucault losses* and *supplementary losses* (FITZGERALD, 1909). These three no-load losses parcels are briefly introduced as follows:

i) *Hysteresis Losses* are the energy dissipation during the movement of the magnetic domain due to the cyclical magnetization. In transformer, hysteresis losses are usually responsible for one-third up to half of the total no-load losses.

ii) *Foucault losses* are introduced in the literature as eddy current losses, which are caused by Joule effect due to the circulation of the induced current inside the core lamination. These losses can be reduced by building the core from thin laminated sheets insulated from each other by thin layer of insulative and inorganic coating to reduce the eddy current.

iii) *Supplementary losses* are the sum of remaining losses in the transformer core that are not well defined in the technical literature, and generally unknown. These losses are still being object of various researches on electrical and metallurgical engineering. The supplementary losses are marginal stray and dielectric losses which occur in the transformer core. The stray losses, due to the stray magnetic field, cause eddy current in the conductor or in surrounding metal and dielectric losses in the insulation materials, e.g. oil and solid insulation of high voltage. The supplementary losses usually are no more than 1% of the total no-load losses and therefore it is estimated by means of empirical values.

The use of new and more efficient electrical steel can reduce these overall no-load losses. The electrical steel specific losses, is defined as losses per unit mass at certain conditions, range roughly from 1.38 to 0.68 W/kg at 1.7T and 50Hz, meaning that depending on the type of material selected, the no-load losses can be reduced by up to 50% from one case to another. Performance of core steels have been improved mainly by introducing thinner gauge materials and improving their orientation (TAKAMIYA et al., 2016).

The use of lower-loss core material will decrease the number of watts lost per kilogram of core, in opposite, substituting for a lower-loss core material will result in an increase in material cost and consequently in total price (ABB, 2004).

During 1980s domain refining was commercialized and made a major step in nominal loss reduction. Figure 2.2 shows the profile of the iron loss improvement since 1970 (TAKAMIYA et al., 2016).

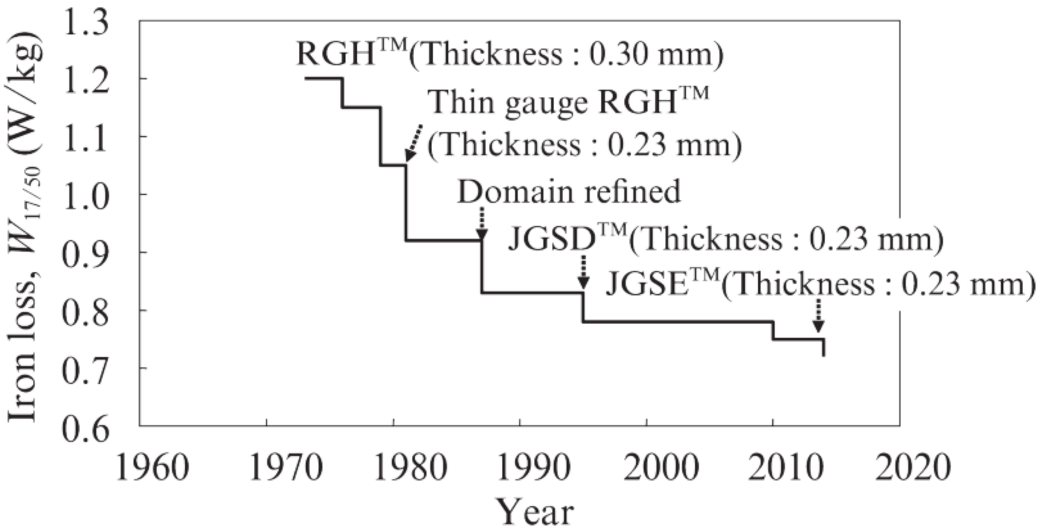

Figure 2.2 – Iron loss improvement 1970-2016.
Source: Adapted from TAKAMIYA et al., 2016

A laser scribed core lamination is used for improved the domain structure of the electric steel, reducing the total no-load loss. Figure 2.3 shows a photography of the grain-oriented steel with laser scribed treatment.

Figure 2.3 – Electrical steel with laser scribed.

Load losses are resulted from the current circulation in the windings and varying with the transformer load. These losses are composed of three components: *resistive losses*, *eddy losses in winding* and *stray losses*. (FITZGERALD, 1909)

i) *Resistive losses* are the most significant component of load losses in power transformers. These losses are resulting due to the winding resistance, leads connection and busbar, also known as DC losses. This component of load loss is the easiest to be predicted accurately.

ii) *Eddy losses in winding* is resulting from eddy currents in conductors exposed to magnetic field. Regardless the type of transformer, Finite Element Method (FEM) tools can be useful during the power transformer design, in order to minimize eddy losses choosing winding conductor which fits better with the leakage flux.

iii) *Stray Losses* are generated by the main leakage flux hitting metallic parts when exposed to magnetic fields and by the currents in the leads and busbar which generate magnetic fluxes as well. These losses can be reduced with the insertion of non-magnetic material, installation of magnetic shunts that work basically as flux collectors, i.e. shielding areas in the power transformer in order to avoid leakage flux through some specific parts (e.g. tank or clamp), where this flux would create higher losses. These losses cannot be calculated easily due to the geometric characteristics of the active parts, therefore 3D modeling by FEM-based computational tools are commonly used. Furthermore, the stray losses cannot be determined separately of the eddy losses by means of measurements.

Auxiliary losses are generated by cooling devices of power transformers, such as fans and/or pumps.

The cooling system is an important feature of the overall transformer lifecycle and efficiency, even auxiliary losses usually are not as significant as the others components of losses it must be well design in order to reduce loss and at the same time quantity of cooling material. Depending on the application of the transformer an intelligent approach should be specified, like a type of cooling media, energy efficiency of the fans or pumps and, the ratio between the operation without forced cooling and with forced cooling.

Currently, electronically controlled fans are used in order to reduce the auxiliary losses in large power transformers when this equipment is not operating in the maximum power.

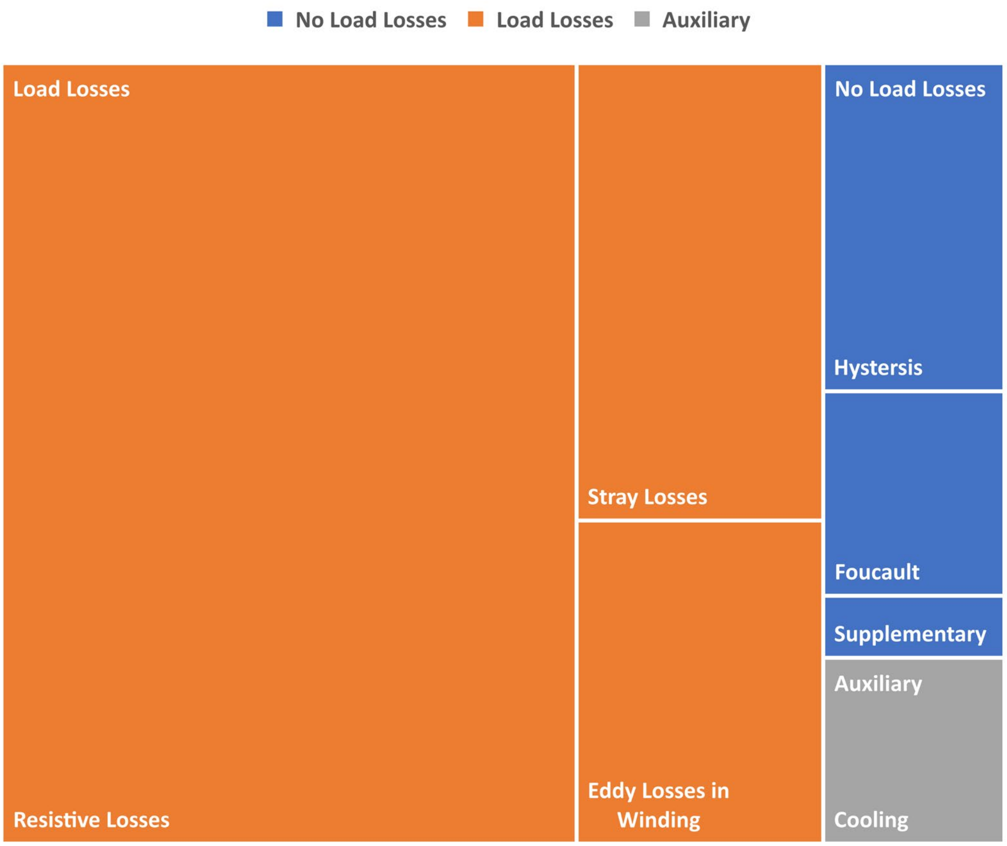

Figure 2.4 – Typical quantity of losses distribution in a power transformer, example.

Figure 2.4 shows that load losses are the most significant component in the total losses of a power transformer, and therefore major thermal dissipation and main driver of the life expectance. In this sense, the winding design concept must be well detailed to avoid as maximum as possible the eddy losses in windings and undesired hotspots. Besides, the hotspot is the main driver of the life expectance of the transformer unit and it should be well predicted and located during the design stage.

2.1. ENERGY EFFICIENCY

Energy efficiency is at the heart of any strategy to guarantee secure, sustainable and inclusive economic growth. It is one of the most cost-effective ways to enhance security of energy supply, to boost competitiveness and welfare, and to reduce the environmental footprint of the energy system. An energy sector transformation of the scale and pace required to achieve the Sustainable Development Scenario depends upon fundamental changes to the way energy is produced and consumed. (PRINDLE, W. et al., 2007).

A sharp pick-up in efficiency improvements is the single most important element that brings the world towards the Sustainable Development Scenario. Energy efficiency is the primary "fuel" of choice in most regions because of its cost-effectiveness. Energy efficiency measures generally offer an attractive payback, although the barriers to their deployment such as access to finance or lack of information have to be successfully addressed. (IEA, 2019).

International efforts to map trajectories towards the achievement of sustainable development goals generally acknowledge the complementarity of renewable energy deployment and energy efficiency measures. (IRENA, 2018). In 2011, the United Nations 'Sustainable Energy for ALL initiative, recognizing the joint role of renewable and efficiency in securing universal access to sustainable energy, set a target to double both the share of renewable energy in global final energy consumption to 36% in 2030 and the rate of improvement in energy efficiency (SEforALL, 2020).

Furthermore, in 2018 the intergovernmental panel on climate change presented several pathways for mitigating climate change that are consistent with a relatively high probability of limiting the long-term increase in global average temperature to 1.5°C above the pre-industrial levels. (ROGELJ et al., 2019).

Wind and solar are the fastest-growing sources of electric power today for a few simple reasons: They are renewable energy sources that do not produce greenhouse gases or other emissions; the "fuel" is free and essentially infinite in supply; and as technology matures, equipment costs continue to drop as already been discussed in the Chapter 1.

Sources currently used to energy demand is limited in nature like fossil, coal and nuclear fuels. In an attempt to rebalance supply and demand, many countries started investing in power generation from renewable resources and energy efficiency programs and more energy performant equipment (BAGGINI & BUA, 2015).

Renewable power capacity is set to expand by 50% between 2019 and 2024, led by solar PV. This increase of 1200 GW is equivalent to the total installed power capacity of the United States today. Solar photovoltaic alone accounts for almost 60% of the expected growth, with onshore wind representing one-quarter. Figure 2.5 shows the capacity growth in renewable sources in GW between 2019 and 2024 considering normal case and the accelerate case (IEA, 2019).

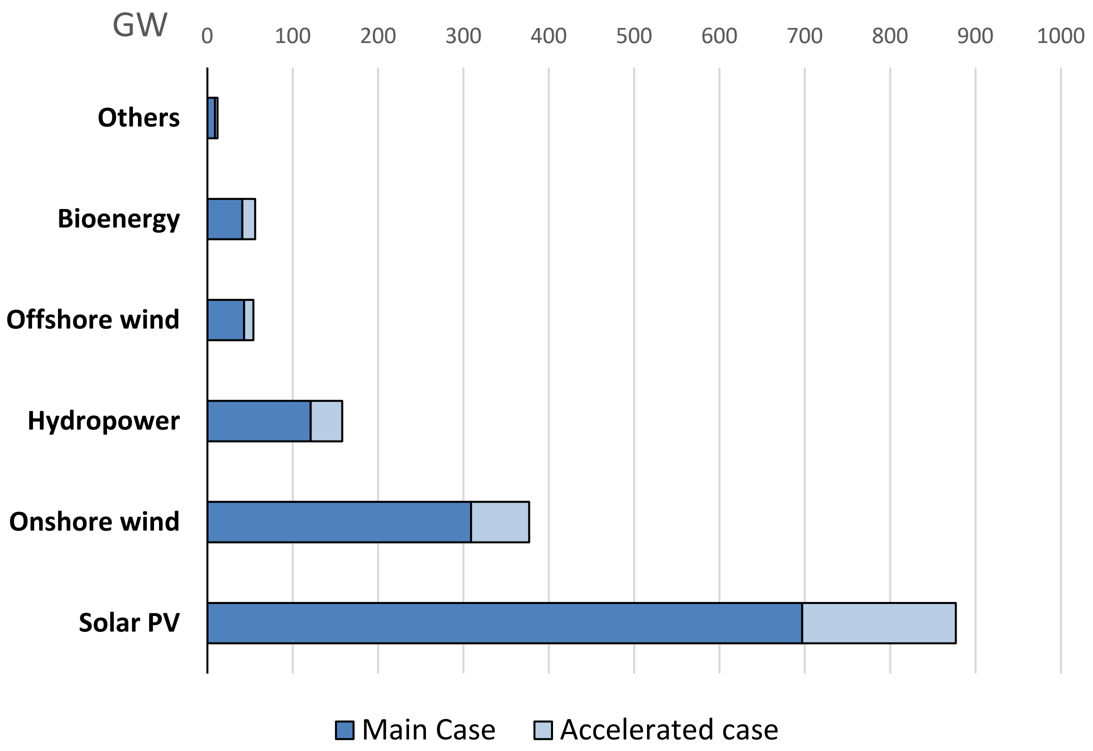

Figure 2.5 – Renewable capacity increase by technology (2019-2024).
Source: Adapted from IEA, 2019.

Solar photovoltaic drives strong rebound in renewable capacity additions. The accelerated case requires that governments address three main challenges:

1) policy and regulatory uncertainty;

2) high investment risks in developing countries;

3) system integration of wind and solar in some countries.

Even if accelerated case is not addressed a substantial grown will be happen in the solar photovoltaic sources.

Energy efficiency has tremendous potential to boost economic growth and avoid greenhouse gas emission. In this sense, the standard IEC TS 60076-20:2017 states: *to promote a higher average level of the energy performance for transformers due to the need for energy saving and reduction of the emission of greenhouse gases*. The IEC international standard proposes methods to specified transformers with higher energetic performance according to loading and operating conditions applicable (IEC, 2017).

Besides, the formulation to efficiency calculation is presented, and its claims that the efficiency index should not be the unique base to choose the transformer. The equipment cost, operational and maintenance cost and the estimate total life cycle should be taken in account to determine the transformer most suitable for the intended application with focus on delivering more cost-effective solutions throughout the life cycle of the transformer.

Several different ways can be used to evaluate the energy efficiency of a power transformer, such as (OJEU, 2014):

- **Maximum no-load and maximum losses at full load** – this metric place two constraints on each design and is closest to that specified in the common test standards. It involves ensuring that a design does not exceed the maximum values of no-load losses and full load losses in watts, when specified separately. This approach for establishing mandatory requirements on transformer performance can be found in economies such as China, Europe Union and United Nations Convention on Climate Change.
- **Maximum combined losses at a specified loading point** – this metric place a single constraint on the design, measured in watts, which is the sum of the no-load losses and the load losses at the specified loading point. This approach for establishing performance requirements on transformers can be found in countries such as India, Japan and Brazil.
- **Percent efficiency at a defined loading point** – this metric is the ratio of the active power in watts delivered by the transformer over the load relative to the active power in watts drawn by it from the source. Percent efficiency varies with load and consequently must be declared at a specified loading point. This approach for establishing mandatory requirements on transformer performance can be found in economies such as Australia, Korea and USA.
- **Minimum efficiency using peak efficiency index (PEI)** – this is an index that was developed by a technical working group supporting the

European Commission's analysis of regulations for large power transformers. The equation for peak efficiency determines the appropriate highest efficiency value of any transformer design at an optimal loading point. This approach for defining efficiency was included in the European eco-design regulation for transformers (OJEU 2014).

2.1.1. MAXIMUM NO-LOAD AND LOAD LOSSES

There are two issues that must be considered during power transformer design: no-load and load losses. These values are obtained from measurement during electrical tests. The main objective is to ensure that the project does not exceed the maximum values of no-load losses and load losses, which are specified separately, i.e. losses in power transformers are limited regardless of your application.

Both IEC 60076 and IEEE C57 standards are based on power performance evaluations of transformers without load in nominal voltage in order to analyze the core magnetization (no-load losses), and with 100% of the load capacity (load losses), (IEC Std 60076, 2018 and IEEE Std C57, 2011).

This normative approach is followed in China, Europe, and the United Nations Convention on Climate Change, where are determined the maximum loss levels for different sizes of transformers. In this sense, no-load losses and load losses are limited to a certain operation margin regardless of the loading level of the power transformer. This is an important issue since it is generally difficult to predict the daily average load, with some degree of accuracy throughout the entire life cycle of the power transformer. With this system, a minimum performance level is guaranteed independently of the load level applied to the transformer.

However, once the no-load losses requirement has been established, an optimum performance point is implicitly obtained, and the minimum manufacture cost can be determined. If the loading corresponding at this optimum efficiency point and minimal production cost is not coincident with the real load of the transformer, a potential energy saving is lost. By this reason, regulators should be careful to define this point to ensure that the proposed requirements do not encourage maximum performance outside of the real load at the transformer will be applied.

Another problem in specifying a maximum no-load and load losses separately is the flexibility reduction during the design process, which implies a major initial cost of the power transformer because of eventual variations on the raw material prices. However, this problem can be mitigated if losses are capitalized, i.e. considering the relationship USD/kW of iron (no-load) and on copper (load) throughout the design and manufacturing process of the power transformer. This analysis leads to an optimum balance between no-load losses and load losses, both below the maximum allowed values.

2.1.2. MAXIMUM COMBINED LOSSES

An alternative way to analyze the power transformer losses is the maximum combined losses, or also called total losses, which basically consists in the sum of the no-load and load losses, given in Watts.

This feature allows the manufacture a higher flexibility at design stage, dividing the losses into an interval between no-load and load losses in order to find the lowest initial cost to the customer. This procedure is widely employed by manufacturers in Japan and Brazil.

A disadvantage of this approach is that the specification of the transformer should select the load point at which the load loss will be warranty, for instance, 60% or 100%, and this load point must be represented at average load level during the entire life cycle of the transformer. If the load level established does not match the actual load of the installation to be fed by this transformer, the best efficiency will not be achieved.

This disadvantage can be overcome if losses are capitalized, as already discussed in the previous approach.

2.1.3. PERCENTAGE EFFICIENCY

Percentage efficiency is a numerical dimensionless parameter, which is similar to the combined value of no-load losses and load losses, since it is based on a single value to limit losses in transformers. The total losses are obtained from the total power of the transformer, and the percentage efficiency is calculated as ratio between the active power delivered to the load (output) and the active power delivered by the generator (input). This value must be defined at a specific load point, since for each demanded power there is a different efficiency. This requirement is mandatory to transformer performance and can be found in countries as Australia, Korea and USA. (FERNANDEZ, 2016)

There is a main advantage of the percentage efficiency instead of maximum losses approach, the first is independent of the technology employed, which allows flexibility to choose materials and design methods in the transformer manufacture. This approach allows the design engineers to decide the losses percentage for operation with and without load, which means a great flexibility during development of an optimized unit according to customer requirements.

In order to get a better point of optimization, the approach of the percentage efficiency index has to be aligned with the specific load level of the transformer during the entire life time, i.e., the specification must be clean in which point of load the losses should be guaranteed, therefore it can be seen as a disadvantage of this method due to the difficult to get this information in the very beginning concept part of the project.

Another important concern about energy losses is the load curve profile demanded from the power transformer, and not solely a specific operating point or average load factor. For the same operation point or average load level, there are innumerous forms of load curve, and therefore, the accumulated losses of a transformer for different load curves are different as well.

Furthermore, end users might not minimize the total cost during the entire life of the asset in case the analysis will be restricted for a specific load factor, so this approach is not indicated to intermittent loading curve as a solar profile when the loading profile is unknown.

The Total Ownership Cost – TOC of the transformer represents an optimization function involving the total losses, manufacturing costs, and optimum average power demand, which is given based on the load profile characteristics. Therefore, the lowest TOC of the power transformer, throughout its life cycle, is calculated based on the cost per kilowatt of losses in the core and windings, i.e. losses capitalization of the power transformer.

2.1.4. PEAK EFFICIENCY INDEX (PEI)

The Peak Efficiency Index (PEI) was proposed by a working group designated to support the European Commission of regulations on power transformers. This index (PEI) is unitless and combines no-load losses and load losses. The peak efficiency equation determines the highest performance value for any transformer design, regardless of the specified load point. The PEI is defined for the point in which the no-load losses are equal to the load losses (IEC, 2017).

This definition of efficiency was included in the European regulation of ecological design for transformers (OJEU, 2014) and in the standard IEC 60076-20 dedicated to the energy efficiency of transformers (IEC, 2017).

This approach has an advantage over other techniques because does not require specifying a loading point. On the other hand, it could lead to level of losses higher than expected if the transformer is designed for the load point related to the minimum manufacturing cost, however, this load point is not necessarily into the load levels in which the transformer operates during its entire lifetime. Some standards proposed by the IEC and CENELEC are suggesting the load level or cost per kilowatt of losses to be included in the bidding process. Therefore, the PEI can be optimized for a specific transformer loading by combining the losses. (IEC, 2017 and CENELEC, 2015)

The transformer efficiency is expressed from the relationship between the output power S_{out} and the input power S_{in}:

$$\eta = 100\frac{S_{out}}{S_{in}}\,(\%) \tag{2.1}$$

The transformer efficiency, at any operating point, is calculated as a function of the: no-load losses at rated voltage and frequency P_0; short circuit losses at the rated current and reference temperature P_{SC}; load factor k and the rated apparent power of the transformer S_r.

$$\eta = 100\left(1 - \frac{k^2 P_{\mathrm{SC}} + P_0}{S_r + P_0 + k^2 P_{\mathrm{SC}}}\right)(\%) \tag{2.2}$$

The load losses are expressed in (2.3).

$$P_k = k^2 P_{\mathrm{SC}} \tag{2.3}$$

The output power P_{out} is calculated as follows:

$$P_{out} = kS_{out} \cos \text{j} \qquad (2.4)$$

And cosφ is the power factor of the load.

The maximum efficiency η_{max} is obtained when the no-load losses are equal to the load losses. This operating point corresponds to the optimum load index C_{opt} (KULKARNI et al., 2004):

$$\eta_{max}(k_{opt}) \rightarrow P_k = P_0 = k^2 P_{SC} \qquad (2.5)$$

$$k_{opt} = \sqrt{\frac{P_0}{P_{SC}}} \qquad (2.6)$$

Substituting the load index for optimal value in the equation (2.2), it is possible to determine the PEI. Assuming the power factor as a per unit value, a population of specific transformers might be compared.

As an example, in the figure 2.6 is presented a 100 MVA power transformer, with no-load losses of 60 kW and 240 kW of load losses at nominal 100 MVA.

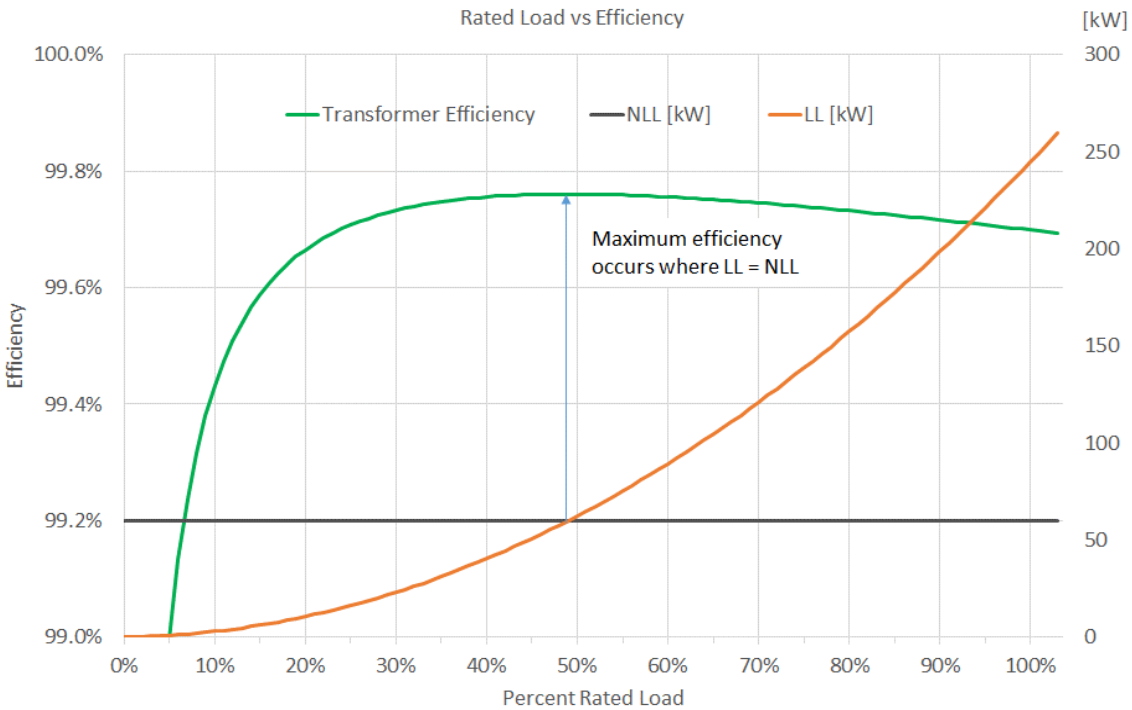

Figure 2.6 – Transformer efficiency: no-load losses and load losses.
Source: Adapted from BAGGINI, 2017.

The maximum efficiency occurs when $P_k = P_0$. This way, equation (2.2) can be restructures as follows:

$$PEI = \eta_{max} = 100\left(1 - \frac{2P_0}{k_{opt}S_r + 2P_0}\right)(\%) \tag{2.7}$$

Therefore, the *PEI* is a function of P_0, P_{SC}, S_r and the power factor of the load cos φ, which is unitary in this case. This approach is useful for comparison of the energy efficiency of large distribution transformer to different primary voltage, which is applied in energetic studies of installed transformers samples. This method focuses on the specific design concept of each transformer unit in terms of component of losses.

In this context, it is possible to conclude that each losses approach, introduced in this section, offers some advantages as well as specific limitations. The best losses analysis method varies according to various technical and economic issues which depend on the load profile and network in which the power transformer will be installed.

2.1.5. STANDARDS OF TRANSFORMER EFFICIENCY

Transformer performance is measured by tests from well-established international standards, which ensure the efficiency, accuracy and reliability of the test methodology. These international standards are established by two well-known organizations: the *International Electrotechnical Commission* – IEC and *Institute of Electrical and Electronic Engineers* – IEEE.

The IEC has published and maintained approximately 19 standards of the IEC-60076 series, in addition to other standards on tap-changers, bushings, terminals and converter transformers. The IEEE has more than 80 standards and guides on power transformers. Several countries have been involved with development and promotion of improvements on energy efficiency in power transformers, according to the well-established IEC-60076 standard. In addition, some countries have made slight modifications in the IEC standards due to specific technical requirements of each local electric grid (IEC Std 60076, 2018 and IEEE Std C57, 2011).

The energy efficiency policies for power transformers, based on the IEC recommendations, are followed by several countries around the world, some of them are standards are: Australia, Brazil, China, Europe Union, India, Israel, Japan, Mexico, New Zealand, the Republic of Korea and Vietnam. (FERNANDEZ, 2016) On the other hand, IEEE standards are widely employed in the USA and Canada.

Although these standards are defined by two distinct institutions, they are not so different in the way in which transformer performance is measured and evaluated. To avoid eventual duplications in the standard definitions, IEC and IEEE have proposed a joint project to stablish a single standard with both logos for transformers and other power devices. (McNELLY et al., 2019). It is expected in the future, IEC and IEEE prioritize the losses measurement within a double-logo procedure, in which standards on energy efficiency in power transformers are established in a joint definition from both institutes.

2.2. CAPITALIZATION

Capitalization is defined as the optimization of technical issues in a given process taken into account a reduced investment and then a minimal final cost. In the case of power transformers, it consists to minimize the total losses, and then searching for the greatest energy savings, for a minimum investment and therefore a reduced final cost. This is not a trivial task, since each power transformer is designed in a customized way, which varies depending on the application and operational conditions (SZWANDER, 1945).

Basically, the capitalization process involves the *Net Present Value* – NPV of the energy losses saving over the lifetime of the transformer. Due to the large numbers of inputs needed with considerable degree of uncertainty, the calculation of kWh saving is not an easy task, for instance, the value of kWh probably will vary along the period, the discount rated over the lifetime should be well estimated to get the NPV of the losses and the duration of the investment must be defined (ABB, 2004).

The investment decision, in case of power transformer, is driven by the requirement to supply power in the present moment, so that the associated loss levels are implicitly and explicitly decided at date of purchase. To select what level of losses is appropriate involves sophisticated financial and engineering judgement and analysis (IEEE, 1991).

Total Cost of Ownership – TCO is used to evaluate the most economic transformer, in which the initial cost and the associated losses are considered together. This way, saving initial purchase costs from buying a low efficiency transformer are balanced by higher level of losses incurred, increasing savings in losses by the higher initial purchase prices.

Asset management feature is the best method for optimization of power transformer design in accordance with customer needs, therefore TCO is encouraged to be used during the procurement process, and according to the initial cost of the transformer should take into account all others associated lifetime costs such as: installation, maintenance, insurance, transportability and end of life disposal (ABB, 2004).

Analogously, the value of the energy saved is characterized by its marginal cost per kWh and should not include fixed costs, such as: renewable taxes, public sector obligation levies, value-added tax and others.

Increase the capitalization value will result in a decreasing loss, up to the point in which the cost of decreasing the losses equalizes the capitalization values, or where the weight associated, or the size exceeds the limits in the specification. The capitalization values represent the avoided costs associated with the marginal kW of iron (no-load losses) and copper losses (load losses) saved.

The no-load losses decrease when the respective capitalization factor increases, which incurs in a major transformer efficiency at any loading level during operation. In this situation, great part of the total losses is attributed to energy dissipation in the magnetic core of the power transformer. On the other hand, if load loss capitalization factor increases, a major part of the total losses of the power transformer is resulting from high loading levels.

In this context, for design of transformers applied to intermittent energy sources, e.g. a GSU transformer in a photovoltaic power plant, the capitalization study must be taken in the account during the procurement stage, from an accurate analysis of the load demand and intermittent generation profile in which this transformer will operate. Thus, a design optimization of the magnetic core and copper windings is required to define the best energy efficiency of the power transformer, since the load and generation characteristics are known. Furthermore, the balance between the no-losses and losses capitalization factors is intrinsically related to mechanical characteristics (e.g. weight) and dimension (e.g. tank size and internal volume) of the power transformer, since modifications in the magnetic core and windings demand more or less raw material, such as: cellulose, mineral oil, iron and copper.

Several parameters influence the capitalized loss values. Some of these parameters must be predicted for a few future years and consequently such predictions are subjective and uncertainties.

Nevertheless, an attempt to analyze the situation to obtain reasonably relevant capitalized loss figures will most likely lead to a more economic choice of transformer than neglecting the cost of the losses completely and just go to the lowest purchase price.

Some parameters must be taken into consideration during the evaluation of a transformer and its application. The energy cost and how this evolves during the year of operation of this transformer.

In a calculation model for capitalized costs of the losses, a sensitivity analysis is used to calculate several alternative increase rates in order to see how the result is influenced.

2.2.1. Capitalization Parameters and Complementary Information

The energy cost per unit, or kWh, is influenced by numerous factors, like supply and demand of electricity, taxes, inflation, political situations and decisions, fuel market prices, climate variations. This parameter may fluctuate during a day or even from one year to another, making a fine-tuned prediction of the evolution energy price is almost impossible. For that reason, some methods are used to predict as precision as possible, like an approximation the evolution of energy costs can be calculated by means of an average increase rate per year.

The load pattern of the transformer is another very sensitive and one of the most important parameters in a transformer capitalization. Depending on the application the transformer can be run fully loaded from the beginning until the end of life, except for shut-down period to maintenance. Transformers for operation in systems for general electricity supply normally have a power rating which is considerably higher than the load just after installation, in order to meet the future needs and possible disturbance situation. In some cases, the initial load may then be even below one half the power rating of the transformer and this low load might prevail for several years before the load current slowly approaches the nominal current of the transformer.

Many transformers are operating satisfactorily after more than half a century or more in service. The considerable accumulated saving potential during this long time should make an investment to achieve low transformer losses quite attractive. The amount of money the purchaser or investor accepts to invest per reduced each kW in loss is, however, determined by the number of years the purchaser is willing to wait until accumulated saving equal the invested amount, possibly also adjust according to the general inflation rate. Before these numbers of years have elapsed, there is no net revenue on the investment. The earnings are coming in the following years. Such an investment will compete with alternative investment objects, considering profitability potential and economic risk level.

Another parameter that should be taken into account is the period in de-energized condition due to maintenance or other reasons that this transformer will be facing. It is a parameter that is not easy to predict in its totality but must be considered during the procurement and specification of a transformer.

The insurance premium has normally not any large influence on the capitalized loss value and may be disregarded. In the same approach is the property tax, that is a certain percentage of the acquisition cost and adds to the operational costs. Rules for depreciation for the equipment vary in each country and after certain number of years, the value of the transformer is written down, and the property tax may disappear.

2.2.2. CAPITALIZATION FORMULA AND MAIN COMPONENTS

The capitalization should concern various other parameters, such as the forecast cost of the energy per year during the transformer lifetime, variable losses in this same period, and then to relate these parameters to future monetary issues to present values applying an appropriate discount rate. Unfortunately, several parameters are not easily available and unreliable to determine the capitalization values with acceptable accuracy, as described in the previous section.

The losses used for capitalization evaluation should include the cooling losses, i.e. energy consumed by the cooling equipment, during the operation. That power consumption can appear when the transformer is operating with the no-load losses or with both, no-load losses and load losses, usually, these equipment are fans and/or oil pumps.

Equation (2.8) introduces the TCO. (SZWANDER, 1945)

$$\mathrm{TCO} = \mathrm{IC} + \mathrm{A}(P_0 + P_{\mathrm{Co}}) + \mathrm{B}(P_{\mathrm{SC}} + P_{\mathrm{CS}} - P_{\mathrm{Co}}) \tag{2.8}$$

Term IC is the *initial cost* of the power transformer. For a more sophisticated evaluation, this initial cost is calculated from the manufacturing price added to installation costs (e.g. foundations and commissioning costs); no-load losses P_0 at rated voltage and frequency; short circuit losses P_{SC} at the rated current and reference temperature; cooling power P_{Co} for no-load operation; and total cooling power P_{CS} for operation at rated power.

The factors A and B are capitalization costs of no-load losses and capitalization costs of load losses, respectively. The losses cost comes into effect during the transformer lifetime; losses costs are therefore converted to the moment of purchase. These factors represent a discounted net present value of the future losses per kW over the lifetime of the power transformer, which depend on transformer loading profile as well as cost of capital (Brealey et al. , 2015) energy market forecasts and expected transformer lifetime.

The no-load losses and associated cooling losses are present as soon as the transformer is energized, therefore the capitalization cost is the energy costs multiplied by the operating time over the full life expectancy of the transformer.

The value of these kWh today is the **A** factor or *no-load loss capitalization value*, normally given in \$/kW of no-load losses, and represents, the net present value of no-load losses saved over the transformer's lifetime.

Correspondingly, a purchaser would be willing to invest up to this amount on extra costs in improving the transformer performance, because if this extra investment will be less than **A**, so there is a positive gain to be made. However, a higher investment in the power transformer incurs in some declining returns, so then the benefits from the extra investment cost more than losses saved, in which stage no further investment will be economic. At this point, the value of the losses saved is balanced by the extra transformer investment cost per kW, and this value is **A** in \$/kW.

To calculate the value of capitalization is needed have some input data where, C is the initial energy cost given in local currency and C_{mid} is the energy cost at the mid-lifetime of the transformer, as expressed in (2.9).

$$C_{mid} = \frac{C + C(1+p)^n}{2} \tag{2.9}$$

The expected lifetime of the transformer is given in years n; the energy increase price per year is p.

Another important variable is the discount rate in the investment *Inv*, in percentage, as also known as *Weighted Average Cost of Capital* – WACC. Basically, it the average rate of return a company expects to compensate all stakeholders. (GITMAN et al., 2011). In other words, WACC represents the minimum return that a company must earn on an existing asset base to satisfy its creditors, owners, and other investors. Usually, companies use the WACC to evaluate if the project investments are viable or not.

$$A = t_{op} C_{mid} \frac{1 - \left(\frac{1}{1+Inv}\right)^{n}}{Inv} \tag{2.10}$$

The operating hours in which the power transformer is energized per year is t_{op}. This term is usually established as 8640 hours, since the power transformer is considered to keep operating at all time. (OROSZ, 2019).

The load loss the capitalization cost of the losses due to load and is highly dependent on the load profile as losses vary with the square of the load. The capitalization of load loss is highly dependent of the load profile once this component of this losses varies with the square of the load.

The way in which losses vary depends on the load profile during a day, week, month, and along the year. Since the load profile characteristics are known, the load loss factor, L_f is calculated, which is defined as the average overtime of the root mean square RMS values of the instantaneous load. Typically, the proportionality constant used is the square of the load factor.

$$B = A \, {L_f}^2 \tag{2.11}$$

Following the same logic as for no-load losses, a purchaser would be willing to back roll up to B, $/kW on extra costs in improving the transformer efficiency, because once this extra investment is less than **B**, there is a positive gain to be made. However, there are declining returns with increasing investment so that at some stage the benefits from the extra investment cost more than the losses saved, in this stage no further investment is economic. At this point, the value injected to saved load losses is balanced by the extra transformer investment cost per kW, and this value is **B**.

Equation (2.12) shows a new formulation to calculate the load loss capitalization, including the integral of the current in a time period t_{op}, as previously introduced and the current rated of the equipment I_{rated}. From this formulation is possible to define the average loading of the transformer during its lifetime.

$$\mathbf{B} = \left(\frac{\int_0^{t_{op}} i(t)\mathrm{d}t}{I_{rated}}\right)^2 C_{mid}\, t_{op}\ \frac{1-\left(\frac{1}{1+Inv}\right)^n}{Inv} \qquad (2.12)$$

The relationship between no-load losses and load losses in transformer selection means, in practical terms, that power transformers operating in full load, as those in industrial/commercial and urban areas, copper losses are predominant and represent an expressive return on investments; whereas transformers operating low load conditions, e.g. solar power plant transformers, a very low investment return on copper losses is observed, and then iron losses are predominant.(IEEE standard C57.120, 1991)

For maximum transformer efficiency the ratio of no-load losses per load losses should be related to the load factor served. When the transformer operates with a unit load factor, probably the optimum balance will be with a transformer with lower load losses because this component is relevant. The opposite is also valid when a small load factor is predicted, the no-load losses become more important.

GSU power transformers represent a special application. Great part of the 24 hours, this power transformer operates without load (no-load) or low load demand, i.e. it is energized and consuming energy from the electrical net system. During the part of the daylight period, the GSU power transformer operates with practically full loading, around 100% of its nominal power. In this sense, capitalization of power transformers applied for solar power systems present several peculiarities which should be taken into account during evaluation of the losses costs.

The purchase decision of a transformer should be based on the optimum design and purchase price that result in the lowest lifecycle cost. The use of TCO method allows the manufacturers to design various customized devices in order to provide an optimal solution by concerning specific requirements from each customer. Thus, both cost of purchase and lifetime cost due to the lost energy are evaluated by using TCO method in order to define an optimum solution that varies according to each customer.

Chapter 3 – BACKGROUND ON POWER TRANSFORMERS AGING

The solid insulation of power transformers is predominantly made of cellulose and, in some specific cases, composed of polymeric aramid materials applied for high temperature applications. In winding conductor, paper insulation is often used where are electrically and mechanically stressed. (BENGTSSON et al., 2018).

In the figure 3.1 is presented a solid insulation inside the transformer discretizing collar, exits, barriers, spacer and strips.

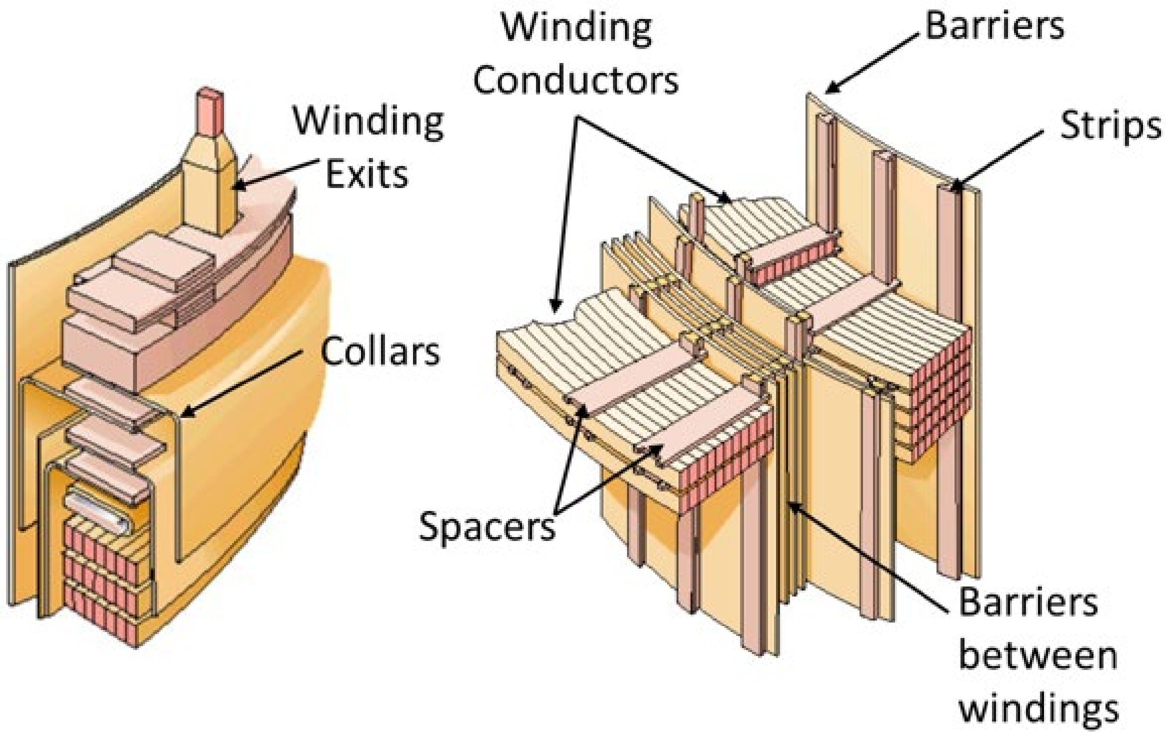

Figure 3.1 – Solid insulation in windings and collars (KAZMIERCZAK, 2020)

Cellulose occurs widely in nature as the constituent of the cell walls of plants. Softwoods like pine or spruce and some hardwoods are used for pulp, which is used in the manufacture of cellulose structure for transformer solid insulation. Cellulose fibers are composed of a complex structure which, at the molecular level, is comprised of chains of anhydro glucose units. (FRIMPONG et al., 2019).

Polymeric aramid materials are often applied in high-temperature solution due to a class of heat-resistant and strong synthetic fibers. These strong synthetic fibers increase the capability to resist high temperatures comparing with cellulose.

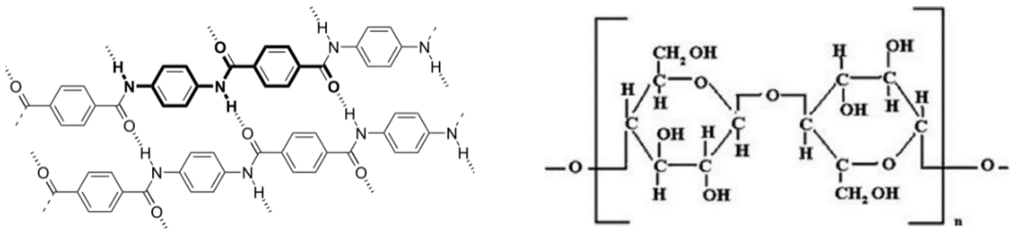

Figure 3.1 – The aramid molecule (left) and cellulose molecule (right).

One of the best cost-efficiency and reliable materials for electrical insulation, in high voltage applications, is the cellulose (solid insulation), which have been widely used since late 1920, due to the availability from natural renewable source. The cellulose into power transformers has two functions: electrical insulation and mechanical support of the windings structure. These two functions are coupled and often should be considered together. Nevertheless, cellulose is hydroscopic, which means that it easily absorbs moisture when exposed to air. The dielectric strength of the cellulose insulation decreases with increasing moisture content, which can be also generated from the mineral oil during electrical stresses.

Two different types of paper are used in a great part of transformer designs: normal kraft paper or thermally upgraded paper. Kraft paper, or also known as non-thermally upgrade paper, is produced from unbleached softwood pulp under the sulphate process without addition of stabilizers. The thermally upgraded paper is a cellulose-based paper which has been chemically modified to reduce the rate in which the paper decomposes.

Moisture and temperature are the two main aging agents in oil and cellulose insulation in power transformers during throughout entire lifetime (KUNG et al., 2017). For example, the lifetime expectance of the transformer is reduced 50% every 6°C increasing in temperature. Moisture shows a similar aging rate; in this sense, both moisture and temperature incur in significant reduction in the lifetime expectance. New technologies have been proposed for oil-immersed transformers in order to minimize the moisture and oxidation effects on insulation lifetime, in which the most important factor is the winding hot spot temperature (ZAREI, 2019).

In this sense, methodologies based on the temperature show to be reliable for lifetime analysis of power transformers.

The temperature range, in which power transformer operates, is defined by international standards in the technical literature. In case the temperature limit exceeds, during overload or very hot ambient temperature, the winding insulation material is progressively degraded and therefore incurring in reduction of the transformer lifetime (FERNANDEZ, 2016).

Power transformers are subject to different types of stresses during the life cycle, which are grouped into thermal, mechanical and electrical. E.g. overload (thermal), short-circuit mechanical forces, fast electromagnetic transients. These stresses are directly related to the operational conditions and load demand characteristics of the system in which the power transformer is installed. In addition, these various stresses are also directly and indirectly associated with insulation degradation/aging due to gas generation during electromagnetic transient events or mechanical stresses (IEEE, Std, 2012).

The insulation aging implies in degradation of mechanical properties of the paper insulation, incurring in possible failures due to mechanical stresses provoked from short-circuit occurred in the external network. If the mechanical stress is strong enough to crack the aged paper insulation, a severe internal short-circuit in the winding may occur, resulting in out-of-operation as a final consequence. (BENGTSSON, 2018) It should be noted that electrical failures in the windings, related to thermal aging, rarely happen solely because of the paper degradation. This is resulting from combination of both aging and mechanical stress.

A well-established method is the Degree of Polymerization, DP, which is used in the transformer industry to track degradation of the paper insulation used inside transformers. The Degree of Polymerization method works well for both new, unprocessed paper, and for aged paper. (FRIMPONG et al., 2020)

Power transforms are usually characterized by an efficiency higher than 99%, i.e. the input and output powers are approximately the same. However, as previously described, a minor amount of power loss occurs during the electromagnetic conversion. This power loss is represented by load losses in the conductors, losses in the electrical steel due to the changing magnetic flux (no-load losses), and losses in metallic tank walls and other metallic structures caused by the stray time varying flux, which induces eddy currents. These losses are directly related to the temperature variation during transformer operation, which must be controlled by the cooling system. (VECHIO, 2007)

The thermal behavior of power transformers has a direct relationship with the aging processes of solid and liquid insulations. A suitable expression describing the aging process would be: "*Irreversible deleterious changes to the serviceability of the transformer*". The main term of this definition is the serviceability, i.e., any change that does not affect the transformer in a definitely way is not accounted or relevant during the aging process. Another statement to describe the aging process may be: "*Such changes are characterized by a failure rate which increases with time*". Thus, from this last statement, the aging can be also defined as the increasing conditional probability of failure with time (CIGRE, 1993).

The characteristic curve that represents the failure rate *versus* time is usually denoted as *bathtub curve* in the technical literature. Such function is given from an interesting analogy with human lifetime. In the early life, high levels of infant mortality are observed, or juvenile failure rate, which decrease to lowest values covering most of the lifetime. However, the failure rate increases abruptly during the last years due to the aging process, resulting from a continuous physical and chemical degradation of active parts and insulation along the life cycle. The total lifetime depends on application and operational conditions in which the power transformer was subjected. (RETTERATH, 2005)

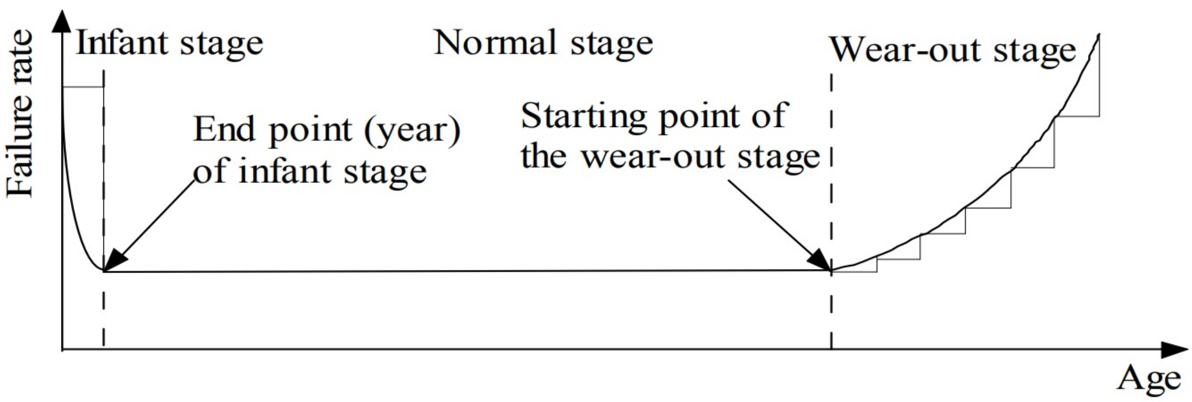

Figure 3.2 – Hypothetical bathtub curve (AHMED, 2011)

At the bottom of the bathtub curve, there is a low value of the failure rate and, in this region, the probability of failure is then independent of the age of the transformer, i.e. any failure occurring during the flat part of the curve is the consequence of a random, extremely severe stress or an abnormal reduction in dielectric strength (CIGRE, 1993).

Large power transformers have an insulating system which consists of organic materials, essentially mineral oil, paper and pressboard. These materials are progressively deteriorated throughout the transformer lifetime due to continuous aging process, which leads to impaired insulation properties and malfunction in operation. These properties are intrinsically related to a time function taken into account variables as temperature, moisture, and various gas contents dissolved in the insulation oil. However, as prior commented and based on the well-established literature (MIKULECKY et at., 2001 and MOSER et al., 1999), the most significant agent during solid and liquid insulation deterioration is the highest temperature levels in some specific operational conditions (e.g. overload demand), during electromagnetic transients, and presence of hotspot in the windings.

The basic literature presents three main mechanisms that contribute to cellulose deterioration during power transformer operation: *hydrolysis*, *oxidation*, and *pyrolysis* (SEN et al., 2011). These aging agents are resulting from presence of moisture, oxygen, and effect of very high temperatures due to hotspots, respectively. These agents are listed as follows:

- *Hydrolysis* (water) – The oxygen bridge between glucose rings is affected by water, causing the rupture of the chains, and reduction of Degree of Polymerization and weakening of fiber.
- *Oxidation* (oxygen) – The oxidation is a process dominant at lower temperature. Oxygen attacks the carbon atoms in the cellulose molecule to form aldehydes and acids, releasing water, CO, and CO_2. Since oxidation releases water, it accelerates the hydrolysis process and the insulation deterioration. Oxygen is derived from either the atmosphere, or from thermal degradation of cellulose. The problem is intensified in presence of catalyst agents, as moisture and copper.
- *Pyrolysis* (heating) – Heat and the resulting high temperatures contribute to the breakdown of individual monomers in the cellulose chain. Thermal degradation of the cellulose also yields free water, as well as certain gases as carbon monoxide CO and carbon dioxide CO_2. High temperature within a power transformer can cause the cellulose insulation to shrink and brittle. This leaves the solid insulation susceptible to failure due to mechanical stress. (SEN et al., 2011).

The transformer winding copper holds its mechanical strength up to several hundred degrees Celsius and the transformer oil maintains its integrity below 140ºC, the paper insulation degrades at temperatures exceeding 90ºC. Also, the moisture content, acidity and oxygen content of the oil have a significantly detrimental effect on insulation life. Therefore, the loading capacity of a transformer is defined in terms of its hotspot temperature and the thermal aging of its insulation (SUSA et al., 2005).

As the temperature of the solid insulation is then considered one of the principal agents during aging process, with time and high temperatures, cellulose insulation is subject to a *thermal depolymerization process*. As the chain of cellulose gets shorter, several mechanical properties of the paper are degraded, e.g. tensile strength and elasticity. Eventually, the paper becomes brittle and unable to withstanding short-circuit mechanical forces and even normal vibrations under nominal operation conditions.

To contain the thermal depolymerization of the celluloses, modern power transformers have used thermally upgraded paper which has a rated hotspot temperature of 110°C. Previous designs of transformers were developed by using conventional kraft paper for a hotspot temperature of no more than 95°C.

According to the international standards the most useful thermal aging criteria is the *Degree of Polymerization* – DP. This aging criteria are suitable to thermal evaluation of solid insulation in power transformers, since cellulose is an organic compound whose molecular structure is characterized by a long chain of glucose rings and monomers (FABRE et al., 1960) and (SHROFF et al., 1985) and (LAMPE et al., 1976).

Degree of molecular polymerization refers to the average number of glucose rings usually from 1000 to 1400 for new material. A single cellulose fiber contains many of these long chains, providing a good mechanical strength in fibers. Hence, it is true that mechanical resistance of the solid insulation is directly related to the length of these glucose chains. In this sense, the DP is an effective way to evaluate the mechanic resistance and functionality of cellulose (IEEE, Std.C57).

In order to apply an absolute time scale to the life measurement, an appropriate end-of-life was defined by international standard. An absolute DP value of 200 for an end point of insulation life was defined. It means that up to 200, the mechanical properties of the cellulose in the solid insulation are maintained.

Figure 3.2 presents per unit transformer insulation life when the insulation employed in the winding is made of cellulose. The utilization of this curve shows the principal variable that affects the thermal life and consequently, the overall transformer life which is the absolute temperature of the hotspot. This specific region will become the weakness part of the transformer in terms of aging.

This graphic also indicates that at 110 °C of absolute temperature in the hotpot, the transformer will be aging at a unity factor. In case the temperature is beyond this value, the aging is accelerated and below the aging is retarded.

This statement means that if a transformer operates with 110°C absolute temperature along its entire life cycle, after 150,000h, this transformer will be reach the end-of-life criteria of 200DP in insulation, if the transformer operates with temperatures below 110°C, it is saving lifetime. On the other hand, if the transformer is working with temperatures above 110°C, therefore it is losing lifetime. (IEEE, 2011)

Experimental evidence indicates that the relation of insulation degradation to time and temperature follows an adaptation of the Arrhenius reaction rate theory. The equation for the curve is based on the winding hotspot θH in °C, which is the absolute temperature.

$$PUL = 9.8.10^{-18} e^{\left[\frac{15000}{\theta H+273}\right]} \tag{3.1}$$

The *per unit transformer insulation life PUL* curve can be used in the following two ways. It is the basis for calculation of the *aging acceleration factor* – F_{AA} for a given load and temperature or for a varying load and temperature profile over a 24h period. F_{AA} has a value greater than 1 for winding hottest-spot temperatures, i.e. higher than reference temperature of 110 °C, and no more than 1 for temperatures below 110 °C. The F_{AA} is expressed as follows:

$$F_{AA} = e^{\left[\frac{15000}{383} - \frac{15000}{\theta H+273}\right]} \tag{3.2}$$

Figure 3.2 shows the aging acceleration factor F_{AA} as a function of the hotspot temperature.

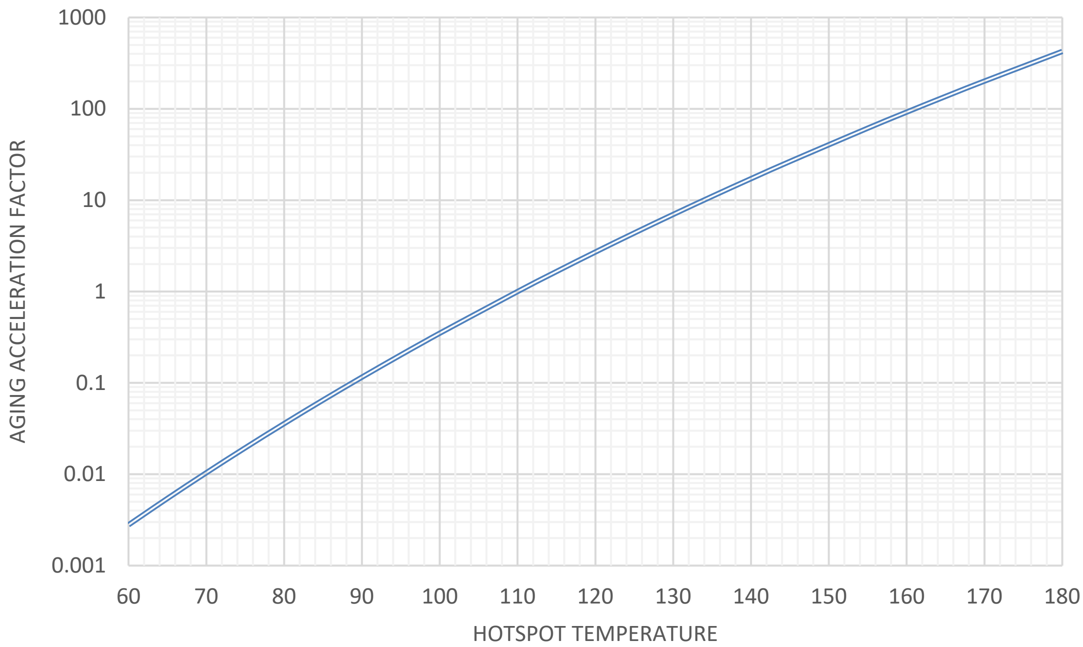

Figure 3.3 – Aging acceleration factor in thermally upgraded paper.
Source: Adapted from IEC Standard, 2016

Figure 3.3 shows that the thermally upgraded paper is sensitive to temperature variation and during an emergency overloading, with hotspots around 140°C, the factor F_{AA} is approximately 17, i.e. one hour operating with temperature 140°C is equivalent to 17 hours aging at rated temperature 110°C.

There are various reasons for power transformers failure, such as excessive overload operation or mechanical stresses (THENBOHLEN et al., 2017). Nevertheless, any transformer will eventually fail due to aging process in the insulation throughout the life cycle, even with a very efficient protection care. In this sense, equation (3.3) may be used to calculate the *loss of life* – *LL* in a determined time interval from t_1 to t_2.

$$LL = \int_{t_1}^{t_2} F_{AA}\, dt \qquad (3.3)$$

The loss of life *LL* is then expressed as the definite integral of the aging acceleration factor F_{AA}, described in (3.2), in each interval of time.

Unfortunately, there is a limited literature available in the public domain discussing failure statistics of transformers. Internal surveys are being conducted by certain countries such as Australia, Brazil, Canada, Germany and Japan (THERNBOHLEN et al., 2017).

The first international survey on large power transformer failure was published in 1983 summarizing the results of the analysis of transformer that failures in the period of 1968 to 1978 (BOSSI et al., 1983). In 2008 Cigré formed a working group *named Transformer Reliability Survey* with the main objectives was: review all existing surveys and study different practices; conduct a new international survey and proposing a uniform way of collect, compile and present those data; and analyze this new data. In December of 2015 the final report will be published.

According to this report presented in 2015 the failures mode were classified as *Dielectric*, when it is related with partial discharge, tracking or flashover; *Electrical*, for instance, open circuit, short circuit, poor joint or poor internal contact; *Thermal*, basically general overheating or localized undesired hotspot; *Physical Chemistry* where can be identified as contamination like moisture, particles, gas or corrosion; and *Mechanical*, i.e., bending, breaking, displacement, loosening. The figure below shows the failure mode for 165 generator step-up transformer and it is the most reliable information in literature.

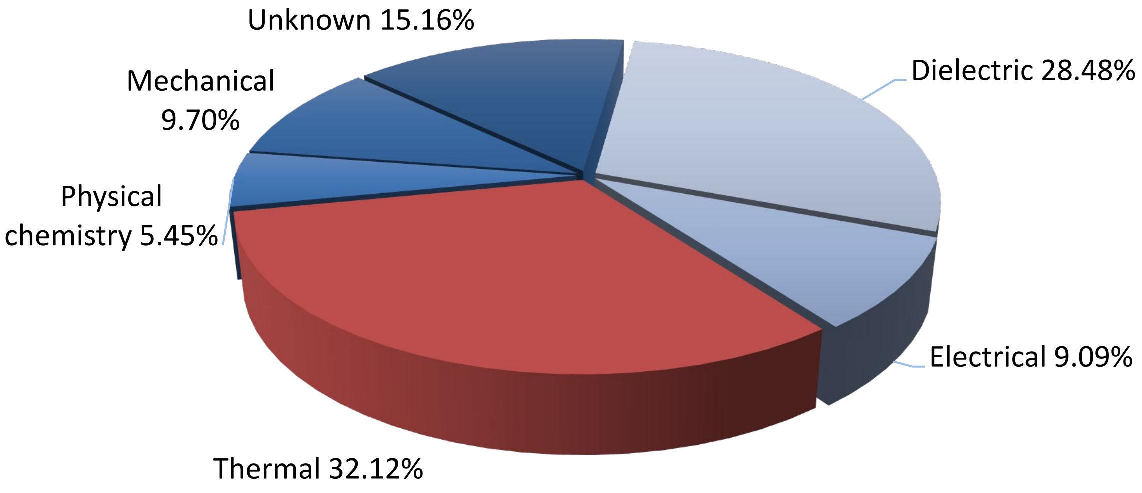

Figure 3.4 – Failure mode analysis of 165 GSU (Cigre, 2015), Adapted

The conclusion shows that dielectric mode failures were among the most prominent, irrespective transformer application and voltage class. Substation transformers were also more prone to mechanical type failures, and GSU transformers to thermal mode failures. This can be explained by the normally higher loading of GSUs compared to substation transformers. (Cigre, 2015).

The thermal failure is the most significant mode of failure in the GSU transformers, as presented in the figure 3.3, based on that, this study has a certain importance in order to avoid undesired temperature which can cause future failure in GSU transformer.

3.1. Economic Analysis and Optimization

Nowadays, there is a constant search for different optimized solutions, combining efficiency and reduce costs, in terms of materials and manufacturing process (GEORGILAKIS et al., 2007). Materials used in power transformers suffer commodities market variation with direct impact on design of a technically and economically optimum transformer. Figure 3.4 shows the variation per year of copper and electrical steel costs, and the ratio copper/e-steel.

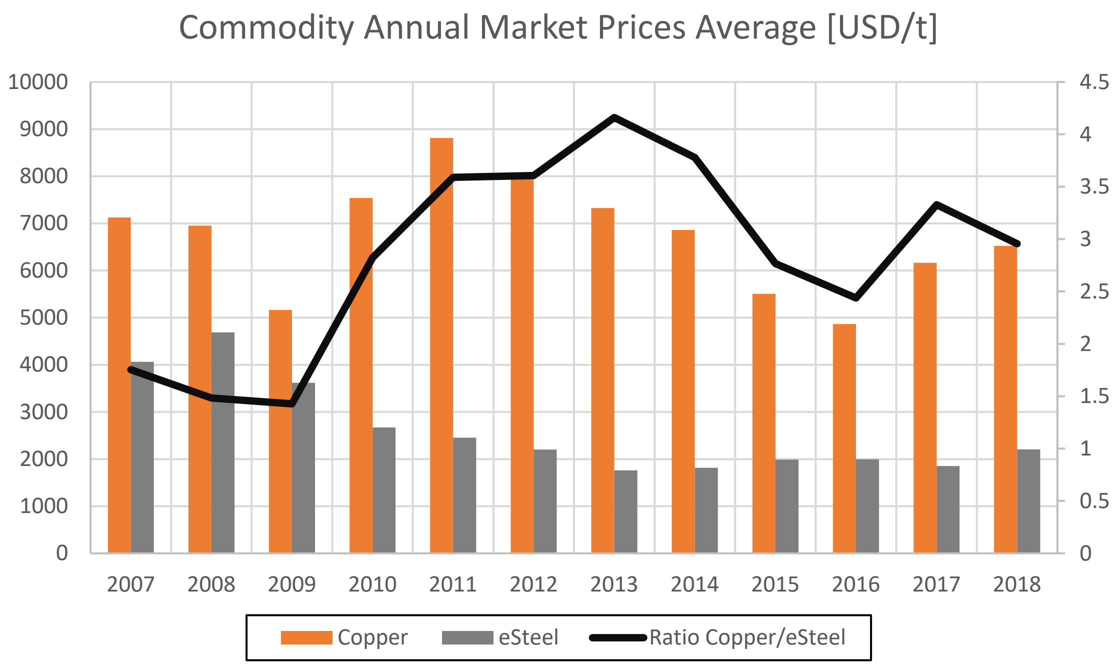

Figure 3.5 – Copper and electrical grain-oriented steel price variation.
Source: Bloomberg, LME and T&D Europe

Figure 3.5 describes that copper and steel varied greatly from 2007 to 2018, which raises the question if the same optimization technics applied during these years are also valid for power transformer design currently. For example, a transformer manufactured in 2009 probably was designed with more copper than power transformers designed in 2011. Basically, the manufactures can vary the quantity of materials in transformer design year by year in order to obtain a best cost-efficiency project.

The optimization process varies depending of the transformer application and customer objective, such as: minimize optimization of unit cost, maximize efficiency, minimize the total life cycle owning cost, meet the guaranteed losses, and reduction of the CO_2 emission footprint. The number of variables varies according to these design objectives. (PHAENGKIEO, 2016).

Usually, computer aided design (CAD) tools are necessary to efficiently solve this multivariable optimization problem. The two main materials of transformer design are copper and steel; however due to the continuous increasing of the computational capacity, many others materials can be optimized as well as analyzed in technical and economic terms, such as: mineral oil, metallic structure of the tank, solid insulation, cooling system and core clamps. These materials can be estimated during the quotation stage.

In this context, computational analysis during design and pricing stages, since there are also economic reasons to prefer units with high energy performance, concerning that losses represent the most significant part of the Life Cycle Cost, especially in an increasing electricity price scenario. (BAGGINI, 2017).

Currently, transformers are designed conservatively to withstand extreme scenarios of loading and weather conditions. These two parameters affect the heat balance in transformers, which consequently affects transformer capacity and life expectancy. Load and weather conditions are variables; therefore, the transformer capacity also changes constantly. When the transformer's loading is increased above nameplate rating and standard load guidelines, the power network operators can have significant level of cost savings and increased return of investment (WARD, 2001).

It is very common to define the active part of the transformer based on the prices of the feedstock, as: copper and silicon steel. Depending on the materials price, the designer can choose a transformer with more copper and less core or vice versa. There are different ways to optimize power transformers in the technical literature (GEORGILAKIS et al., 2007 and JUDD & KRESSLER, 1977). Power transformer is a prototyping industry, it means that the same specifications can be attended by distinct designs. An objective function for optimizing power transformer design can be expressed in (3.4): (HURLEY et al., 1998).

$$\boldsymbol{min\ Cost} = \boldsymbol{min} \sum_{i=1}^{n} \boldsymbol{uc_i\, w_i} \tag{3.4}$$

Where $\boldsymbol{uc}$ represents the unit cost of the copper, steel, solid insulation, mineral oil, tank structure, core clamps, cooling system and so on given in (USD/kg), and $\boldsymbol{w}$ is a weight value applied to each material $\boldsymbol{uc}$ in kg. Others important accessories can be included in the total material cost of the transformer, such as: bushing, tap-changes, electronic devices, monitoring system, and pumps and fans.

The optimum Total Owning Cost – TOC can be calculated from the capitalized loss values, and if the loading curve is previously known, the TOC and aging process can be easily determined. The balance between material and cost must be reach, for example, more materials means lower losses and vice-versa. Morover, very heavy or height transformer could become non-transportable by normal highway and it can cause price increase in the transportation.

Another important cost driver is the liquid used for cooling and insulating the transformer. This is a key factor for determining special thermal requirements for most accessories in the power transformer. Thus, when an optimum solution is determined, all accessories should be verified in order to check if the insulation and cooling fluids are adequate for such optimum solution. Otherwise, the optimum solution must be found considered all accessories.

Leads and cable must be properly designed to guarantee the transformer operation under overloading and high temperatures, independently of the solid and liquid insulation. Other components (bushings, tap-changer, insulation, tank structures) must be also designed to operate during high temperatures and current density. In addition, the internal structure of power transformers must be totally sealed from the external environment in order to avoid any contact with the air moisture, which causes oxidation of the mineral oil and inner structures of the transformer (RUBIO et al., 2012).

In this system, the interior of the transformer shall be sealed from the atmosphere throughout the total temperature range of operation. The aim of this system is to avoid any contact with the external air where has moisture and it causes oxidation on the transformer oil and decreases life expectance.

Chapter 4 – DYNAMIC LOADING AND RESULTS

The technical literature introduces the concept of *Dynamic Transformer Rating* – DTR taken into account varying load profile and environmental conditions. This index indicates the power transformer load above the nameplate without incurs in adverse effects on the transformer's total lifetime or increases the risk of failure (LAHOTI et al., 1981). A general definition for dynamic loading could be given by the maximum loading in which the transformer may acceptably sustain under time-varying load and/or environmental conditions (LACCHMAN et al., 2003).

Most power transformers operate with dynamic loading through its entire lifetime, on some periods it exceeds the nameplate rating, and situations where environmental or transformer conditions lie outside the design characteristics, dynamic loading may be lower than nameplate information. The basis of dynamic loading includes the insulation oil thermal time-constant, ambient temperature, and issues related to the cumulative thermal aging process in which electric insulation is subject. Nevertheless, the technical literature shows that dynamic loading can be justified without encroaching on normal life expectancy or with an acceptable loss-of-life (BENKO et al., 1979). Furthermore, the appropriate analysis of the dynamic loading could optimize the characteristics of power transformers to be installed, and therefore result in more economy and saving on investment costs. So far, a limited number of publications have been addressed in this subject (LACCHMAN et al., 2003).

In this context, some models are described in the technical literature to evaluate the transformer insulation lifetime taken into account bottom and duct oil rises, fluid viscosities, and specific heats of materials as well as other important parameters applied for the proposed methodology (hotspot gradient, oil rise over ambient, hotspot time constant, top oil time constant, total harmonic losses, no-load losses, exponential power of loss *versus* temperature, loading, and ambient temperature). (IEEE, 2011).

4.1. BACKGROUND AND METHODOLOGY

Power transformers are usually sized and designed in a very conservative way, to withstand extreme combined scenarios of loading and weather condition, which rarely come together in practice, and the temperature is an important variable during design process (PACHECO et al., 2019).

There are two methods to calculate the hotspot temperature, which are described in detail by the IEEE Standard: *top-oil model* and *bottom-oil model*. The first one, the temperature rises over ambient to determine the winding hottest-spot temperature during an overload. This method was proposed in early 40s, when there were only a few experimental investigations in winding hotspot temperature during transient loading conditions. In the 1990s, some researches proved that the oil temperature into the winding cooling duct increases rapidly at a time-constant of the duct is equal to the winding, during the overload condition (AUBIN et al., 1992; PIERCE, 1992). Such researches shown that, during the transient condition, the oil temperature adjacent to the hotspot location is higher than the top oil temperature in the tank. For air-natural and air-forced cooling models, this phenomenon results in winding hotspot temperature higher than predicted by the top-oil model. On the other hand, more input information is needed in order to obtain more accurate and reliable results. In this sense, the *bottom-oil model* shows to be more accurate, since it takes into account additional variables, such as: type of liquid, winding duct temperature, cooling model, ambient temperature, loading changes during a load cycle, resistance and viscosity variation. In this research, the IEEE Annex G model (bottom-oil model) has been used because it yields more accurate winding losses and hottest-spot calculation (SEN et al., 2011; ZAREI et al., 2019). In addition, this model is suitable, during the specification process and design review, because all parameters are available.

Overload implies in some risks during power system operation, especially when the load profile exceeds the nameplate rating of some power devices in the system. In these terms, this thesis proposes also to identify such risks and to determine limitations and guidelines, in order to minimize risks to an acceptable level. The proposed methodology is based on thermal models using the DTR approach for a real case on a GSU power transformer installed in a large photovoltaic power plant.

The pieces of information obtained from the thermal model are used to perform the reliability analysis, specifically on lifetime loss. Thereafter some improvements are suggested and discussed based on the DTR and other indexes, such as:

- Optimization of the transformer size;
- Variation of no-load losses;
- Limiting accessories;
- Capitalization analysis;
- Efficiency analysis.

This method starts by calculating and optimization of some power transformers in a wide range of input power, from 50 MVA to 175 MVA with steps of 25 MVA. All cases were calculated by using the same procedure, which is well established in the technical literature and industry proceedings. The technical specification is the similar for all transformers, and the unique variation is the power:

- Power Input, P_{input} in MVA: 50, 75, 100, 125, 150 and 175;
- High Voltage: 230 kV ±10% with tap changer;
- Low Voltage: 34.5 kV;
- Impedance at last stage of cooling: 12%;
- Maximum Total Losses at ONAF bases: 0.4%;
- Connection: Ynd1;
- No-load losses capitalization: 2500 USD/kW;
- Load Losses capitalization: 2500 USD/kW;
- Loading Profile: 1.0 p.u. (flat curve);
- Ambient Temperature: 30°C (continuous);
- Maximum hotspot rises allowable: 80 °C;
- Maximum top oil rises allowable: 65 °C;
- Maximum mean winding rises allowable: 65 °C;

- Type of oil: Mineral;
- Solid insulation material of the winding: Thermo-established paper;
- Winding conductor material: copper;
- Total lifetime considered: 150000 hours as per IEEE standard.

This method uses as input data: the no-load and load losses capitalization taken into account the best available electrical steel in terms of cost-benefit because it is possible to insert as input, the price of each kind core steel available, for instance, regular grain-oriented, Hi-B or laser scribed. Normally, high quality material has lower losses and higher prices, however, depending the capitalization factor it is possible to optimize the overall transformer core.

Several output parameters are obtained from this optimization process (GEORGILAKIS et al., 2007), however, only seven of these data are needed as input information on this method, so for each parameter, a fitting a curve is generated to determine an equivalent equation, in order to be able to get any size of the transformer through these curves. These parameters are resistivity losses, PW; winding eddy losses, PE; stray losses, PS; core losses, PC; weight of the core and coils, WCC; weight of the tank, WTANK; and volume of fluid, GFLUID. Figures from 4.1 to 4.7 show the graphics related with these parameters. The optimization process generated all these parameters and the numerical regression was used to fit the best curve.

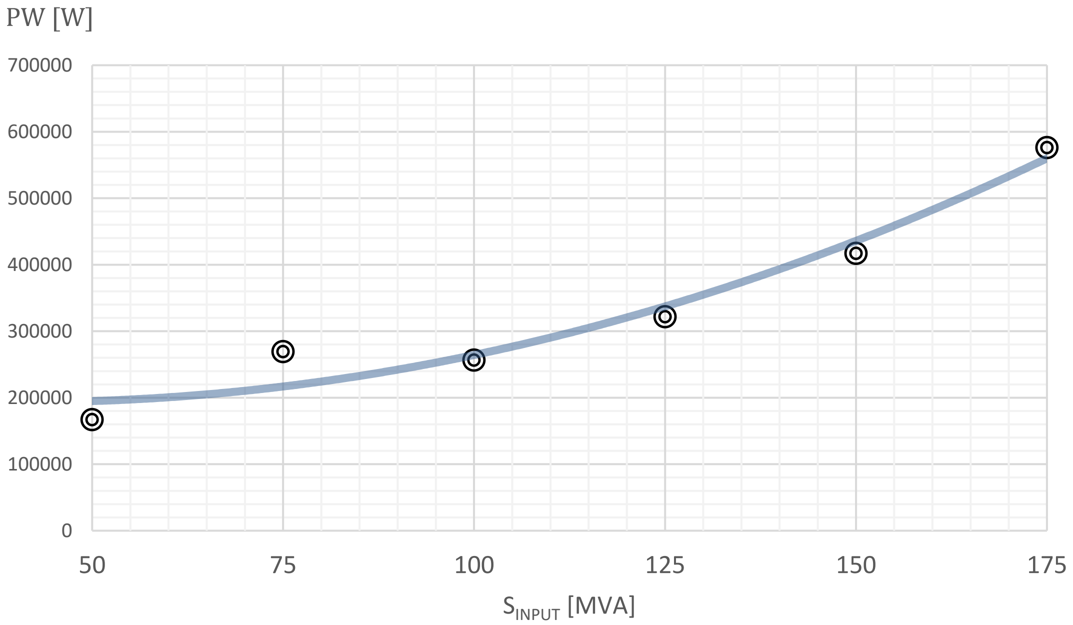

Figure 4.1 – Resistivity losses *versus* input power.

The fitted equation (4.1) encountered according to the points defined by the optimization process for resistivity winding losses parameters, previously described in the figure 4.1, in which the coefficient of determination R^2 equal to 0.9572.

$$PW = 20.454\, S_{input}^2 - 1682.2 S_{input} + 227954 \tag{4.1}$$

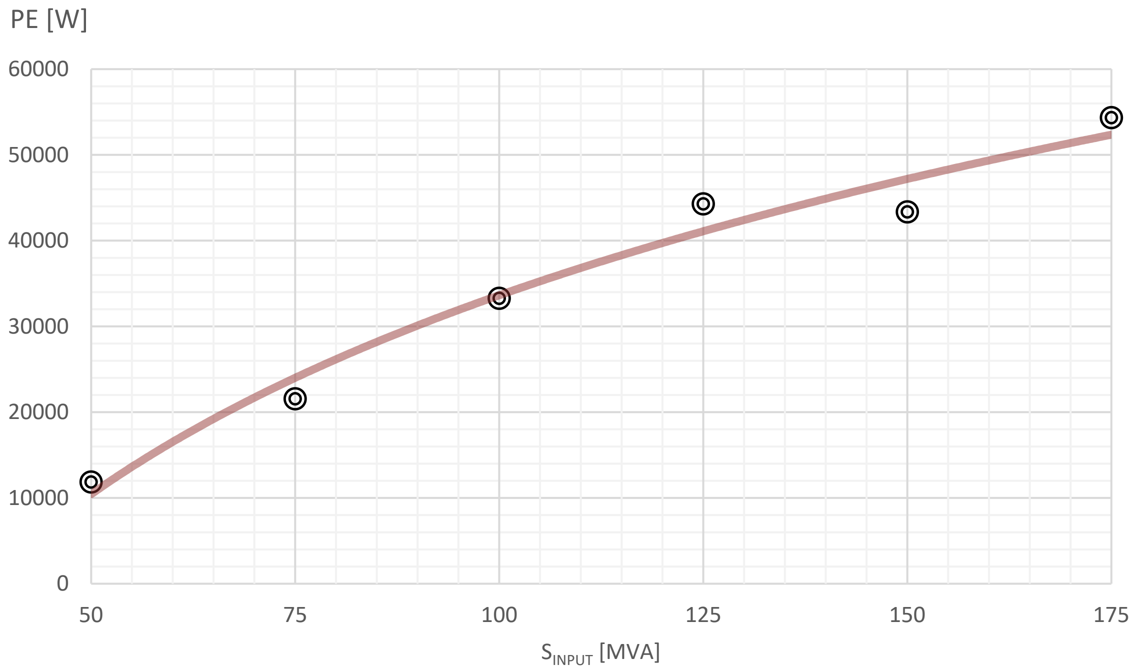

Figure 4.2 – Winding eddy losses *versus* input power.

Based on the optimization points and curve in the figure 4.2, equation (4.2) is fitted for the winding eddy losses parameters, in which the coefficient R^2 is 0.9704.

$$PE = 33454\ln(S_{input}) - 120431 \tag{4.2}$$

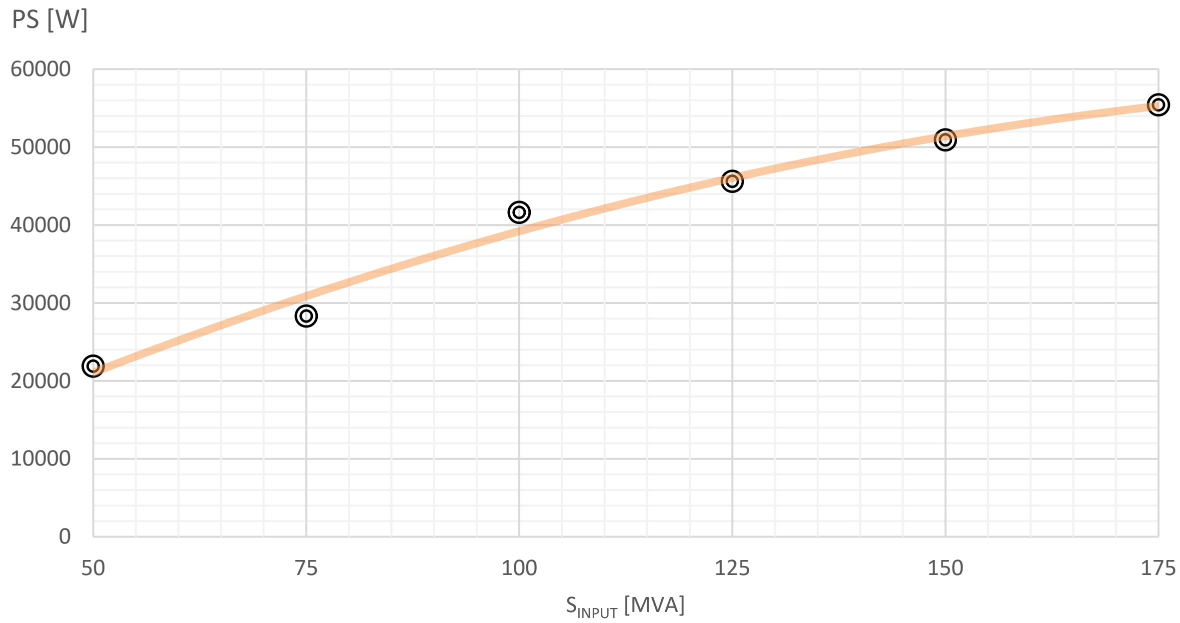

Figure 4.3 – Stray losses *versus* input power.

Equation (4.3) is obtained by fitting the function from the points defined by the optimization process for the stray losses parameters PS, with the coefficient R^2 equal to 0.9842.

$$PS = -1.1896\, S_{input}^{2} + 541.22\, S_{input} - 3019.4 \quad (4.3)$$

The fitting obtained from optimized points is shown in figure 4.4, related to the no-load losses and the equivalent expression in (4.4). The determination coefficient R^2 is 0.9797.

$$PC = 3522.6\, S_{input}^{0.6273} \quad (4.4)$$

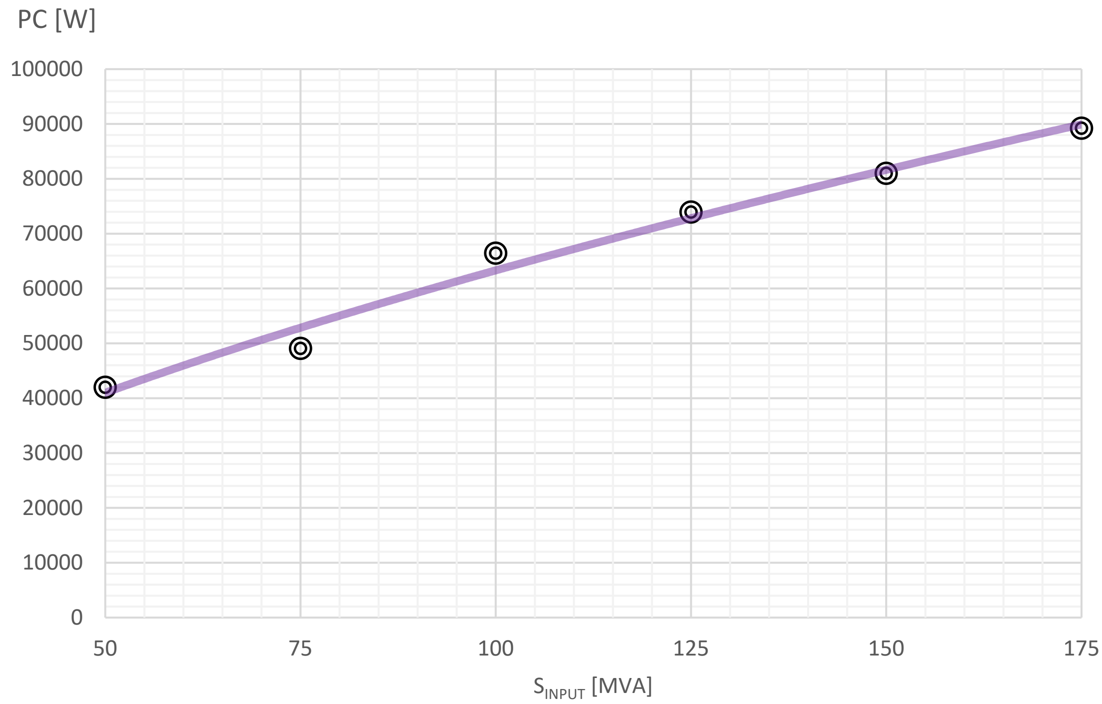

Figure 4.4 – Core losses *versus* input power.

The same fitting procedure is applied for the weight of the transformer core WCC and tank WTANK, and volume of fluid GFLUID, which are described in figures 4.5 to 4.7, respectively. The respective equations are expressed in (4.5) to (4.7) as follows:

$$WCC = -1.9898\, S_{input}^{2} + 1029.4 S_{input} + 10863 \tag{4.5}$$

$$WTANK = 32854 \ln\left(S_{input}\right) - 105015 \tag{4.6}$$

$$GFLUID = 39.509\, S_{input} + 3558.9 \tag{4.7}$$

The coefficient R^2 for (4.5) to (4.7) are 0.9823, 0.9525 and 0.9431, respectively.

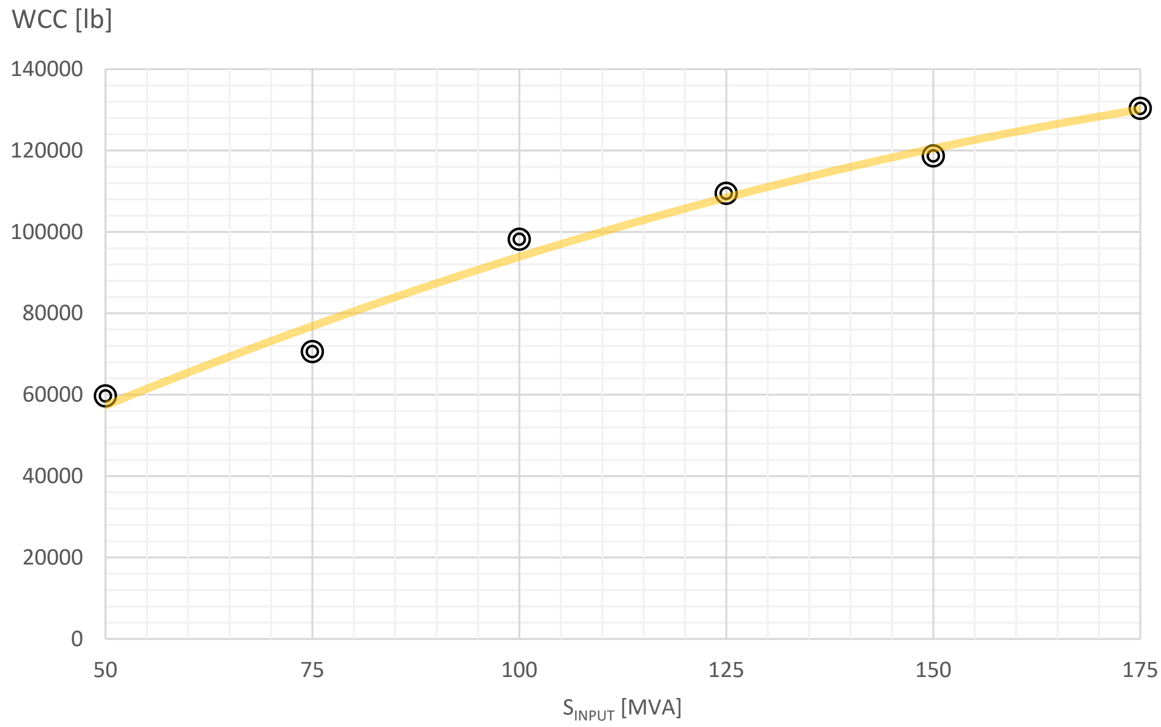

Figure 4.5 – Weight of the core and coils *versus* input power.

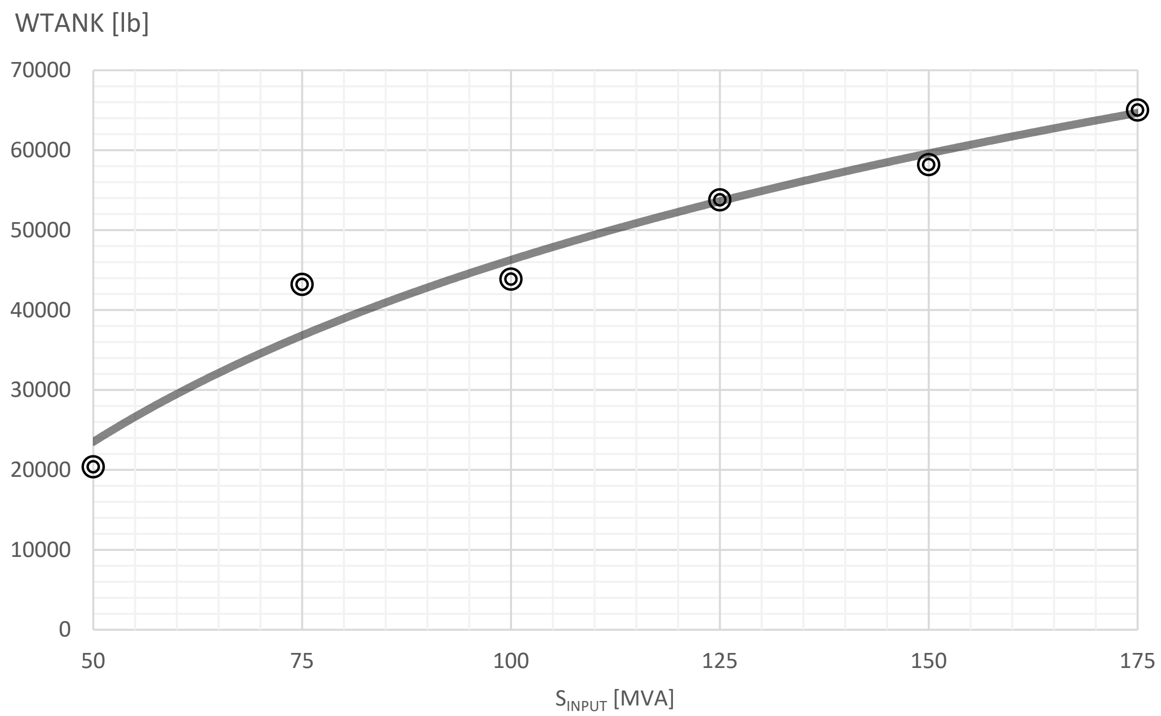

Figure 4.6 – Weight of the tank *versus* input power.

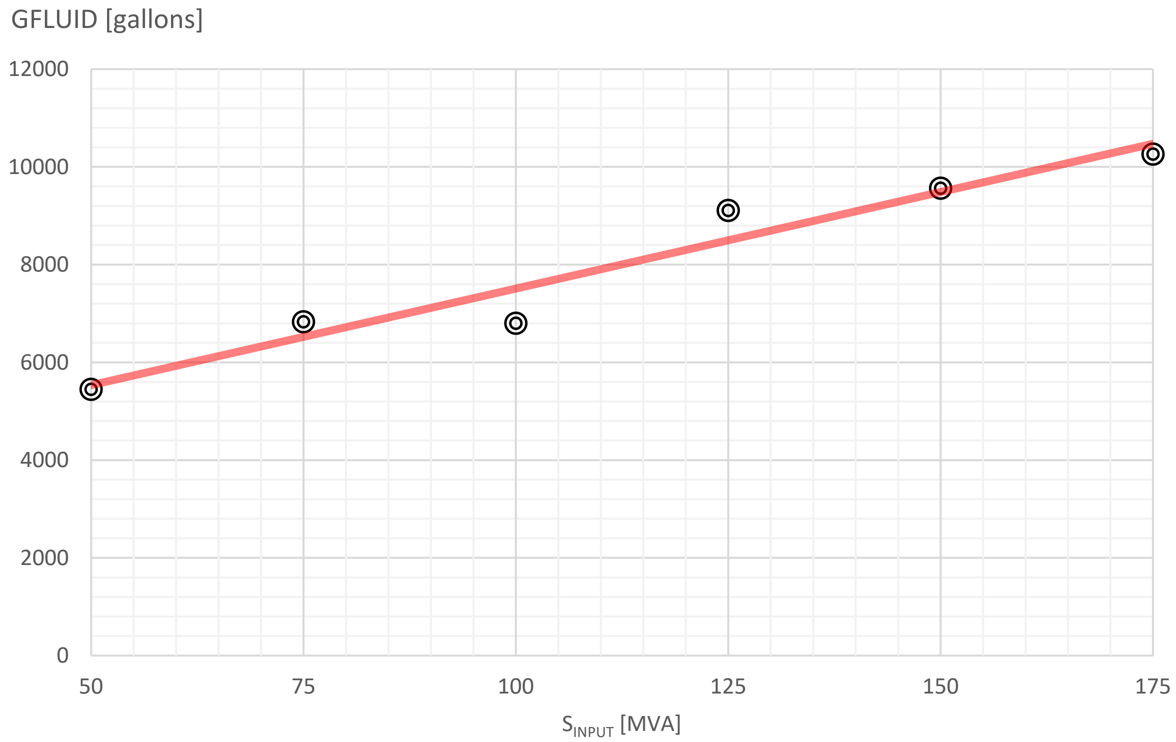

Figure 4.7 – Volume of fluid versus input power.

Therefore, equations (4.1) to (4.7) are obtained according to the technical literature and optimization process, as functions of the power input in the transformer S_{input}:(PHAENGKIEO, 2016; GEORGILAKIS et al., 2007; HURLEY et al., 1998)

Resistivity Losses	$PW = 20.454\, S_{input}^2 - 1682.2 S_{input} + 227954$
Winding Eddy Losses	$PE = 33454 \ln(S_{input}) - 120431$
Stray Losses	$PS = -1.1896\, S_{input}^2 + 541.22\, S_{input} - 3019.4$
Core Losses (no-load)	$PC = 3522.6\, S_{input}^{0.6273}$
Weight of core and coils	$WCC = -1.9898\, S_{input}^2 + 1029.4 S_{input} + 10863$
Weight of tank	$WTANK = 32854 \ln(S_{input}) - 105015$
Volume of fluid	$GFLUID = 39.509\, S_{input} + 3558.9$

Dimensioning the power transformer for a solar power plant without taking into consideration the loading profile could overestimate the total size of the equipment. A recent publication showed a real case example in which a 25 MVA rated power transformer was used to attend a 20 MW solar farm (SINGH et al., 2018). As a solar farm will operate only a few hours a year at the maximum capacity this over dimensioning utilizes more material and increase the total size, weight, footprint, and raw material consumption, so this approach could have been used to dimensioning this equipment.

The proposed method starts input data considering a continuous load for the whole day, i.e., flat curve and ambient temperature according to standards (IEEE, 2012). Figure 4.8 shows the workflow of the method, in which the initial power S_{input} is the maximum total power S_{max} of the solar farm.

The first step of the proposed optimization algorithm is the insertion of Smax, ambient temperature, loading curve function, hotspot limit, top oil limit, and equivalent aging equal unitary. Thereafter, the second stage, represented by the second block, the parameters' values like i) resistivity losses; ii) eddy losses; iii) stray losses; iv) core losses; v) the weight of the core and coil; vi) weight of the tank and; vii) the volume of fluid; receives a value related to the function of the total power to the correspondent parameter. After that, the Annex G algorithm of the IEEE Standard is started. The detailed information of the run Annex G is encountered in Annex A of this thesis.

The output data of this calculation are maximum hotspot and maximum top oil temperature under the loading curve profile, and equivalent aging calculated. The algorithm verifies if one of these three outputs is overtaken the limited values imposed from the data came from the well established international standard. In case no constrain is found, a reduction of 1 MVA in the total size of the transformer is performed and the loop continues, otherwise, the algorithm stops and shows the latest calculation value of the power which is approved in these three criteria.

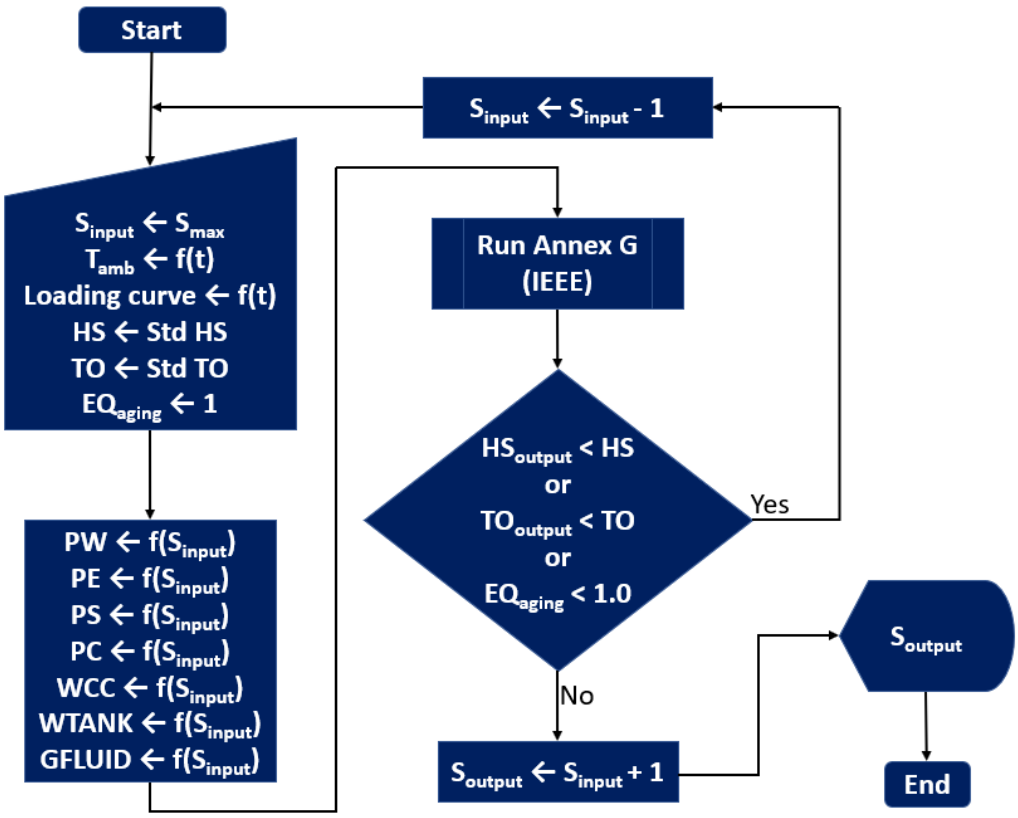

Figure 4.8 – Method workflow.

The ambient temperature T_{amb} is a time-dependent variable which is presented as an array of values. The maximum step considered is one hour, i.e., temperature measurements are hourly collected and inserted in the optimization algorithm. The loading curve in which the GSU transformer is submitted throughout an entire year is also a time-dependent function that represents one of the most important and sensible input information in the proposed model. In case no access to the entire year information, can be realized probability model as describle in the section 4.5 of this thesis.

In addition, the maximum hotspot and the maximum top oil temperature as per international standards (IEEE, 2011), *Std HS* and *Std TO* respectively, are needed in the optimization algorithm. Both variables, hotspot and top oil are considered long-time emergency loading instead normal cycle, since the total time with solar radiation during a day is not 24 hours neither few minutes.

Long-time emergency loadings permit the hotspot and top oil temperature exceed the normal cycle temperatures and may be applied to transformers carrying noncontinuous loads. In this research, the same temperature limit established in the IEEE guide is considered, i.e. 140 °C for hotspot and 110 °C for top oil temperature (IEEE, 2011). These temperature values are defined in accordance with the thermal limits of the mineral oil and thermo-upgraded insulation paper. In the case of the utilization of high-temperature class materials like aramid paper and/or ester fluid, these values can be increased and, consequently, the size of the transformer can be reduced even more.

Loss of insulation life must also be analyzed in order to be accepted as equal or more than 1.0 p.u. at equivalent aging, *EQ aging*, so this variable is a unitary value to be compared with the calculated equivalent aging facing the loading and temperature curve. If eventually one of these three variables do not exceed the maximum allowed, the calculation decreases the total size of this transformer in 1 MVA until converge to the optimum transformer size attending all restrictions.

4.2. REAL LOADING CURVE - EXAMPLE

The real loading curves and seasonal behavior of the ambient temperature are used to perform the analysis of loss of life. Therefore, a real case example is presented in figure 4.9, in which the hourly average temperature per day is described throughout a year.

	Average - Temperature [°C]												
h	Jan	Feb	Mar	Apr	May	Jun	Jul	Aug	Sep	Oct	Nov	Dec	Annual
0	13.39	13.85	13.52	12.00	10.06	8.88	7.66	8.82	9.01	9.95	10.85	12.07	10.82
1	12.71	13.16	12.94	11.32	9.30	7.96	6.67	7.71	8.02	8.96	10.04	11.32	9.99
2	12.03	12.48	12.37	10.64	8.54	7.06	5.69	6.63	7.08	7.97	9.23	10.58	9.17
3	11.35	11.80	11.80	9.96	7.79	6.18	4.70	5.57	6.16	6.98	8.42	9.83	8.36
4	10.66	11.12	11.23	9.28	7.02	5.33	3.76	4.57	5.27	6.04	7.61	9.15	7.57
5	10.10	10.43	10.66	8.60	6.26	4.53	2.83	3.69	4.44	5.22	6.80	8.51	6.82
6	10.75	10.14	10.08	7.92	5.52	3.76	2.18	2.97	3.86	6.29	8.80	10.07	6.84
7	12.30	12.17	11.89	9.45	6.48	3.81	2.14	3.98	6.89	8.75	10.96	11.89	8.37
8	14.07	13.93	13.61	11.59	8.97	6.75	5.66	6.96	9.85	11.43	13.15	13.76	10.79
9	15.78	15.66	15.30	13.68	11.55	9.89	9.15	10.32	12.71	13.97	15.17	15.57	13.21
10	17.34	17.23	16.81	15.59	13.89	12.84	12.36	13.41	15.32	16.22	16.94	17.17	15.41
11	18.65	18.57	18.07	17.17	15.89	15.32	15.10	16.00	17.46	18.08	18.36	18.47	17.25
12	19.71	19.63	19.05	18.38	17.42	17.21	17.22	17.99	19.08	19.50	19.42	19.48	18.67
13	20.46	20.39	19.72	19.15	18.39	18.40	18.62	19.28	20.13	20.43	20.12	20.16	19.60
14	20.86	20.81	20.06	19.49	18.81	18.91	19.26	19.90	20.59	20.87	20.43	20.49	20.03
15	20.97	20.91	20.07	19.37	18.59	18.66	19.05	19.83	20.41	20.80	20.36	20.49	19.95
16	20.66	20.57	19.58	18.62	17.54	17.42	17.71	18.71	19.33	19.96	19.70	20.02	19.15
17	19.90	19.76	18.64	17.31	15.86	15.34	15.46	16.71	17.47	18.47	18.50	19.07	17.70
18	18.76	18.56	17.39	16.35	15.01	14.39	14.39	15.50	15.59	16.57	16.92	17.77	16.42
19	17.52	17.74	16.72	15.57	14.16	13.44	13.31	14.29	14.45	15.41	15.88	16.79	15.43
20	16.63	16.91	16.04	14.80	13.31	12.49	12.24	13.08	13.30	14.26	14.85	15.81	14.46
21	15.74	16.09	15.37	14.03	12.46	11.54	11.17	11.86	12.19	13.10	13.81	14.83	13.50
22	14.88	15.26	14.69	13.25	11.61	10.59	10.10	10.65	11.07	11.95	12.77	13.85	12.54
23	14.01	14.44	14.01	12.48	10.76	9.64	9.03	9.44	9.96	10.79	11.73	12.87	11.58

Figure 4.9 – Annual average temperature.

Figure 4.9 represents the average temperature mapping in a year. In this specific case, higher temperatures are observed around 13 up to 15 hours, i.e., from 1:00 pm to 3:00 pm. The highest ambient temperature values throughout the year are verified in January/February and November/December. At the same time, during these same months, the highest generate levels are also observed, as described in figure 4.10.

The average temperature mapping and average load are related to a largely urban and industrial area in South America since the summer season is from December to March in the South hemisphere. Therefore, great power demand is required for residential/commercial air conditioning and many other cooling applications.

	Average - Load												
h	Jan	Feb	Mar	Apr	May	Jun	Jul	Aug	Sep	Oct	Nov	Dec	Annual
0	0.00000	0.00000	0.00000	0.00000	0.00000	0.00000	0.00000	0.00000	0.00000	0.00000	0.00000	0.00000	0.00000
1	0.00000	0.00000	0.00000	0.00000	0.00000	0.00000	0.00000	0.00000	0.00000	0.00000	0.00000	0.00000	0.00000
2	0.00000	0.00000	0.00000	0.00000	0.00000	0.00000	0.00000	0.00000	0.00000	0.00000	0.00000	0.00000	0.00000
3	0.00000	0.00000	0.00000	0.00000	0.00000	0.00000	0.00000	0.00000	0.00000	0.00000	0.00000	0.00000	0.00000
4	0.00000	0.00000	0.00000	0.00000	0.00000	0.00000	0.00000	0.00000	0.00000	0.00000	0.00000	0.00000	0.00000
5	0.00000	0.00000	0.00000	0.00000	0.00000	0.00000	0.00000	0.00000	0.00000	0.00000	0.00000	0.00000	0.00000
6	0.04320	0.00128	0.00000	0.00000	0.00000	0.00000	0.00000	0.00000	0.00011	0.06357	0.17788	0.14437	0.03606
7	0.56622	0.38394	0.25553	0.13740	0.03921	0.00074	0.00079	0.06273	0.33777	0.66302	0.77259	0.72366	0.32836
8	0.85470	0.80368	0.75843	0.67256	0.57210	0.43960	0.45061	0.62905	0.78625	0.89257	0.92994	0.89028	0.72283
9	0.93673	0.90655	0.87848	0.78989	0.69243	0.64748	0.66558	0.77556	0.87863	0.94621	0.97252	0.96354	0.83741
10	0.96434	0.93647	0.90481	0.81875	0.70951	0.68348	0.69645	0.79714	0.89035	0.95442	0.97861	0.98066	0.85913
11	0.95732	0.94619	0.90864	0.81845	0.71672	0.67459	0.69485	0.78907	0.88512	0.95248	0.96806	0.97365	0.85659
12	0.96022	0.94383	0.90553	0.81061	0.70947	0.66205	0.68671	0.77545	0.87561	0.94644	0.96000	0.97284	0.85022
13	0.95948	0.94246	0.90657	0.80350	0.70598	0.66427	0.68643	0.77404	0.87352	0.94324	0.96285	0.96677	0.84858
14	0.93665	0.93698	0.90026	0.79650	0.70577	0.66826	0.68971	0.77401	0.86920	0.93175	0.95171	0.95313	0.84229
15	0.92526	0.91725	0.88529	0.77295	0.67949	0.65578	0.67323	0.76337	0.85362	0.90516	0.93793	0.92506	0.82398
16	0.86955	0.87086	0.83096	0.70348	0.58211	0.54831	0.59720	0.68809	0.78220	0.82933	0.87132	0.86727	0.75272
17	0.74038	0.74810	0.64593	0.37144	0.16359	0.11383	0.20198	0.33402	0.45888	0.56118	0.69375	0.72394	0.47832
18	0.33407	0.27612	0.09201	0.00033	0.00000	0.00000	0.00000	0.00000	0.00091	0.03193	0.12843	0.25443	0.09235
19	0.00000	0.00000	0.00000	0.00000	0.00000	0.00000	0.00000	0.00000	0.00000	0.00000	0.00000	0.00000	0.00000
20	0.00000	0.00000	0.00000	0.00000	0.00000	0.00000	0.00000	0.00000	0.00000	0.00000	0.00000	0.00000	0.00000
21	0.00000	0.00000	0.00000	0.00000	0.00000	0.00000	0.00000	0.00000	0.00000	0.00000	0.00000	0.00000	0.00000
22	0.00000	0.00000	0.00000	0.00000	0.00000	0.00000	0.00000	0.00000	0.00000	0.00000	0.00000	0.00000	0.00000
23	0.00000	0.00000	0.00000	0.00000	0.00000	0.00000	0.00000	0.00000	0.00000	0.00000	0.00000	0.00000	0.00000

Figure 4.10 – Annual average load.

In figure 4.10, the maximum top generation of the solar power plant is 1.0 p.u., so then the maximum average of 0.98 p.u. occurs at 10:00 am in December, i.e. the intermittent behavior of photovoltaic power generation demands only a few hours per year for the nominal rated power of the GSU transformer.

Running the loading curve with the data from the figure 4.9 and 4.10 according *bottom-oil model*, the curve in figure 4.11 is obtained. The blue curve represents the average loading in which the maximum loading is no more than 0.9 p.u.; the gray curve is the dynamic profile of the hotspot temperature inside the winding, with a maximum temperature of 80 °C approximately.

Top oil and bottom oil are represented by yellow and green curves respectively and the orange bars mean the ambient temperature. The figure 4.11 is the annual average temperature and loading, considering that 1.0 p.u. is 100 MVA, the output data is:

- Maximum hotspot temperature of 79.84 °C at 15 hours and 00 minutes;
- Maximum top fluid temperature of 64.35 °C at 15 hours and 21 minutes;
- Equivalent aging: 0.178805 p.u. for 10 minutes and 44 seconds a day.

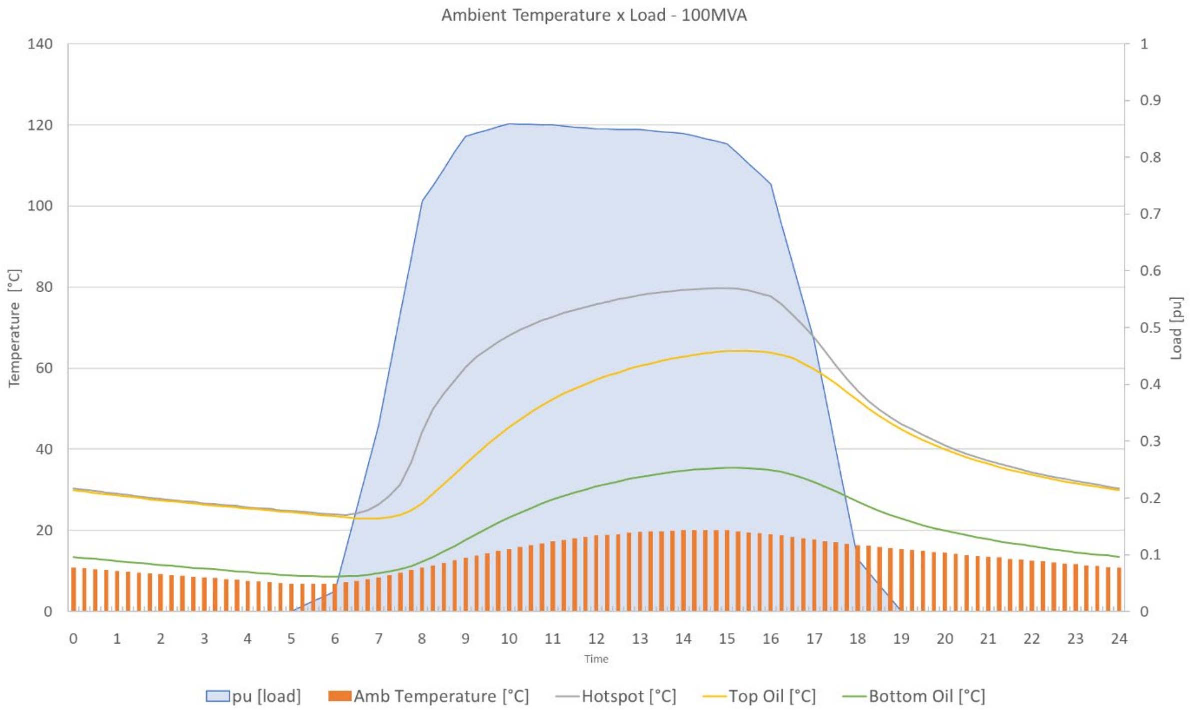

Figure 4.11 – Annual average loading and temperatures for a 100-MVA transformer.

A transformer with thermally upgraded paper can operate for the entire life with 110 °C in the hotspot (IEEE, 2011 and IEC, 2018), it means that, if the transformer faces a constant loading and a constant temperature, the equivalent aging factor is unitary value, i.e., after 150,000 h the DP of the paper will reach the end-of-life criteria. In case of the aging factor is bigger than 1.0 p.u., which means that the transformer has been accelerated aging and vice-versa.

Modern generator step-up transformer utilizes an on-load tap changer, OLTC, on the high voltage side, and none regulation on low voltage side. As the high short-circuit power appears on the high voltage side, so depending on the voltage level of the high voltage system, the regulation relay will fetch the correct position of the OLTC. Based on that, these transformers can operate with maximum induction on the linear region of the saturation curve differently from the old transformer designs that do not have installed automatic voltage regulation and for that needs to be designed with some clearance on the saturation.

In order to check the model used in this approach was run a flat loading curve with a flat temperature curve to verify if the calculation of the aging factor is correct. Figure 4.12 shows the line of loading at 1.0 p.u. and the hotspot with temperature of 110 °C. The aging factor of this curve in figure 4.12 is 1.0 p.u.

The real loading curve and ambient temperature are input data which have to be insert in the workflow method presented in figure 4.8. Figure 4.13 shows the calculated values of the hotspot absolute temperature, top oil absolute temperature and equivalent aging in hours.

In figure 4.14, the maximum hotspot, top oil temperatures and equivalent aging as per standards are the dashed lines gray, yellow and green respectively. The minimum transformer size for the top oil temperature point of view is 63 MVA, for hotspot temperature is 64 MVA and 68 MVA for the minimum equivalent aging. In this context, the minimum allowable transformer size is 68 MVA.

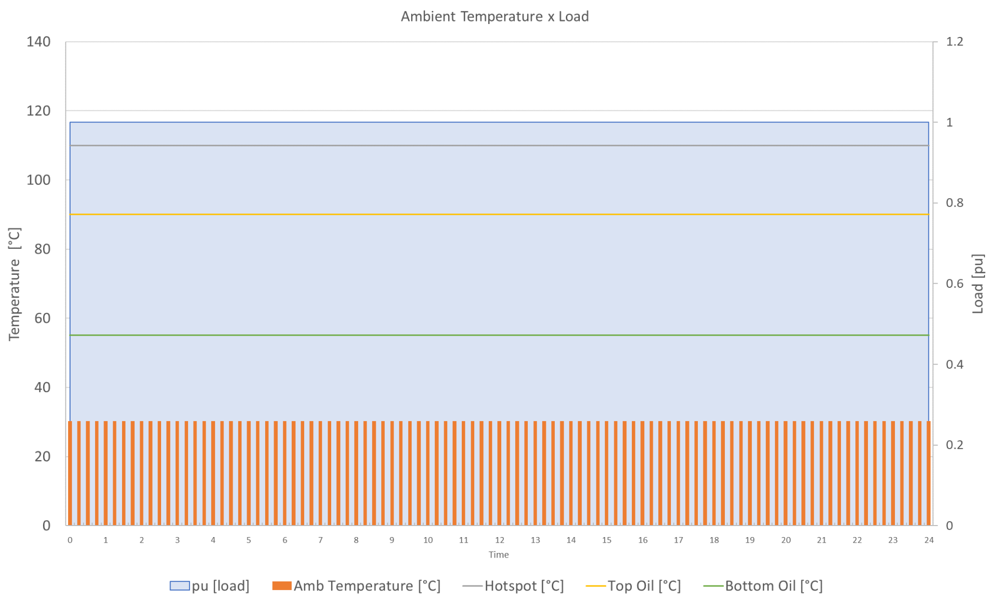

Figure 4.12 – Flat loading and temperature curve for 100 MVA transformer.

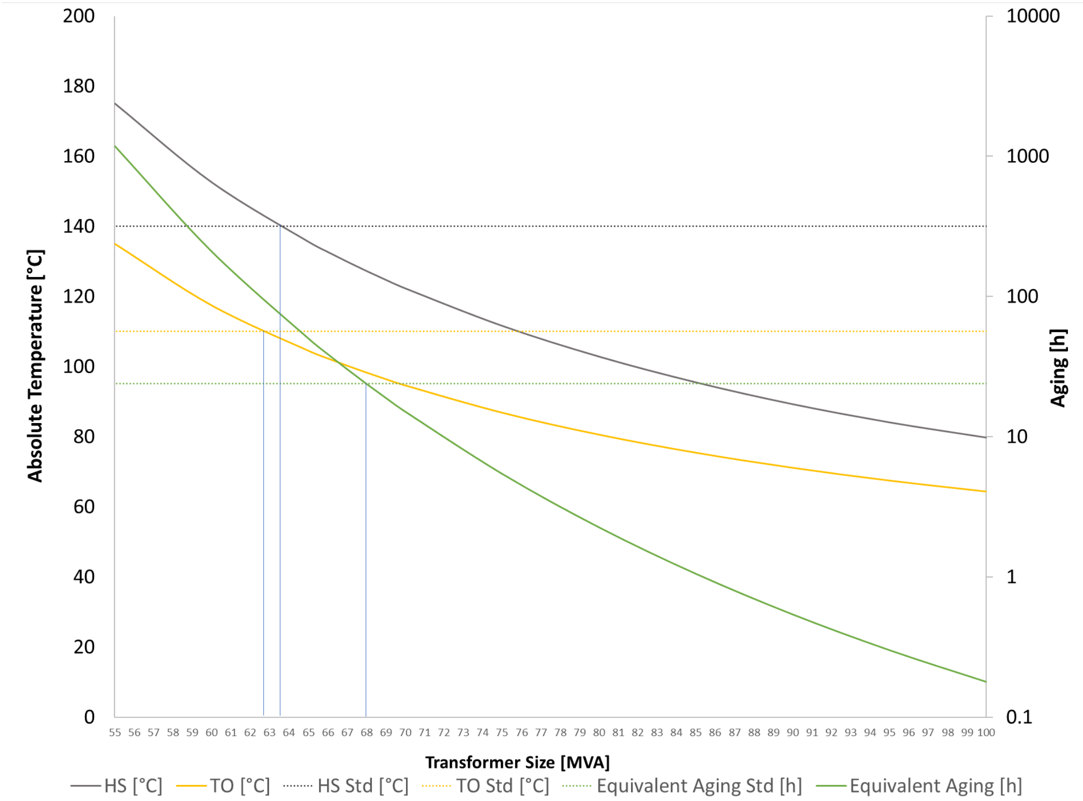

Figure 4.13 – Absolute temperature of hotspot and top oil, equivalent aging limits.

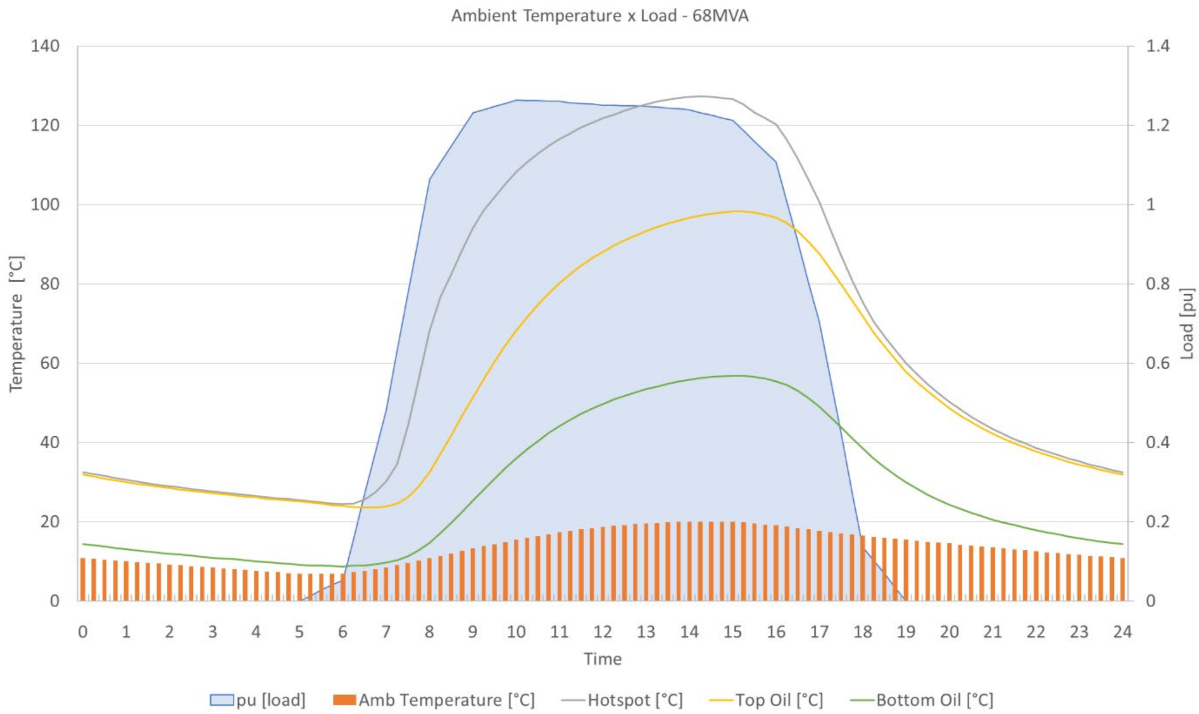

Figure 4.14 –Annual average loading and temperatures for a 68 MVA transformer.

The same loading curve and temperature profile are applied for a 68-MVA transformer in order to verify the maximum temperature of the hotspot and top oil:

- Maximum hotspot temperature of 127.30 °C at 14 hours and 09 minutes;
- Maximum top fluid temperature of 98.28 °C at 15 hours and 09 minutes;
- Equivalent aging of 0.99439 p.u. for 23 hours and 52 minutes a day.

Thereafter, determining the minimum and technically viable size of the power transformer, the formulation of the loss's capitalization is applied to determine the minimum TOC. In this sense, 68 MVA represents the lowest size for the GSU transformer, so then this value should be verified if meet with the minimum TOC as well.

4.3. TEMPERATURE CORRECTION

This method also corrects the effect of the losses on the equipment lifetime based on the temperature levels in which it is exposed. Thus, during colder months, losses are lower than other months compare with the same load. In the cold days, when the transformer starts the operation at the beginning of the morning, the ambient temperature is low and due to the thermal inertia of the whole equipment, sometimes the transformer does not reach the higher temperature because there is no enough time to stabilize the oil temperature, consequently, the load losses are less.

The figure 4.15 shows the temperature diagram inside the transformer, where it is possible to observe the cooling media flow path inside the equipment. Point 1 and 1` is the lowest temperature found in the equipment, also known as Bottom Oil. As the heat-generating sources are the windings and the core, the oil flows through two elements, and the temperature increases progressively from the bottom to highest parts of the tank, as described in figure 4.15.

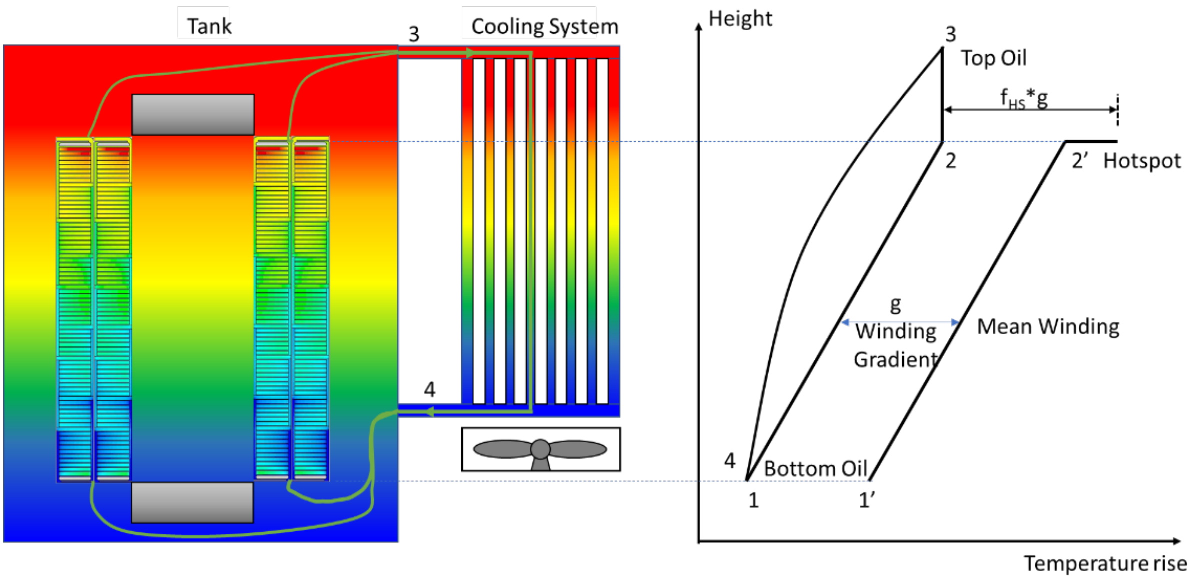

Figure 4.15 - Temperature map *versus* tank height.

Inside the winding is the highest temperature found in the transformer, representing the most critical aging agent in power transformers. The temperature at the hottest region is not linear and it is governed by a hotspot factor that is calculated by the ratio between the maximum and average losses in the conductors. On the top of the winding, due to the leakage flux generated from the windings, a stray flux impinging in the upper and lower turns and it generates concentrated losses on this region. On the bottom turns, this effect os not important because it is surrounding by colder oil, but on the top turns a combination of these two factors must be considered.

The number 3 in figure 4.15 indicates the top oil temperature that represents the maximum temperature in the tank and at this temperature the inlet oil on the cooling system. On the other hand, point 4 is the lowest temperature that returns to the tank after cooling down in the cooling system.

The winding gradient is defined as the difference between the average temperature around the winding and the average temperature of the tank. (CIGRE, 2016). The calculation of the average winding temperature is necessary because it is the real temperature in which the winding is facing. This parameter is one of the most important data during the transformer acceptance test because it is directly related with the load losses and efficiency of the equipment.

In order to clarify, the way that the mean winding temperature is measure on the test laboratories is not simple because this measure must be done thought indirect measure. During the short-circuit test, circulate the nominal current in the windings until stabilizing the oil. Thereafter, the transformer must be completely shut down and disconnected from the source to be possible to measure the at hot resistance. This resistance must start to measure a few moments after shut down in order to get a curve of resistance versus time and through the extrapolation of this curve to the time equal zero, it is possible to know which is the average winding temperature when nominal current is flowing.

The mean winding absolute temperature MO_{abs} is another important index to determine other parameters, as the top oil TO, bottom oil BO, hotspot temperature HS, hotspot factor f_{HS}, and the ambient temperature. Equation (4.8) calculates the temperature which the winding is subjected.

$$\mathrm{MO}_{abs} = \frac{(TO-BO)}{2} + \frac{(HS-TO)}{f_{HS}} + T_{amb} \tag{4.8}$$

Figure 4.16 shows the temperatures inside the transformer, and the dotted curve represents the average temperature at the windings.

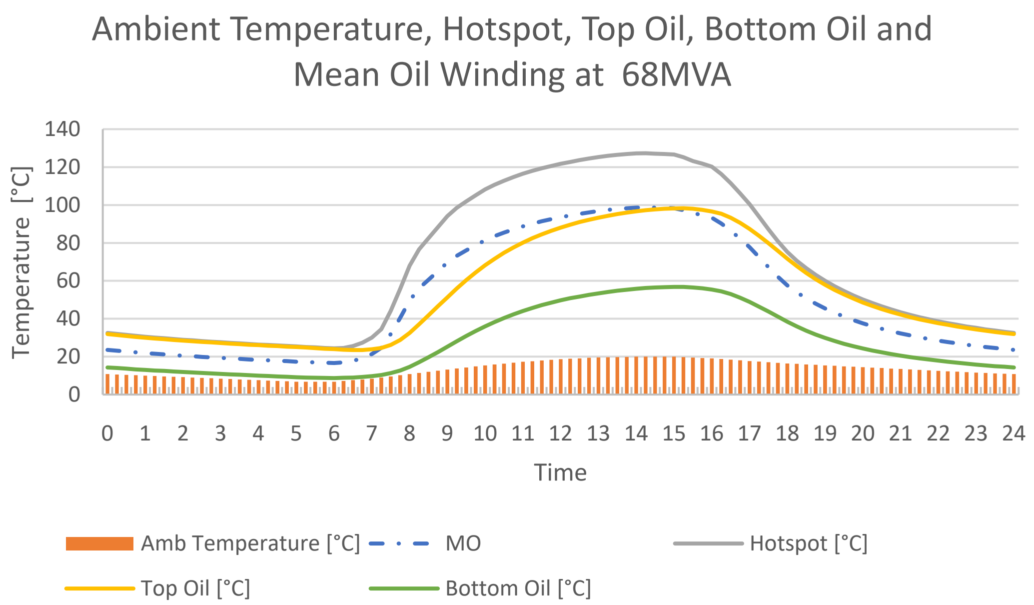

Figure 4.16 – Ambient temperature and temperatures into the 68-MVA transformer.

In this figure, it is possible to observe that the thermal inertia of the winding, represented by MO, is higher than thermal inertia of the 68-MVA transformer as a whole, represented by TO. In this sense, the thermal stability will never be achieved in a power transformer with the loading profile of a solar plant.

It is well known that smaller power transformers, operating in overloaded conditions, results in higher temperatures on the windings and insulation, therefore a temperature correction procedure is necessary in order to avoid any mistake during design process. For temperature corrections in the windings, it is necessary to distinguish the types of associated losses are being considered. For ohmic losses PW and winding eddy PE, the correction factor is directly proportional to the temperature, as expressed in (4.9). (IEC 60076-1, 2011).

$$f_{PW} = f_{PE} = \frac{(234.5+T_{\theta})}{(234.5+T_{ref})} \tag{4.9}$$

The f_{PW} and f_{PE} are the correction temperature factor to ohmic losses and eddy losses respectively. Tref is the reference temperature defined in the standard which is normally 75°C to non-thermally upgraded paper and 85°C to thermally upgraded paper and, T_θ is the temperature which the material is submitted.

For stray losses PS occurs the opposite phenomenon, i.e., it means that as higher the temperature is, lower the stray losses because of the greater conductivity in metallic parts, as demonstrated in (4.10). (IEC 60076-1, 2011). The f_{PS} is the correction temperature factor to stray losses.

$$f_{PS} = \frac{(234.5+T_{ref})}{(234.5+T_{\theta})} \tag{4.10}$$

This way, the load losses *LL* are calculated as a function of the dynamic temperatures of the power transformer, as expressed in (4.11).

$$LL = f_{PW}PW + f_{PE}PE + f_{S}P \tag{4.11}$$

The load loss has a direct influence on the temperature which the winding is inserted. Considering a 100 MVA transformer and apply (4.1), (4.2) and (4.3) at 75°C the ohmic losses are 264.274 kW, the winding eddy losses are 33.630 kW and the stray losses are 39.206 kW, in case, the reference temperature change to 45°C, the ohmic losses become 238.658 kW, the winding eddy losses become 30.370 kW and the stray losses become 43.414 kW, resuming the load losses at 75°C is 397.11 kW while the load losses at 45°C is 372.442 kW, 7.8 % lower, i.e., this shows the importance to correct the losses through the real temperature during loading cycle and ambient temperature.

The load factor is one of the most important information needed during the transformer procurement. There are two concepts of load factor presented in the literature, where the load factor can be defined by the average loading or the average overtime of the root mean square RMS values of the instantaneous load (SZWANDER, 1945; IEEE, 1991). In addition, it is proposed a novel approach for correction of the RMS loading based on the real temperature inside of the power transformer winding taken into account the temperature correction factor.

The mean winding temperature is usually specified as a rise temperature, however, the real load losses are calculated at absolute temperature, so the ambient temperature has a direct influence on the load losses of the transformer. There are two standards values indicative of the "*mean winding temperature*": 55 °C rise when non-thermally upgraded paper and, 65 °C rise when the thermally upgraded paper is used. In the IEEE standard the ambient temperature is fixed at 20 °C, so, in order to compare the load losses at the same base, the procurement engineer must define the temperature reference. In the industry, there are two temperature references used, 75 °C or 85 °C and, the load loss values are warranted at a reference load and temperature.

This work proposes a correction of the load losses at a real temperature instead of a fixed temperature and it is discussed below.

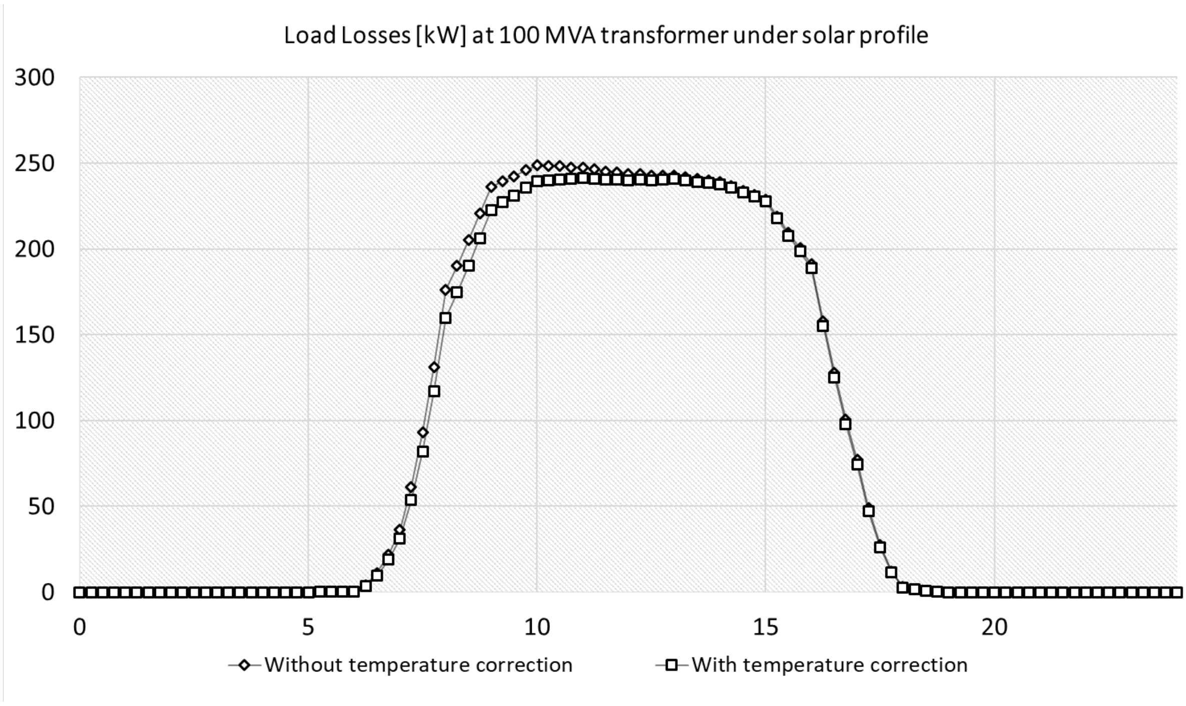

Figure 4.17 – Comparison of load losses with and without temperature correction.

Figure 4.17 shows a simulation with 85°C as losses reference called “without temperature correction” and the other curve is the real temperature profile, which is denoted as “with temperature correction”. Basically, it is possible to observe that the losses are highly dependent of the temperature, the optimum transformer size can by determined by comparing these two results. As previously introduced, the losses vary with the load profile during a determined time period, and the load factor L_f can be represent as two different approaches:

- Average loading;
- Average overtime of the root mean square RMS values of the instantaneous load.

This thesis proposes the third approach method which is recalculate the load losses and consider this value to optimize the equipment and recalculate the TOC.

- Average overtime of the root mean square RMS values of the instantaneous load considering instantaneous temperature correction.

The average loading is described as the arithmetical average of the load along the entire year. For non-intermittent load applications, this approach has a very good performance, as well established in the technical literature, so the load factor L_f is calculated by (4.12).

$$L_f = \frac{1}{h}\int_0^h f_{load}(t)\,dt \tag{4.12}$$

The time function f_{load} is represented in figure 4.17, in which the load loss factor is calculated from a definite integral throughout a year (total period), where h is the number of hours in one year. The figure represents the per unit load of a real profile studied in these. The data inserted in this figure was collected during an entire year considering the solar radiation of the 8760 hours of the year, with step of one minute, so the total number of points in this graphic is 525600.

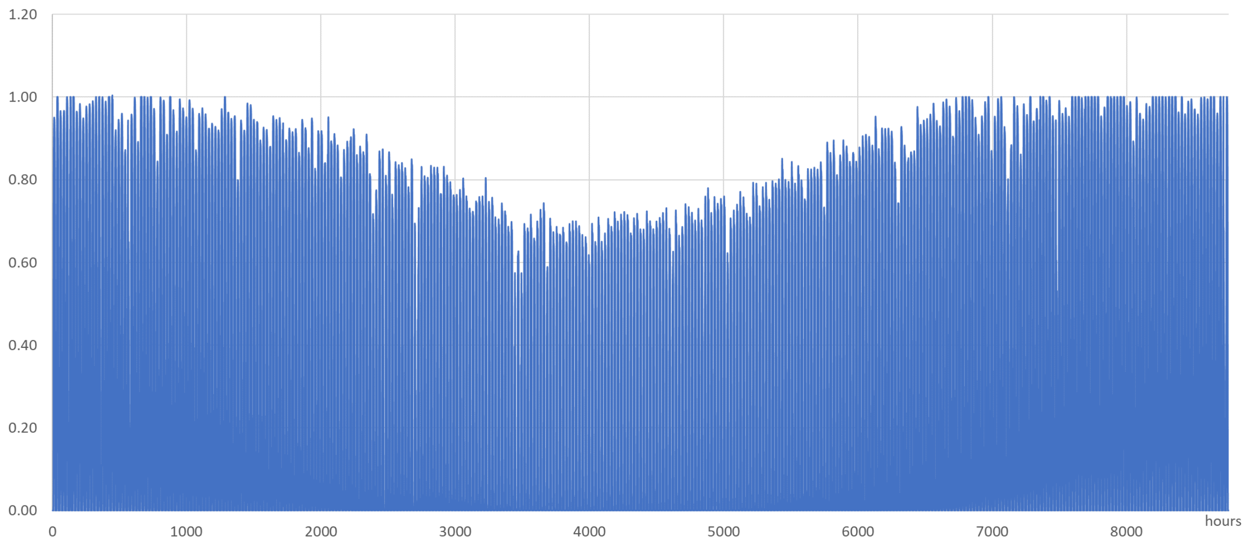

Figure 4.18 – Per unit solar radiation along the year.

Average RMS overtime represents a more suitable method for intermittent energy sources. The load loss factor L_f is given in (4.13) as follows. (KENNEY, 1962)

$$L_f = \sqrt{\frac{1}{h}\int_0^h f_{load}(t)^2\,dt} \tag{4.13}$$

Finally, the conventional expression of the loading function in (4.13) is reformulated taken into account the temperature correction f_{temp}, such as described in (4.14).

$$L_f = \sqrt{\frac{1}{h}\int_0^h f_{temp}(t)^2\,dt} \tag{4.14}$$

Figure 4.18 shows the load factor calculated by using the three different methods. For a 100-MVA GSU transformer, the average loading based on the solar energy profile in figure 4.17 is around 58.9%, in which the conventional RMS overtime is 50.4% and 51.2% when RMS with temperature corrections.

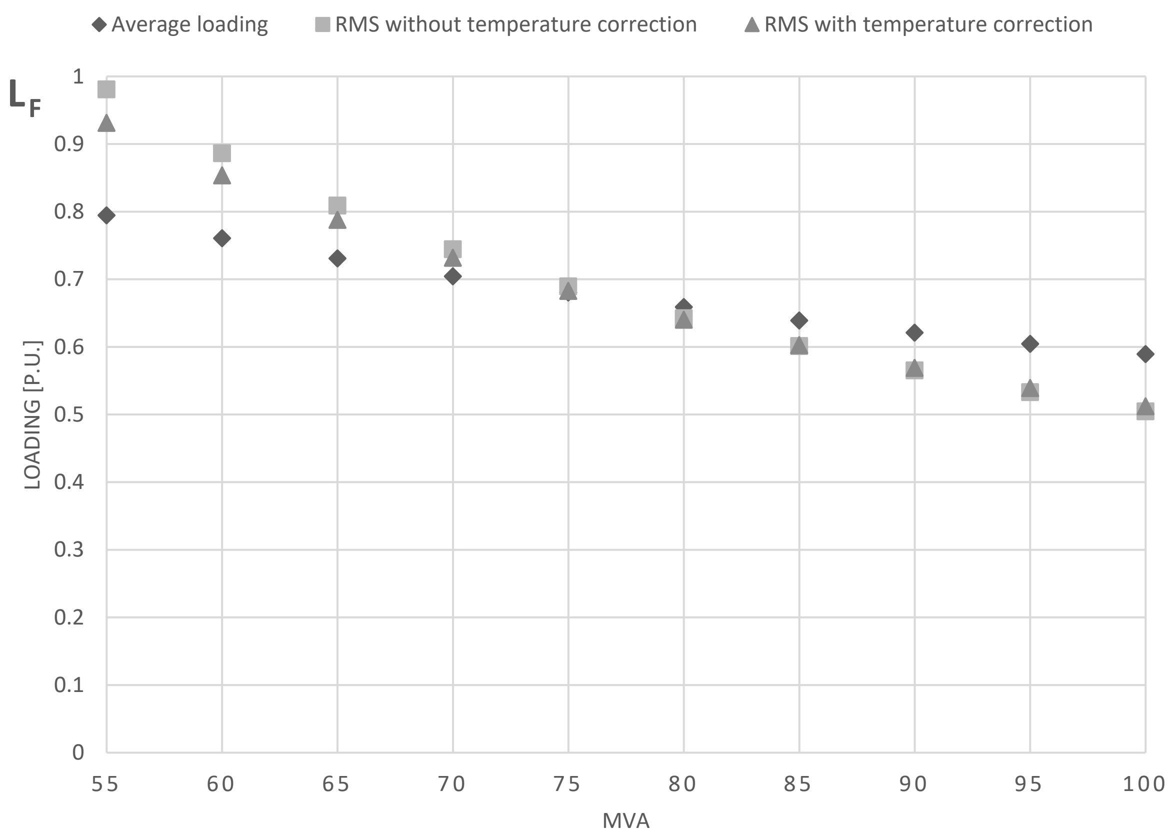

Figure 4.19 – Load loss factor *versus* transformer size.

On the other hand, power transformers with almost half size, 55 MVA, the average load factor is no more than 80%, while for RMS load factor without temperature correction this value is 98% and RMS load factor with temperature correction is 93.1%. For solar application, transformer almost does not operate near of the temperature referred on technical standard, i.e., around 85°C, due to the large load variation, so, when the temperature is corrected through this method proposed a bigger gap appears when light equipment is compared, it is because, as smaller the equipment, higher temperature of operation and consequently the correction of the temperature get more evident.

The method which utilizes average load has been presented a good approach, however, when the load variation increases, this method shows a not real composition of load losses, an example if a 100 MVA transformer is substitute for 80 MVA transformer, the equivalent increase of loading is 25% higher but, it can be applied only for constant loading or with small variations if some error are acceptable, for that reason for intermittent loading the RMS load factor approach capture the real load.

In order to simulate the real case and calculate the TOC to compare the both RMS load approach with and without temperature correction, some values were inserted in the model to perform a sensibility test. The average energy price of the first year in operation is 0.02033 USD/kWh which was taken of the closed price of the last auction of solar power plant in Brazilian regulation marketing according presented in the figure (1.10). The average annual increase in energy cost is 1.52% per year according to a weighted index of the energy price provided by the World Bank (STATISTA, 2020). Figure 4.20 shows the price of the worldwide energy indexed.

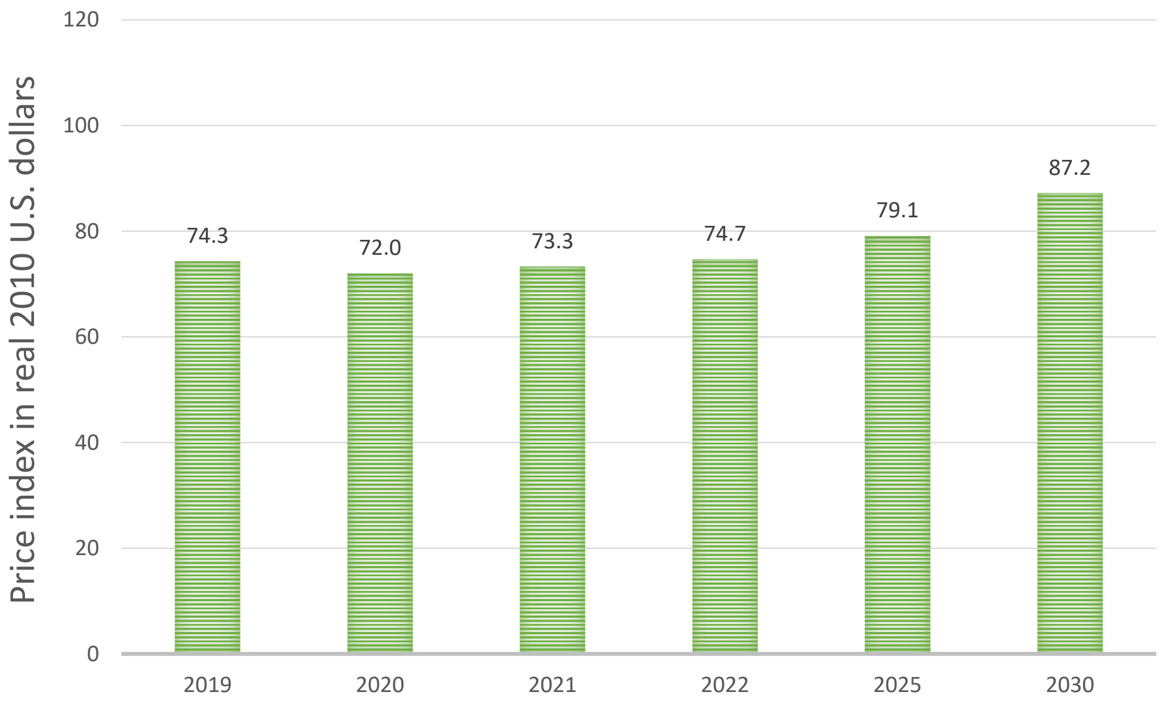

Figure 4.20 – Price index of energy worldwide from 2019 to 2030 in U.S. dollars, price index in 2010.

Source: Adapted from Statista, 2020

From 2020 to 2030, the average increment is from 72.0 to 87.2, so, the annual average increase estimate price is 1.52% per year in the next 10 years. Another important data that the investor must inform is the weighted average cost of capital, WACC, that has been discussed before. The estimated WACC of the energy transmission companies is 6.6% per year (LAM,1998) and this value is used in this example.

The investor must have as input data the cost of the transformer installed and commissioned in the substation, i.e., it is the final price given from the manufactured. The transformer equipment has a big correlation with commodities prices due to the big amount of material used in the manufacture. For that reason, a good way to obtain the initial price of the investment, IP, to have a knowledge of the prices of the main transformer elements needed. A good approximation way to get the initial investment cost of the transformer is given by (4.15),

$$\text{IPrice} = f_{price}(m_{copper}w_{copper} + m_{iron}w_{iron} + m_{oil}w_{oil}) \quad (4.15)$$

The m_{copper} is the total mass of the copper and w_{copper} is the price of the copper given in kg/USD; m_{iron} is the total mass of the iron electric steel and w_{iron} is the price of the iron given in kg/USD and; m_{oil} is the total mass of the oil and w_{oil} is the price of the cooper given in kg/USD. Morover, only these three cost drives do not give the total cost of the equipment, for that reason, a factor price, f_{price}, is insert in this model to consider all others elements costs like: engineering costs, manufacture costs, others materials, taxes, transportation, installation, commissioning and the profit of the manufacture. As this value will never be encountered in the literature because it is part of the business strategy, in order to obtain a final price of the equipment, a factor price chosen is 2.8, i.e., the estimate value of the price of the equipment is three times the values of the sum of copper, iron and oil.

These materials have their price vary daily according to the commodities price, so this example was chosen 8.00 USD per kilogram of the copper, w_{copper}, 2.00 USD per kilogram of the core steel, w_{iron}, and 1.00 USD per kilogram of the mineral oil, w_{oil}. Summarizing, the input data used in this test are:

- ❖ Average energy price of the first year in operation 0.02033 USD/kWh;
- ❖ Average annual increase in energy cost rated of 1.52%;
- ❖ Number of years before the invested amount shall be paid back: 17.12 years which is equivalent at 150.000h;

- Weight average cost of capital of 6.6%;
- Copper cost: 8.0 USD/kg;
- Iron cost: 2.0 USD/kg (electrical steel core material);
- Oil cost, : 1.0 USD/kg;
- Factor price, f_{price} = 2.8.

The total cost of ownership is calculated according to equation (2.8). The table below shows the TOC calculated, in kUSD, by using the three methods introduced previously in this section.

Table 4.1 – Initial Cost and TOC *versus* transformer size using RMS approaches with and without temperature correction.

Power [MVA]	**100**	**95**	**90**	**85**	**80**	**75**	**70**	**65**	**60**	**55**
Initial Cost [kUSD]	444	429	413	396	379	361	343	324	304	284
TOC [kUSD] - RMS	751	744	738	734	**733**	737	745	762	791	837
TOC [kUSD] - RMS - with temperature correction	757	748	741	735	732	**731**	735	745	763	792

Table 4.1 shows that there is a different optimum point when temperature correction is considered. The first row shows the initial cost calculated through (4.15) and as smaller as the transformer, lower the initial prices. This statement makes sense once no financial input is inserted to calculate the initial cost, on the other hand, when TOC is calculated is it possible to observe that, there is a minimum optimum transformer size. The green color means the lower TOC prices and red color shows the higher TOC. For RMS approach without temperature correction, the second row, the optimum point is a transformer with 80 MVA rated power and TOC equals 733 kUSD, and when the temperature correction is considered a 75 MVA transformer is encountered with 731 kUSD. As previously analyzed, the minimum allowable transformer size is 68 MVA due to the technical limitations of aging, top oil, and hotspot temperature. If the procurement engineer only is taken into consideration the technical

limitation, probably the 68 MVA transformer will be chosen because will be the most economical transformer. For that reason, it is very important to understand the full concept of the TOC in order to reanalyze, and, according to this example, the optimum transformer is 75 MVA when all criteria are checked.

In terms of energetic efficiency, figure 4.20 shows the efficiency index comparing these two different approaches and the peak efficiency index, PEI, which is obtained when the no-load losses are equal to the load losses presented in (2.7).

A more realistic data of the efficiency index is presenting in the figure (4.20) when the calculation considered a specific loading of the transformer, in this case it is the real load loss factor calculated for each approach, i.e., for 75 MVA transformer the RMS without temperature correction is: 68.96% and with temperature correction is 68.30%.

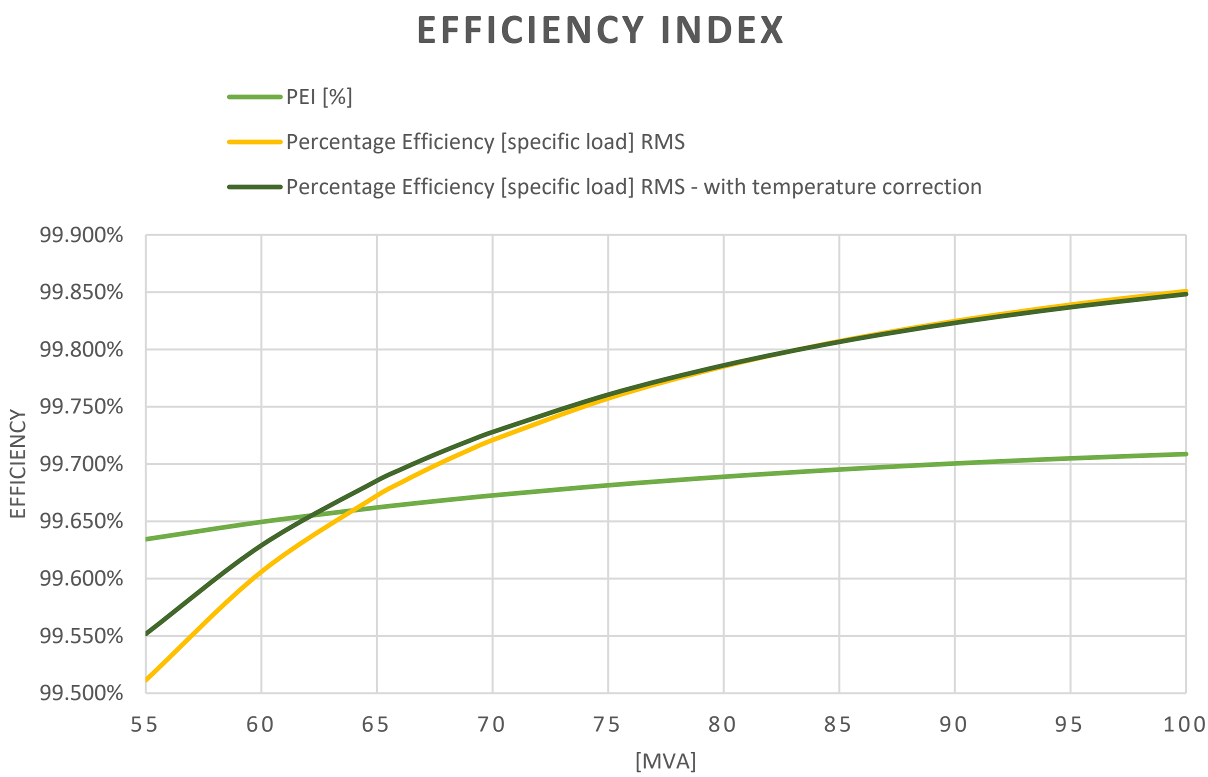

Figure 4.20 – Efficiency index of specific load and PEI.

In this example, for RMS with temperature correction higher index compared with PEI is seen when the transformer is chosen is bigger than 63 MVA. The PEI has a lower index because this index is calculating when the no-load losses are equal to the load losses per definition, i.e., in power transformer units it usually occurs at low load which makes this transformer with high efficiency at low loads. The proposed method also increases the transformer efficiency at the specific load which this equipment will operate along the entire year, became more compact and efficient.

According to the example exposed in this thesis, it is possible to reduce the total rated power in 25%, from 100 MVA to 75 MVA when the new approach is applied. The no-load losses will be reduced from 63.3 kW to 52.9 kW as presents in table 4.2. This means low energy consumption for the entire life of the transformer.

Table 4.2: Mass and losses comparison

Power [MVA]	Core [kg]	No-load losses [kW]	Cooper [kg]	Load losses at 100 MVA [kW]
65	75%	48.3	72%	595.0
70	78%	50.6	76%	533.0
75	82%	52.9	81%	483.1
80	82%	55.0	85%	442.4
85	90%	57.2	89%	408.8
90	93%	59.3	93%	380.7
95	97%	61.3	97%	357.1
100	100%	63.3	100%	337.1

At the same base rated, the load losses are bigger because the quantity of cooper material is approximately 19% lower, on the other hand, a transformer with 75 MVA will operate less than 20% at overload condition. Comparing the no-load loss, from 100 MVA to 75 MVA the no-load losses came from 63.3kW to 52.9kW, a reduction of 19.6% of this loss component that is presented for the entire life of this transformer.

4.4. Real loading curve with Reactive Dispatch - example

The share of photovoltaic farms is increasing in the energy mix as power systems move away from conventional carbon-emitting sources. Photovoltaic farms are equipped with an expensive power converter, which is, most of the time, used well below its rated capacity (LOURENÇO et al., 2018). Currently some photovoltaic plant is eligible for receiving payment on the active power losses due to reactive power generation, which either reduces its active power output or requires power to be drawn from the grid. (HAGHIGHAT, 2010).

The same approach presented in subchapter 4.3 is now presenting considering reactive dispatch. The quantity of the reactive dispatch has obtain from the literature (LOURENÇO et al., 2018). Figure 4.21 represents the quantity of reactive dispatch of photovoltaic plant which provides nearly a full reactive dispatched all the time during night-time and early morning.

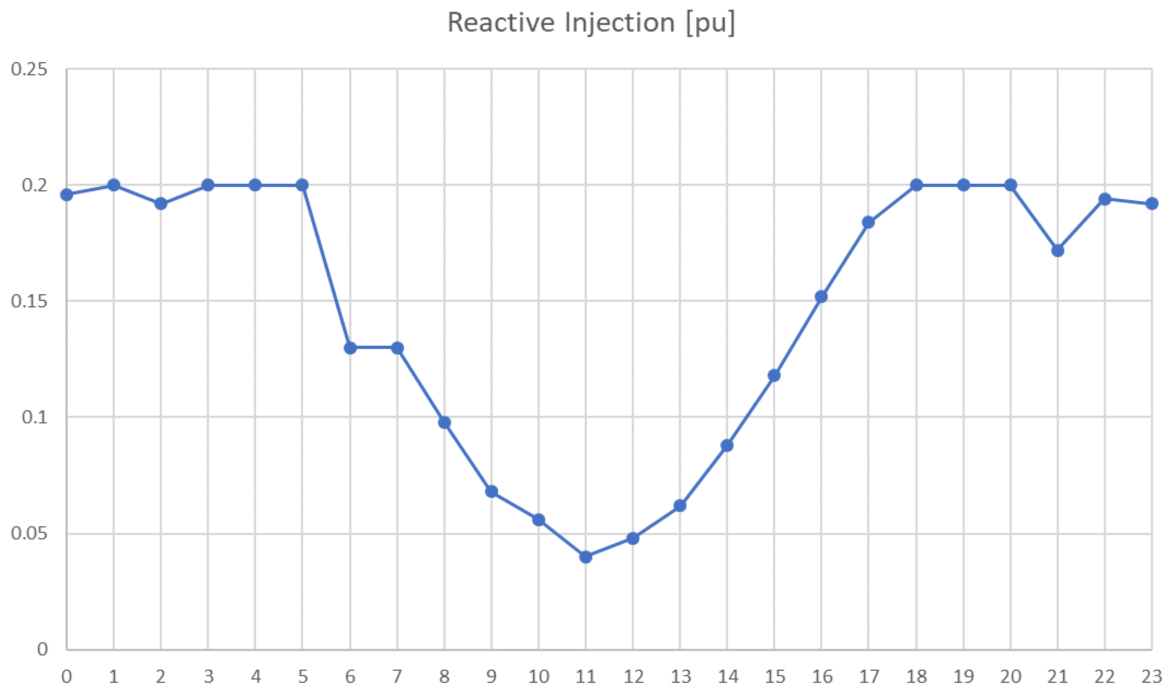

Figure 4.21 – Example of a reactive injection on the grid in a solar power plant.

Considering the dispatch of reactive power in a photovoltaic power plant it is observed that there is an increase in the load of transformer that will operate in the substation. Figure 4.22 shows the average load curve of the loading of the transformer and the figure 4.21 above is added to the quantity of load of the transformer.

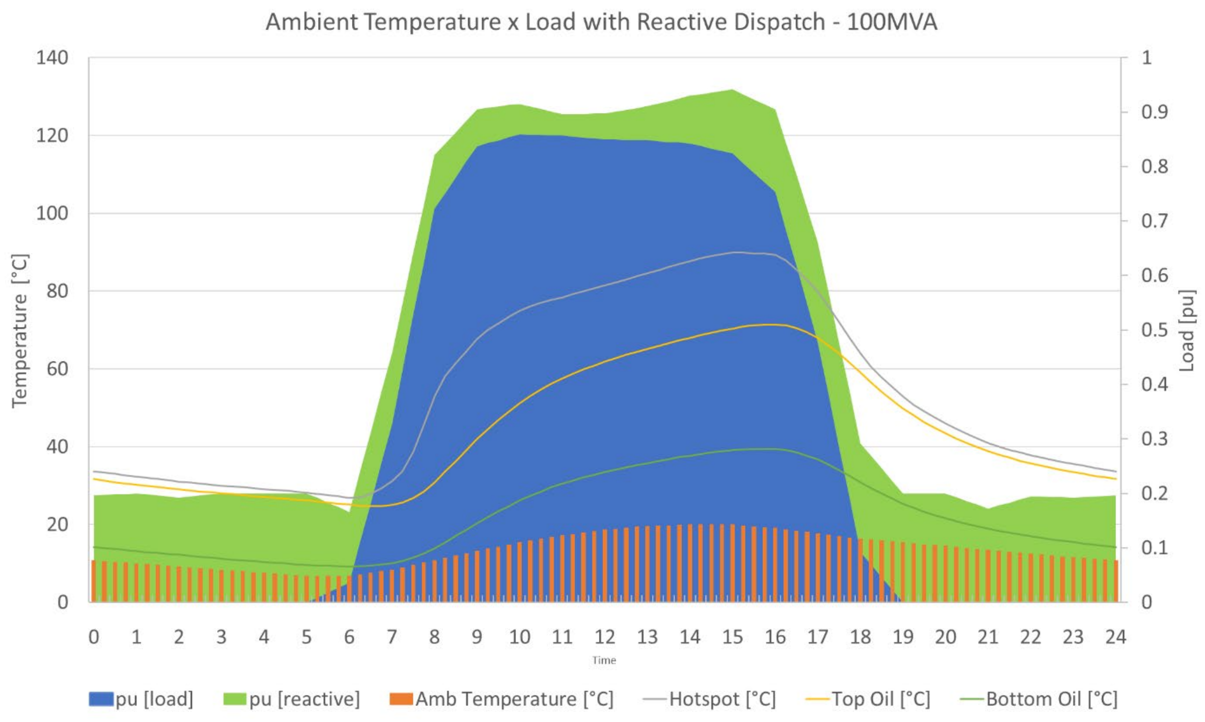

Figure 4.22 – Annual average loading and temperatures for a 100-MVA transformer and the average reactive power dispatch.

Redoing the same calculations already presented in the previous sessions 4.2 and 4.3 in which the TOC and temperature correction are calculated with the same assumptions used previously, we obtain:

Table 4.3 – Initial Cost and TOC *versus* transformer size using RMS approaches with and without temperature correction adding the reactive dispatch.

Power [MVA]	**100**	**95**	**90**	**85**	**80**	**75**	**70**	**65**	**60**	**55**
Initial Cost [kUSD]	444	429	413	396	379	361	343	324	304	284
TOC [kUSD] - RMS	812	809	**808**	810	817	830	851	883	933	1008
TOC [kUSD] - RMS - with temperature correction	817	812	809	**808**	811	818	831	851	883	930

According to the same methodology approach, in the case of the same equipment for the reactive injection, it is necessary to acquire an equipment with at least 85MVA of power in order to obtain that all the criteria are satisfied. Such analysis is of paramount importance for the purchaser of the equipment, since if the equipment is dimensioned or does not consider the use of reactive, the useful life of the equipment can be reduced considerably.

4.5. PROBABILISTIC ASSESSMENT ON SOLAR RADIATION & TRANSFORMER AGING

Procurements generally select the size and overload the transformer, following the international standards. This model provides the deterministic calculation of transformer loss-of-life at given elevated hotspot temperature. With this approach, the exact mean ambient temperature and, the transformer hotspot temperature values are assumed known (SEN et la, 2011).

As the solar radiation is radiant energy emitted by the sun from a nuclear fusion reaction that creates electromagnetic energy (CODDINGTON et al., 2016) and the balance of incident solar radiation that is absorbed or reflected by Earth's surface and atmospheric components, such as clouds and gases, with the radiation that the earth–atmosphere system emits to space defines Earth's radiation budget (Loeb et al., 2009).

The radiation that impinging in the solar panel will be not constant along the entire life, and it can cause a large variation along the year due to many reasons like: season of the year, longitude, latitude, altitude, weather and other. However, in the real practical application, because of the number of variables appointed, the exact amount of overloading is extremely difficult to set.

Some statistical approaches, like Monte-Carlo, to evaluate these parameters are using in the literature (SEN et al., 2011). This approach can provide a more flexibility and better results. To perform an analysis using solar irradiance values from a typical day, a set comprising 2000 synthetic series was used in this thesis. The synthetic series were generated using a methodology that is under development by colleagues from the electrical engineering department at the University of Sao Paulo. This method, that is yet to be published, relies on k-means clustering to model the deterministic component of the solar irradiation and a kernel density distribution for modeling its stochastic component. The synthetic series generated for this analysis correspond to the solar irradiance from a Northeastern region city in Brazil.

Figure 4.23 below represent the boxplot of this data series generate by k-means clustering.

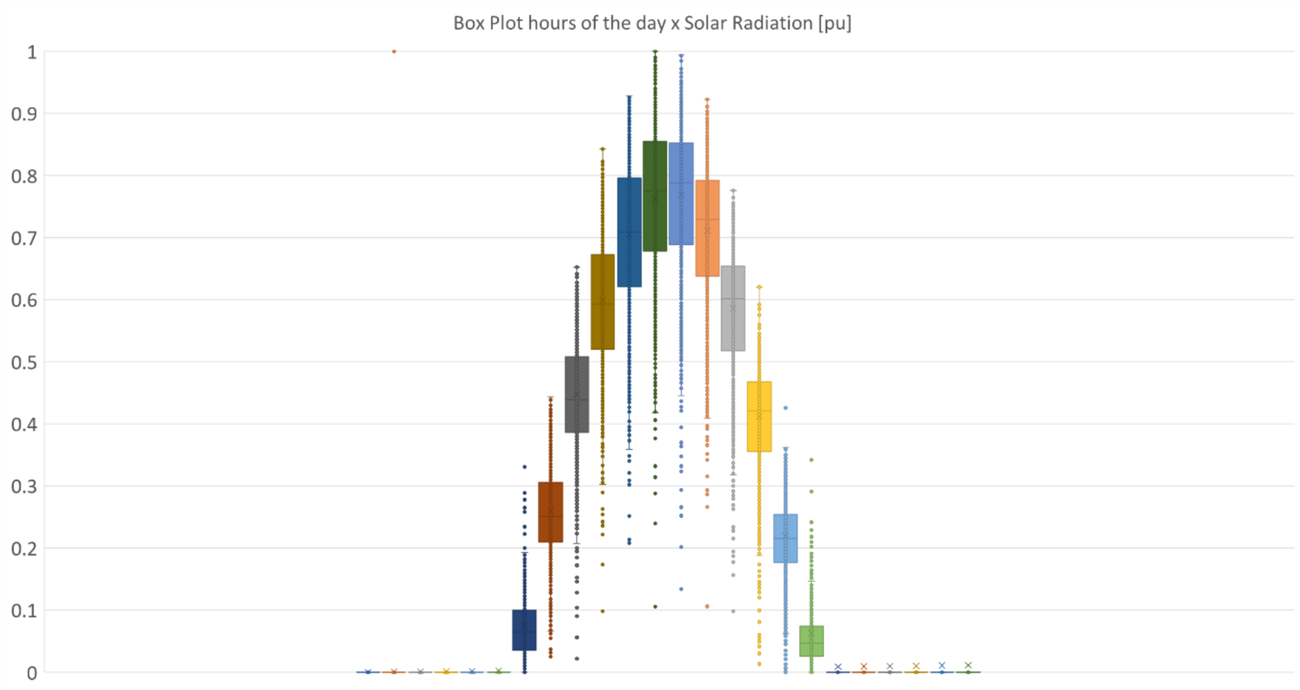

Figure 4.23 – Box plot per hour of the day *versus* solar radiation in per unit

Table 4.4: Statistical data of the generated curves

Hour of the day	0 to 5	6	7	8	9	10	11	12	13	14	15	16	17	18 to 23
Sample Size	2000	2000	2000	2000	2000	2000	2000	2000	2000	2000	2000	2000	2000	2000
Position Measures														
Average	0.000	0.072	0.257	0.444	0.595	0.701	0.757	0.763	0.706	0.579	0.405	0.212	0.054	0.000
Median	0.000	0.065	0.251	0.439	0.593	0.709	0.775	0.788	0.730	0.602	0.421	0.215	0.047	0.000
Mode	0.000	0.014	0.245	0.415	0.528	0.736	0.932	0.930	0.787	0.765	0.485	0.152	0.028	0.000
1st quartile	0.000	0.036	0.210	0.387	0.521	0.621	0.678	0.689	0.638	0.518	0.356	0.177	0.026	0.000
2nd quartile	0.000	0.065	0.251	0.439	0.593	0.709	0.775	0.788	0.730	0.602	0.421	0.215	0.047	0.000
3rd quartile	0.000	0.100	0.306	0.508	0.672	0.796	0.855	0.853	0.792	0.654	0.467	0.254	0.075	0.000
Dispersion Measures														
Standard Deviation	0.000	0.045	0.068	0.086	0.101	0.119	0.125	0.121	0.114	0.100	0.085	0.060	0.036	0.000
Variance	0.000	0.002	0.005	0.007	0.010	0.014	0.016	0.015	0.013	0.010	0.007	0.004	0.001	0.000
Average Deviation	0.000	0.036	0.055	0.069	0.083	0.096	0.101	0.097	0.092	0.080	0.067	0.047	0.028	0.000
Maximum	0.000	0.331	0.444	0.653	0.843	0.929	1.000	0.995	0.923	0.776	0.621	0.426	0.342	0.000
Minimum	0.000	0.000	0.026	0.022	0.098	0.208	0.106	0.134	0.106	0.099	0.014	0.001	0.000	0.000
Interquartil interval	0.000	0.064	0.096	0.122	0.152	0.175	0.176	0.164	0.154	0.136	0.112	0.077	0.048	0.000
Amplitude	0.000	0.331	0.418	0.630	0.744	0.721	0.894	0.861	0.817	0.678	0.607	0.425	0.342	0.000
Coefficiency variation	N/A	62.398	26.590	19.260	17.040	16.936	16.572	15.838	16.170	17.272	20.898	28.309	66.575	N/A

Evaluating the data presented in the figure above, it is possible to create a histogram data from each hour of the day and the probability of occurance can be represented by the figure 4.24.

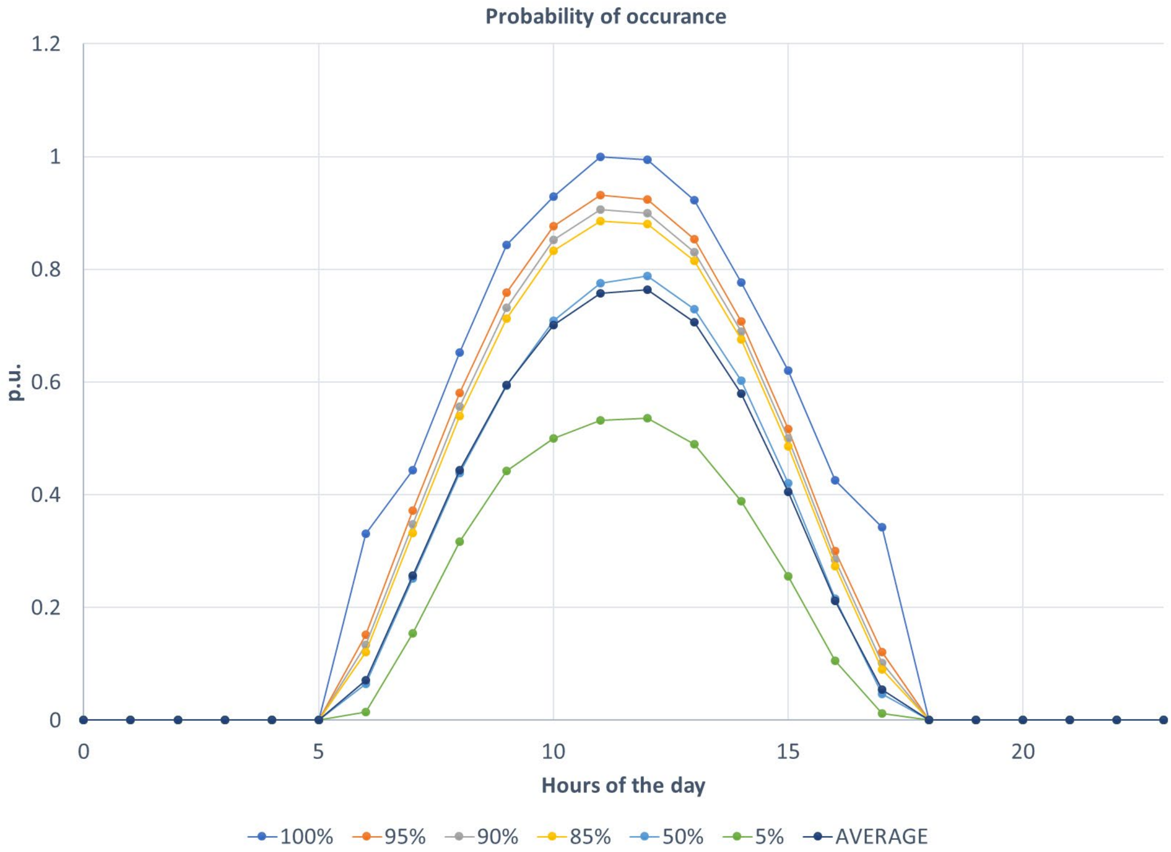

Figure 4.24 – Probability of occurance of radiation

Based on the curves found by the k-means clusters method, computer simulations were performed in order to find the loss-of-life for each type of curve used. If the equipment is dimensioning for the maximum irradiation, i.e., 100% curve (blue in the figure below), the aging rate is 1.00 p.u. for the transformer sized for that curve. Performing the same analysis for 95% and 90% it is observed that there is a significant decrease in aging by 0.30 p.u. and 0.20 p.u., as shown in the figure 4.25.

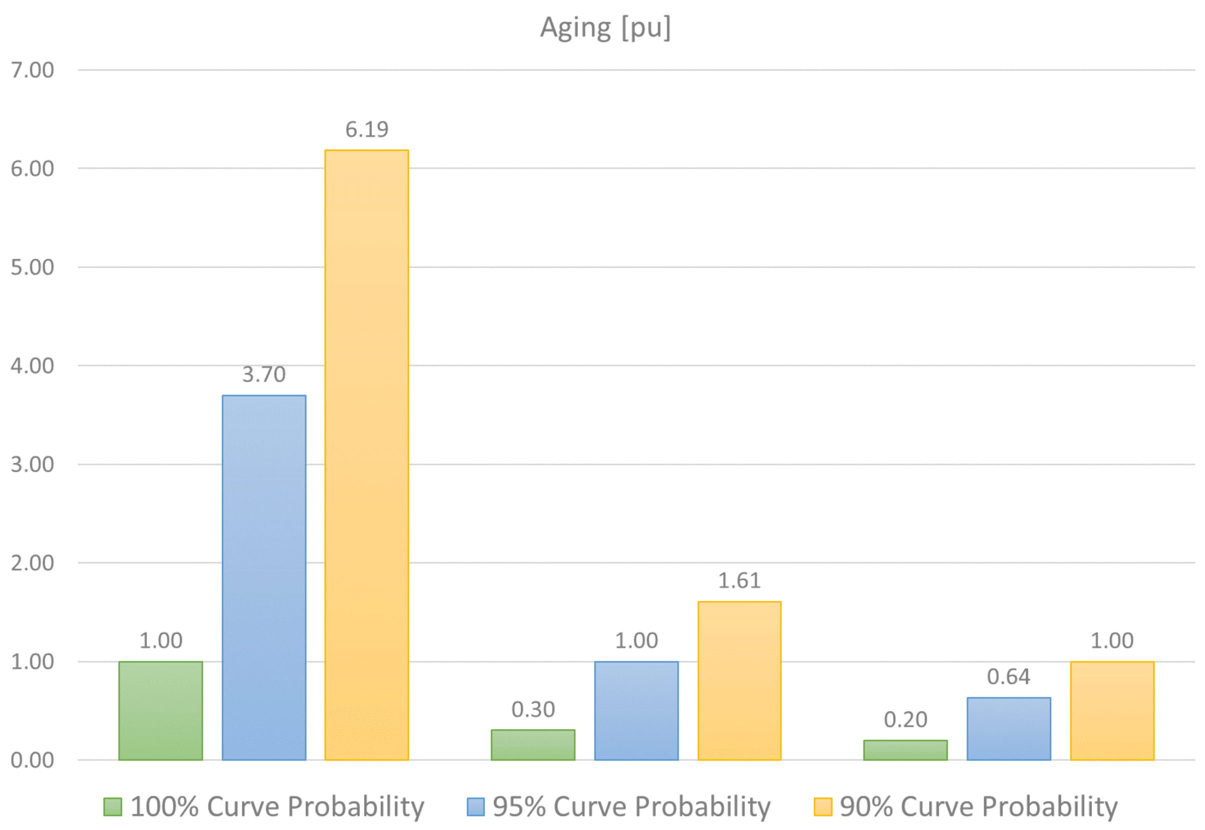

Figure 4.25 – Aging and curve of probability

If the transformer is dimensioned to reach 1.00 p.u. with the 95% probability irradiation curve, the aging value for a day which the curve reaches 100%, i.e., extreme irradiation, is 3.7 p.u. of aging which means that on this specific day the transformer will aging 3.7 times the normal aging expected. In addition, such results are analyzed by the proposed method in order to avoid that the maximum temperatures of the hotspot and top oil for the long and short-term loading limits are not exceeded.

In this thesis has not been considered the reduction of efficiency of the solar panels, obviously, in case of has this consideration has taken into account, there will reduce the total size of the power transformer even more, however, valuing the security of the facilities and by the possibility of the owners of the photovoltaic farm change the solar panel for a new one with more efficiency, this consideration was neglected.

Chapter 5 – CONCLUSIONS AND DISCUSSIONS

The knowledge and optimization process in this thesis are the result of decades of experience in power transformer design and manufacturing. The empiric and experimental technical knowledge, accumulated along the years in the factory floor, is also documented in this thesis as part of the proposed optimization method. Although experienced engineers have very deep knowledge about technical issues, sometimes financial issues are neglected during the procurement process, even more, when the power transformer is going to be installed to an intermittent power resource. Thus, this thesis has a double task, to document the well-established experimental knowledge as well as the development of a novel technique for the optimization of large power transformers designed in the context of new applications involving renewable energy

A high safety factor does not have a direct relationship with the high quality of the overall system neither higher prices, therefore the goal of the proposed method is an optimization process for dimensioning a GSU power transformer for photovoltaic power plants considering not only the conventional real loading curve and the ambient temperature which the transformer will operate throughout its lifecycle. In this context, the new optimization method is formulated considered these two last characteristics and in addition the correction of the mean oil temperature of the winding and the financial data to find the overall transformer dimensioning technically and financially.

Technically this work also aimed to deal with two issues, encountered by utilities, energy generators, and finance area, without any clear answer until now: *how to optimize transformer size in a new project with real loading and temperature curve*; **and** *this technically optimized transformer fulfill all economic criteria*. Both items together fit the final cost-effective transformer for a new installation.

Two very well-established concepts of load factor were presented in this thesis, the first one defined the load factor by the average loading and the second defined by the average overtime of the RMS value of the instantaneous load. The first shows an adequate performance for cases with low load variations during the evaluated period, and the second represents a modern approach taken into account very high load changes throughout the evaluated time period, but this last one does not consider correction by the ambient temperature. The model presented in this thesis where besides using the RMS of the instantaneous load it is considering the temperature correction jointed with the total ownership cost.

Even though the method technique developed here is independent of the type of transformer as size, cooling system, design etc., the numerical example demonstrates the principles are limited to mineral oil-cooled power transformer applied for a solar application. This method could easily be expanded to other types of the transformer and varied applications.

A few researches on this subject were found in the technical literature, however, the temperature correction inside the winding is not considered in this same research, and neither a joint relationship is defined on the total ownership cost of the power transformer. In this context, this method is efficient and more appropriate for its intended purpose because find the most suitable technical equipment comparing its financial inputs data like the price of energy, WACC of the investor and transformer life expectance, therefore, it is an original method that has great potential to assist in the design of transformers for systems with intermittent loading.

It is possible to observe the importance of acquiring reliable data on the loading and the ambient temperature of the installation site of the equipment, as well as the concepts of the weighted average cost of capital of the investor/buyer of the transformer, reliable estimates on the growth of the electricity values and the concept of capitalization of losses over the useful life of the equipment.

Although in recent years, some investors have reduced attention to the topic of losses capitalization, just focusing on the initial price of the transformer, or not distinguishing the difference between the capitalization of no-load losses and the capitalization of load losses. To avoid a reduction in the revenue of electricity production, a deep analysis in this context was done which has demonstrated the importance to take into account the loading profile and the huge difference between capitalization of no-load and load losses.

Another relevant conclusion is that the peak efficiency index may not be the best way to compare transformer efficiency for in solar energy applications. The best way to define the most efficient transformer is by analyzing the efficiency at a specific load, because the transformer with higher PEI are larger, with no technical or economic advantage for solar application.

These methods of energy efficiency were developed for GSU power transformers design, more specifically for power transmission systems with conventional hydro and thermal generation. With the increasing advent of renewable energy sources, e.g. photovoltaic, it is possible to verify a gap in the technical literature concerning intermittent energy sources. Moreover, this proposal methodology can be expanded for analysis in high-temperature transformers also considering other variables, such as: the solid insulation moisture, hotspot temperature, top oil temperature, and end-of-life criteria for high-temperatures materials applied in this transformer.

According to the standards, ester fluids combined with aramid solid insulation have a higher temperature of operation which increases the ability to overload the power transformer, generating higher revenues during peak demand periods without compromise the transformer life. The ester fluid, differently of the mineral fluid, reduces the risk of environmental fines and can have insurance benefits because the chance to explode is small. In some countries, the applicable laws and regulations determine how fines are imposed and high biodegradability and non-toxicity ester liquids leakage can be disposed of through normal.

High-temperature materials and aging control through dynamic overloadability allows a much more compact and efficient transformer design. The size reduction is particularly valuable for photovoltaic power plants, wind offshore power stations, urban substations, and others. Generator step-up transformers applied to photovoltaic power plant are unique because:

- experience intermittent loading that follows weather conditions and has an upper limit corresponding to the installed generators or more;
- must fulfill the minimum efficiency according to the current standards;
- no-load losses have a significant impact on the capitalization scenario;
- reliability of transformer in the grid.

Currently, the digitalization of a substation and consequently the power transformer digitalization has become massive. Power transformers already commissioned and in operation can be monitored with digital and electronic equipment that can estimate the end-of-life of this asset. For brand new equipment, the investor should consider additional investment in the monitoring system which besides estimate the end-of-life of the transformer can evaluate many other parameters, such as: on-line dissolved gas generation, non-expected high temperature, hotspot, and failure initiation.

Even with all analyses described in this thesis, to dimensioning the total size of the transformer, it is recommended to monitoring a transformer during its entire life in order to provide actionable information that supports effective operations, maintenance actions, and predictive maintenance actions to avoid the possible risk of failures. As presented in this work, the transformer population distribution failure has been governing by the bathtub curve and, in a few cases, early failures can occur.

In addition, the proposed optimization method can be improved in order to provide a more detailed knowledge on the solar loading curve and temperature. Monte Carlo based methods have been proposed to randomly create a set of data points corresponding to a transformer loading at ambient temperature. This well-established probabilistic method can be applied to the proposed optimization method in further researches. This thesis used probabilistic data generated by a synthetic series in order to present the importance of the knowledge of solar radiation and the necessary consideration for the procurement engineer.

Besides that, some modern photovoltaic plant is eligible for receiving payment on the active power losses due to reactive power generation and this approach was presented and conclude that must be taken into account during the procurement process, even more, the credits which the generator will obtain during the reactive dispatch has to be part of the TOC equation.

From the finance point of view, a Sharpe ratio can be studied for this purpose. The Sharpe ratio it has been one of the most referenced risk/return measures used in finance world and this ratio is used to help investor understand the return of an investment compared ti its risk. The risk of failure or aging according to a random load curve and the TOC can be studied to fit an optimum risk/return utilizing the method presented in this thesis.

The novel methodology proposed in this work which carried out dynamic loading models applied with TOC analysis can reduce the weight of the transformer approximately 25%, considering the same thermal material class, bringing better cost-benefit, and longer service life with higher reliability to the investor.

An effective change in the global energy policy requires a fundamental upgrade in the way energy systems are conceived and operated. This requires long-term energy system planning and changes to a more holistic policymaking, more coordinated approaches across sectors and countries. It is critical in the power sector, where timely infrastructure deployment and the redesign of sector regulations are essential conditions for cost-effective integration of solar and wind generation on a large scale as well as other renewable energy sources. These energy resources will become the backbone of the electric power system by 2050.

Currently, there is no technical literature that reports how the calculation of the transformers applied to large solar plants is carried out. Based on the methodology currently applied by IEEE Loading Guide, it is possible to optimize from a technical point of view. On the other hand, this thesis presents arguments for the needs to analyze the equipment from the economic point of view in addition to the assessment of the ambient temperature in which the equipment will be installed.

The thesis supports that it is necessary to observe three issues, and mainly disagreeing with the normalized currently data used by most of the procurement of transformers. This three issues are: *i) Method of Technical Optimization; ii) Method of Financial Optimization and iii) Ambient Temperature*. The equipment is marked by the temperature values according to the international standards, however, the optimum point of the equipment can be only found in the current ambient temperature.

REFERENCES

- ABB Transformer Handbook, Zurich, Switzerland, 2004.
- ABSOLAR. Associação Brasileira de Energia Solar Fotovoltaica, http://www.absolar.org.br/infografico-absolar-.html., 2019.
- AHMED, E. B. BU-ELANIEN; SALAMA, M. M. A., BARTNIKAS, R. A new techno-economic replacement technique for transformer, *IEEE Power and Energy Society General Meeting,* Detroit, MI, USA, 2011.
- AMOIRALIS, E. I.; TSILI, M. A.; KLADAS, A. G. Power transformer economic evaluation in decentralized electricity markets, *IEEE Trans. Industrial Electronics*, v. 59, n. 5, p. 2329-2341, 2012.
- ANEEL. Matriz de Energia Elétrica, download: 01-04-2020. http://www2.aneel.gov.br/aplicacoes/capacidadebrasil/OperacaoCapacidadeBrasil.cfm
- AUBIN, J.; LANGHAME, T. Effect of Oil Viscosity on Transformer Loading Capability at Low Ambient Temperatures, *IEEE Transactions on Power Delivery*, v. 7, n. 2, p. 516–524, April 1992.
- BAGGINI, A. et al. Accelerating the Global Adoption of Energy-Efficient Transformer, *UM Environment – GEF United for Efficiency* (U43), 2017.
- BAGGINI, A.; BUA, F. Power transformer energy efficiency program: a critical review, *IEEE,* 2015.
- BENGALI, S.; The biggest solar parks in the world are now being built in India., *L.A. Times*, download: 19-03-2018. http://www.latimes.com/world/asia/la-fg-india-solar-20180319-story.html, 2018.
- BENGTSSON, C; KRAUSE, C.; MIKULECKY, A.; SCALA, M.; LESSARD, M.C.; MELZER, L.; HURLET, L.; RAJOTTE; C. Insulation condition during transformer manufacturing, *Cigre A2 – Reference Paper, ELEKTRA*, n 229, 2018.
- BENKO, I.S. et al. Loading of substation electrical equipment with emphasis on thermal capability, Part II—Application, *IEEE Trans. Power App. Syst., vol.* PAS-98, pp. 1403–1419, July/Aug. 1979.

❖ BOICE, D. G.; GURSKY, R. J.; TRAD, J. B. Cost of electrical power system losses for use in economic evaluations, *IEEE Trans. Power Systems*, v. 4, n. 2, 586-593, 1988.

❖ BOSSI, A.; DIND, J.; FRISSON, J; KHOUDIAKOV, U.; LIGHT, H. An international survey on failures in large power transformers in service, *Electra*, 1983.

❖ BRANDÃO, L. Piauí instalada a maior usina de energia fotovoltaica da América Latina., *Piauí Hoje*, October, 11st, 2018, download: 07-06-2020. http://piauihoje.com/noticias/piaui-instala-a-maior-usina-de-energia-fotovoltaica-da-america-latina/.

❖ BREALEY, R.; MYERS, S.; ALLEN, F. Principles of Corporate Finance - *McGraw-Hill/Irwin Series in Finance, Insurance and Real Estate*, 12th Edition, 2016.

❖ CALIL, W. V. Determinação do fator de correção para cálculo de perdas magnéticas em núcleos de transformadores de potência pelo método de elementos finitos - *Dissertação de Mestrado, Escola Politécnica, Universidade de São Paulo, São Paulo.* doi:10.11606/D.3.2009.tde-14082009-164110, download: 27-12-2019. www.teses.usp.br.

❖ CALIL, W. V.; MELO, A. S.; AVELINO, P. A. Avaliação técnico-financeira em transformadores de potência para usinas fotovoltaicas, *Inter. Workshop on Power Transformers Equipment Substations and Materials*, Recife, Pernambuco, Brazil, 2016.

❖ CENELEC, BS EN 50629:2015 Energy performance of large power transformers (Um > 36 kV or Sr ≥ 40 MVA), 2015.

❖ CHARALAMBOUS, C. A.; MILIDONIS, A.; LAZARI, A.; NIKOLAIDIS, A. I. Loss evaluation and total ownership cost of power transformers – part I: a comprehensive method, *IEEE Trans. Power Delivery,* v. 28, n. 3, 1870-1880, 2013.

❖ CHARALAMBOUS, C. A.; MILIDONIS, A.; NIKOLAIDIS, A. I.; LAZARI, A. Loss evaluation and total ownership cost of power transformers – part II: a comprehensive method, *IEEE Trans. Power Delivery,* v. 28, n. 3, 1881-1889, 2013a.

❖ CIDADE VERDE, Maior usina solar da América do Sul entra em operação no interior do Piauí, photo download: 08-06-2020: https://cidadeverde.com/noticias/315867/maior-usina-solar-da-america-do-sul-entra-em-operacao-no-interior-do-piaui, 2020

❖ CIGRE Working Group 12.09 Lifetime Evaluation of Transformers, *Électra Magazine*, No 150, 1993.

- CIGRE Working Group A2.37, Transformer Reliability Survey, *Technical Brochure,* No 642, December, 2015.
- CIGRE Working Group A2.38, pages 39 - 51 – Transformer Thermal Modelling, *Technical Brochure*, No 659, October, 2016.
- CODDINGTON, O.; LEAN, J. L.; PILEWSKIE, P.; SNOW, M.; LINDHOLM, D. A Solar irradiance climate data record, *American Meteorological society*, pp 1265-1282, July, 2016
- ENERDATA 2019 Global Energy Statistic Yearbook- https://yearbook.enerdata.net/renewables/renewable-in-electricity-production-share.html, 2019.
- FABRE, J. and PICHON, A. Deterioration Processes and Products of Paper in Oil Application to Transformers, *CIGRE Paper 137*, 1960.
- FERNANDEZ, F. O. Aportaciones a la clasificación energética de transformadores de potência, *Thesis Doctoral*, Universidad de Cantabria, 2016.
- FITZGERALD, A.E., KINGSLEY, C., UMANS, S.D. Electric machinery, *6th Edition McGraw-Hill series in electrical engineering. Power and Energy*. ISBN 0-07-112193-5, 1909.
- GAMA, P. H. R. P; AOKI, A. R.; LUIZ, C. M., VECENTINI, E., SOUZA, M. L. M.' Geração Fotovoltaica de Energia no Brasil, *CIGRÉ-Grupo de Trabalho C6*, 2013.
- GEORGILAKIS, P. S.; AMOIRALIS, E. I. Spotlight on Transformer Design, *IEEE Power & energy magazine*, January/February, 40-50, 2007.
- GEORGILAKIS, P. S.; AMOIRALIS, E. I. Distribution transformer cost evaluation methodology incorporating environmental cost, *IET Generation Transmission & Distribution*, v. 4, n. 7, 861-872, 2010.
- GITMAN, L. J.; JUCHAU, R. H., FLANAGAN, J. Principles of Managerial Finance, *6th edition*, 2011.
- Global Energy Statistic Yearbook, download: 05-04-2019. https://yearbook.enerdata.net/renewables/renewable-in-electricity-production-share.html, 2019.

- HAGHIGHAT, H.; KENNEDY, S. A model for reactive power pricing and dispatch of distributed generation, *In Proceedings of the IEEE Power and Energy Society General Meeting*, Providence, RI, USA, 25–29, pp. 1–10, July, 2010.
- HURLEY, W.G.; WOLFLE, W.H.; BRESLIN, J.G. Optimized transformer design: Inclusive of high-frequency effects, *IEEE Transactions on Power Electronics*, vol 13, no. 4, pp. 651-659, 1998.
- IEA (2019), Renewables 2019, *IEA*, Paris, download: 05-08-2020. https://www.iea.org/reports/renewables-2019., 2019.
- IEA, Installed power generation capacity by source in the Stated Policies Scenario, 2000-2040, IEA, Paris , download: 16-01-2020. https://www.iea.org/data-and-statistics/charts/installed-power-generation-capacity-by-source-in-the-stated-policies-scenario-2000-2040, 2020.
- IEA, Renewables 2019, IEA, Paris https://www.iea.org/reports/renewables-2019., 2019.
- IEC Power Transformers – Part 1: General, *International Standard IEC 60076-1,* ed 3.0, 2011.
- IEC Power Transformers – Part 2: Temperature rise for liquid immersed transformer, *International Standard IEC 60076-2*, ed 3.0, 2011.
- IEC Power Transformers – Part 20: Energy efficiency, *Technical Specification IEC TS 60076-20*, ed.1.0, 2017.
- IEC Power Transformers – Part 7: Loading guide for mineral-oil-immersed power transformers, *International Standard IEC 60076-7*, ed 2.0, 2018.
- IEEE Guide for Loading Mineral-Oil-Immersed Transformers and Step-Voltage Regulators, *IEEE standard C57.91.2011*, 2011.
- IEEE loss evaluation guide for power transformers and reactors, *IEEE standard C57.120.1991*, 1991.
- IEEE Standards for Design, Testing, and Application of Liquid-Immersed Distribution, Power, and Regulating Transformers Using High-Temperature Insulation Systems and Operating at Elevated Temperatures, *IEEE standard C57.154.2012*, 2012.
- IRENA, International Renewable Energy Agency, Global Energy Transformation: A Roadmap to 2050, Abu Dhabi – April 2018 , download: 08-10-2019.

http://www.irena.org/publications/2018/AprGlobal-Energy-Transsition-A-Roadmap-to-2050, 2018.

- JIAO. Y., CFD Study on the Thermal Performance of Transformer Disc Windings without Oil Guides, *M.Sc. thesis, KTH School of Industrial Engineering and Management*, 2012.
- JUDD, F.; KRESSLER, D. Design optimization of small low-frequency power transformers, *IEEE Transactions on Magnetics*, vol. 13, no. 4, pp. 1058-1069, 1977.
- LOS ANGELES TIMES, The biggest solar parks in the world are now being built in India, Shashank Bengali, Los Angeles Times, 2018, photo download: 07-06-2020: https://www.latimes.com/world/asia/la-fg-india-solar-20180319-story.html, 2018
- KAZMIERCZAK, J. Power Transformer 101, *Virtual Red TIE/Customer Transformer Training (CTT)*, ABB, 2020.
- KENNEY, J. F. and, KEEPING, E. S. Root Mean Square in Mathematics of Statistics, *3rd edition, Princeton*, NJ, pp 59-60, 1962.
- KULKARNI, S. V., KHAPARDE, S.A. Transformer Engineering: Design and Practice, *CRC Press*, 2004.
- KUNG, P.; ISDINGA, R.; DURAND, V., LU, H.; KAHRIZI, M. Simultaneous Measurement of Hot Spot Temperature and Trace Moisture in a High Voltage Operating Transformer Using a Fiber Optics Sensor Pair, *The 20th International Symposium on High Voltage Engineering*, Buenos Aires, Argentina, 2017.
- LACHMAN MF, GRIFFIN PJ, WALTER W, WILSON A. Real-time dynamic loading and thermal diagnostic of power transformers, *IEEE Trans Power Delivery*, 2003.
- LAHOTI BD, FLOWERS DE. Evaluation of transformer loading above nameplate rating. *IEEE Trans Power App Syst*, 1981.
- LAM, P. The rate of return for electricity distribution networks. *Independent Pricing and Regulatory Tribunal of New South Wales*, Discussion Paper DP-26, November 1988.
- LAMPE, W.; SPICAR, E. The Oxygen-Free Transformer, Reduced Aging by Continuous Degassing, *CIGRE Paper 12-05*, 1976.
- LAZARI, A. L.; CHARALAMBOUS, C. A. Life-cycle loss evaluation of power transformers serving photovoltaic plants in vertically integrated and decentralized systems, *IET Generation Transmission & Distribution*, v. 9, n. 8, 759-766, 2015.

- ❖ LAZARI, A. L.; CHARALAMBOUS, C. A. Probabilistic total ownership cost of power transformer serving large-scale wind plants in liberalized electricity markets, *IEEE Trans. Power Delivery*, v. 30, n. 4, 1923-1930, 2015.
- ❖ Loeb, N. G., B. A. Wielicki, D. R. Doelling, G. L. Smith, D. F. Keyes, S. Kato, N. Manalo-Smith,T. Wong, Toward optimal closure of the earth's top-of atmosphere radiation budget. *J. Climate*, 22, 748–766, doi:10.1175/2008JCLI2637.1, 2009.
- ❖ LOURENÇO, L. F. N.; MONARO, R. M.; SALLES, M. B. C.; CARDOSO, J. R.; QUÉVAL, L. Evaluation of the Reactive Power Support Capability and Associated Technical Costs of Photovoltaic Farms' Operation, *Energies 2018*, 11, 1567, 2018.
- ❖ MELO, A. S.; CALIL, W. V., Hot Spot Control of Structural Parts Due to High Current Leads in Power Transformers by Means of the 3D-FEM, 3th International Colloquium Transformer Research and Asset Management, Split, Croatia, 2014.
- ❖ McCARTHY, J.: Analysis of Transformer Ratings in a Wind Farm Environment, *Masters Dissertation*, Dublin, Technological University Dublin, 2010.
- ❖ McNELLY, S.; FORSYTH, B.; TENEYNHUIS, E.; Transformer Committee, Annual Report – 2018", *IEEE Power and Energy Society*, 2019.
- ❖ MILULECKY, A.; CABRAJAC, S.; GOZEC, Z. Research on Insulation Aging on Transformer Models, *IEEE SDEMPED*, Grado Italy, September 2001.
- ❖ MORAES, H.; Maior usina solar da América do Sul entra em operação no interior do Piauí, Cidade Verde, January 14th, 2020, download: 07-06-2020. https://cidadeverde.com/noticias/315867/maior-usina-solar-da-america-do-sul-entra-em-operacao-no-interior-do-piaui., 2020.
- ❖ MOSER, H. P.; DAHINDEN, V. Thermal aging of oil/Transformer board insulation system *Transformer board II*, second edition, Printing Styrian, Graz, pp. 149-156, 1999.
- ❖ OJEU (2014), Commission Regulation (EU) No. 548/2014 of 21 May 2014 on implementing Directive 2009/125/EC of the European Parliament and of the Council with regard to small, medium and large power transformers, *Official Journal of the European Union,* download: 07-01-2020. http://eur-lex.europa.eu/legal-content/EN/TXT/?uri=OJ:L:2014:152:FULL., 2020.

- OLIVARES, J. C.; LIU, Y; CANEDO, J. M.; ESCARELA-PEREZ, R.; DRIESEN, J.; MORENO, P. Reducing losses in distribution transformers, *IEEE Trans. Power Delivery*, v. 18, n. 3, 821-826, 2003.
- OROSZ, T.; POÓR, P.; and PÁNEK, D., Power Transformer Design Optimization for Carbon Footprint, *Electric Power Quality and Supply Reliability Conference (PQ) & Symposium on Electrical and Mechatronics (SEEM)*, pp 1-4, Kärdla, Estonia, 2019.
- PACHECO, P.; CUESTO, M.; BURGOS, M., Sizing Step-up Transformers for Solar Generation based on Load Profiles Predictability, *6th International Advanced Research Workshop on Transformers (ARWtr)*, Cordoba, Spain, October 2019.
- PHAENGKIEO, D.; RUAUNGSINCHAIWANICH, S. Optimization of three-phase transformer design using adaptive genetic algorithm, *IEEE 19th International Conference on Electrical Machines and Systems (ICEMS)*, Japan, November, 2016.
- PIERCE, L. W. An Investigation of the Thermal Performance of an Oil Filled Transformer Winding, *IEEE Transactions on Power Delivery*, vol. 7, no. 3, pp. 1347–1358, July 1992.
- PIERCE, L.W. Predicting Liquid Filled Transformer Loading Capability, *IEEE Transactions on Industry Applications*, vol. 30, no. 1, pp. 170-178, January 1994.
- PORTAL SOLAR; Piauí terá maior parque solar da América do Sul, *Portal Solar*, download: 07-06-2020 - https://www.portalsolar.com.br/blog-solar/energia-solar/piaui-tera-maior-parque-solar-da-america-do-sul.html, 2019.
- PRINDLE, W. et al. The Twin Pillars of Sustainable Energy: Synergies Between Energy Efficiency and Renewable Energy Technology and Police, *Washington, DC: American Council for the Energy-Efficiency Economic (ACEEE)*, May, 2007.
- REN21. 2019. Renewables 2019 Global Status Report, *Paris: REN21 Secretariat,* ISBN 978-3-9818911-7-1
- RETTERATH, B. E., VENKATA, S. S., CHOWDHURY, A. A. Impact of time-varying failure rates on distribution reliability, *International Journal of Electrical Power & Energy System*, vol. 27, no. 9-10, pp. 682-688, 2005.
- ROFELJ, J. et al. Chapter 3: Mitigation pathways compatible with 1.5°C in the context of sustainable development, in Valerie Masson-Delmotte et at., eds., Global Warming of 1.5°C,

Geneva: Intergovernmental Panel on Climate Change, 2019, download: 09-07-2019. http://www.ipcc.ch/sr15

- RUBAAI, A., Computer Aided Instruction of Power Transformer Design in the Undergraduate Power Engineering Class, *IEEE Transactions on Power System*, Vol. 9, No3, pp 1174-1181, 1994.
- RUBIO, V.; CALIL, W.; INHASZ, J. Development of a program for the determination of the temperature at transformers copper bus bars by calculating their dimensionless numbers, *Proceeding of the 11th Biennal Conference on Engineering Systems Design and Analysis*, ESDA3023-82023, Nantes, France, 2012.
- SEforALL, 2020 - Sustainable Energy for ALL "About us" , download: 01-03-2020. https://www.seforall.org/about-us, 2020.
- SEN, P.K.; PANSUWAN, S.; MALMEDA, K.; MARTINOO, O.; SIMOES, M. G. Transformer Overloading and Assessment of Loss-of-Life for Liquid-Filled Transformers, *PSERC Publication* 11-02, 2011.
- SHROFF, D. H. and STANNET, A. W. A Review of Paper Aging in Transformers, *IEE Proceedings*, vol. 132, pt. C, no. 6, Nov. 1985.
- SINGH, G; McGUINNESS, S; MILLER, C.; STEPHENS, M.; McGRANAGHAN, M. Effects of PV Transformer Energization on Power Quality, *18th International Conference on Harmonics and Quality of Power (ICHQP)*, ISSN: 2164-0610, Ljubljana, Slovenia, 2018.
- STATITA (2020), Price index of energy worldwide from 2013 to 2030, *Statista*, , download: 08-08-2020. https://www.statista.com/statistics/252795/weighted-price-index-of-energy/, 2020.
- SUSA, D.; LEHTONEN, M.; NORDMAN, H. Dynamic thermal modelling of power transformers, *IEEE Trans Power Delivery*, Vol 20 N° 1: 197–204. https://doi.org/10.1109/ TPWRD.2004.835255, 2005.
- SZWANDER, W. The valuation and capitalization of transformer losses, *Journal of the Institution of Electrical Engineers*, Part II: Power Engineering, vol. 92, no. 26, pp. 125-134, April, 1945.
- T. Kanungo, D. M. Mount, N. S. Netanyahu, C. D. Piatko, R. Silverman and A. Y. Wu, An efficient k-means clustering algorithm: analysis and implementation, *IEEE Transactions on*

Pattern Analysis and Machine Intelligence, vol. 24, no. 7, pp. 881-892, doi: 10.1109/TPAMI.2002.1017616, July, 2002

- TAKAMIYA, T.; HANAZAWA K.; SUZUKI, T. Recent Development of Grain-Oriented Electrical Steel in JFE Steel, *JFE Technical Report*, no 21, 2016.
- TENBOHLEN, S.; JAGERS, J.; VAHIDI, F., Standardized Survey of Transformer Reliability, *Conference Proceedings of ISEM*, 593-596, 2017.
- TOBAR, A. C.; MASSAGUÉ, E. B.; PEÑALBA, M. A.; MELLMUNT, O. G. Topologies for large scale photovoltaic power plants, *Renewable and Sustainable Energy Review*, v. 59, 309-319, 2016.
- VECHIO R.M.; POULIN, B.; FEGHALI, P. T.; SHAH, D. M.; AHUJA, R. Transformer Design Principles, *2nd Edition CRC Press*, 2007. ISBN 978-1-4398-0582-4
- WARD, B. H. A Survey of New Techniques in Insulation Monitoring of Power Transformers, *IEEE Electrical Insulation Magazine*, 0883-7554/01, 2001.
- ZAREI, T.; MAROZOVKA, K.; LANERYD, T.; HIBER, P.; WIHLÉN, M.; HANSSON, O. Reliability considerations and economic benefit of dynamic transformer rating for wind energy integration, *Elsevier Electrical and Power Energy Systems*, v. 106, 598-606, 2019.

ANNEX A – IEEE ALTERNATIVE THERMAL MODEL, ADAPTED FROM (SEN ET AL., 2011)

Transformer's overall life expectancy and overloading capabilities depend on several factors. However, it is determined primarily by the winding hottest-spot temperature. The overloading guideline and the corresponding loss-of-life calculation as presented in the ANSI/IEEE C57.91-1995 is available in the Appendix.

Four modes of cooling most commonly employed in liquid filled transformers are:

- Natural convection of oil and natural convection of cooling air over the radiator (OA);
- Natural convection of oil with forced convection of air over the radiator – either single stage (OA/FA) or multiple stages (OA/FA/FA);
- Directed forced oil flow and forced airflow (DFOA);
- Non-directed forced oil flow; and forced airflow (NDFOA).

The IEEE Classical model uses the top-oil temperature rise over ambient temperature to calculate the winding hottest-spot temperature. Recent investigations (PIERCE, 1992 and PIERCE, 1994) have shown that during overloads the temperature of the oil in the winding cooling ducts rises rapidly at a time constant equal to that of the winding (contrary to the oil). During this transient condition, the oil temperature adjacent to the hottest-spot location is higher than the top-oil temperature in the tank. The calculations in Annex G are based on Pierce, 1994 and account for the type of fluid, cooling mode, winding duct oil temperature rise, resistance and viscosity changes, stray losses, eddy current losses, hottest-spot location, ambient temperature, and load changes.

The principle of the model is governed by two basic heat transfer equations:

Heat balance equation: $Q_{GEN} = Q_{ABS} + Q_{LOST}$

Where, Q_{GEN} is heat generated by heat sources, Q_{ABS} is heat absorbed in heat sources, and Q_{LOST} is the heat lost to cooling medium.

And heat absorption equation: $Q_{ABS}= M\ C_P\ \Delta T$

Where, M is the mass of absorbed material and CP is the specific heat of material, and ΔT is the temperature difference.

The hottest-spot temperature of the model is made up of the following components:

$$HS = T_A + \Delta T_{BO} + \Delta T_{WO} + \Delta T_{HS|WO} \quad \text{(A.1)}$$

Where, ΔT_{BO} is bottom-oil rise over ambient, ΔT_{WO} is duct-oil rise at winding hottest-spot location over bottom-oil, $\Delta T_{HS|WO}$ is winding hottest-spot rise over adjacent duct-oil temperature at hottest-spot location.

The calculation consists of a number of iterations of small time interval, ΔT. All variables are updated for every iteration. All equations use actual temperature, and not the temperature rise.

DUCT-OIL TEMPERATURE

Within the winding, the heat generated, absorbed and lost by the winding is defined by:

$$Q_{WGEN} = K^2\left(T_{KW}\ P_{WR} + \frac{P_{ER}}{T_{KW}}\right)\Delta t$$

$$Q_{WLOST} = \left(\frac{T_W - T_{DAO}}{T_{WR} - T_{DAOR}}\right)^{\frac{5}{4}}\left(\frac{\mu_{WR}}{\mu_W}\right)^{\frac{1}{4}}(P_{WR}+P_{ER})\Delta t \qquad \text{, for OA, FA, NDFOA}$$

$$Q_{WLOST} = \left(\frac{T_W - T_{DAO}}{T_{WR} - T_{DAOR}}\right)(P_{WR}+P_{ER})\Delta t \qquad \text{, for DFOA}$$

$$Q_{WGEN} - Q_{WLOST} = Q_{WABS} = M_W\ C_{PW}\ \Delta T_W \quad \text{(A.2)}$$

Where: Q_{WGEN}, Q_{WABS}, and Q_{WLOST} is the heat generated, absorbed and lost in time interval (Δt).

K is the transformer loading in per-unit.

T_{KW} is the winding resistance correction factor.

P_{WR} and P_{ER} are the winding and eddy current losses at rated load.

T_W is the average winding temperature.

T_{WR} is the average winding temperature at rated load.

T_{DAO} is the average duct-oil temperature.

T_{DAOR} is the average duct-oil temperature at rated load.

μ_W is oil viscosity in the duct.

μ_{WR} is oil viscosity in the duct at rated load.

M_W is mass of the winding.

C_{PW} is the specific heat of the winding.

The new value of the average winding temperature is calculated from ΔT_W from equation (A.2).

$$T_{W,new} = T_{W,old} + \Delta T_W \tag{A.3}$$

The duct-oil temperature rise is given by:

$$\Delta T_{TDO|BO} = (T_{TDOR} - T_{BOR})\left(\frac{Q_{WLOST}}{(P_{WR}+P_{ER})\,\Delta T}\right)^x \tag{A.4}$$

Where, $\Delta T_{TDO|BO}$ is the duct-oil temperature rise over bottom-oil temperature, T_{TDOR} and T_{BOR} is the top-duct oil and bottom-oil temperature, and x is exponent of duct-oil rise (0.5 for OA, FA, NDFOA and 1.0 for DFOA).

The duct-oil temperature rise gives the update to T_{TDO}, T_{DAO}, and T_{WO} as:

$T_{TDO} = T_{BO} + \Delta T_{TDO/BO}$

$$T_{DAO} = \left(\frac{T_{TDO}+T_{BO}}{2}\right)$$

$$T_{WO} = T_{BO} + HHS\ \Delta T_{TDO|BO}$$

Where, HHS is the location of hottest temperature of the winding, hotspot. It is equal to 1.0 when the hottspot is at the top of winding and equal to 0.0 when at the bottom.

HOTTEST-SPOT TEMPERATURE

In finding the hotspot temperature, it is assumed that the entire winding is at the hotspot temperature. The winding loss at hotspot temperature is:

$$P_{WHSR} = T_K\ P_{WR}$$

$T_K = \left(\frac{234.5+T_{HSR}}{234.5+T_{WR}}\right)$ for copper winding and

$T_K = \left(\frac{225+T_{HSR}}{225+T_{WR}}\right)$ for aluminum winding.

Where P_{WHSR} is the winding loss at hottest-spot temperature, T_K is the temperature correction factor, T_{HSR} is the hottest-spot temperature at rated load.

Similar to the duct-oil temperature, within the winding at hotspot location, the heat generated, absorbed and lost by the winding is defined as:

$$Q_{HSGEN} = K^2\left(T_{KHS}\,P_{WHSR} + \frac{P_{EHSR}}{T_{KHS}}\right)\Delta t$$

$Q_{HSLOST} = \left(\frac{T_{HS}-T_{WO}}{T_{HSR}-T_{WOR}}\right)^{\frac{5}{4}}\left(\frac{\mu_{HSR}}{\mu_{HS}}\right)^{\frac{1}{4}}(P_{WHSR}+P_{EHSR})\Delta t$, for OA, FA, NDFOA

$$Q_{HSLOST} = \left(\frac{T_{HS}-T_{WO}}{T_{SHR}-T_{WOR}}\right)(P_{WR}+P_{ER})\Delta t \qquad \text{, for DFOA}$$

$$Q_{HSGEN} - Q_{HSLOST} = Q_{HSABS} = M_W\ C_{PW}\ \Delta T_{HS} \tag{A.5}$$

Where: Q_{HSGEN}, Q_{HSABS}, and Q_{HSLOST} is the heat generated, absorbed and lost in time interval (Δt).

T_{KHS} is the winding resistance correction factor.

P_{HSR} and P_{EHSR} are the winding and eddy current losses at rated load at hotspot temperature.

HS is the hottest-spot temperature.

T_{HSR} is the hottest-spot temperature at rated load.

μ_{HS} is the oil viscosity at hottest-spot location.

μ_{HSR} is the oil viscosity at hottest-spot location at rated load.

The new value of hottest-spot temperature is calculated from ΔT_{HS} of equation (A.5)

$$T_{HS,new} = T_{HS,old} + \Delta T_{HS} \tag{A.6}$$

BULK-OIL TEMPERATURE

The model considers the heat that is generated, absorbed, and lost (to the air)

$$Q_{OGEN} = Q_{WLOST} + Q_{Stray} + Q_{Core}$$

$$Q_{OLOST} = \left(\frac{T_{OAVG}-T_A}{T_{OAVGR}-T_{AR}}\right)^{\frac{1}{y}} P_{TR}\ \Delta T$$

$$Q_{WLOST} + Q_{Stray} + Q_{Core} - Q_{OLOST} = \sum MC_P\ \Delta T_{OAVG} \tag{A.7}$$

Where: Q_{OGEN} ,Q_{WLOST} ,Q_{Stray} ,Q_{Core} , and Q_{OLOST} is the heat generated in oil, heat lost form winding to oil, stray loss heat, core loss heat, and the heat lost.

T_{OAVG} is the average bulk-oil temperature, $(TO + T_{BO})/2$.

T_{OAVGR} is the average bulk-oil temperature at rated load.

y is the exponent of average oil rise as per table below.

P_{TR} are the total transformer losses at rated load.

ΣMC_P is the summation of the product of mass and specific heat of tank, core, and oil excluding winding.

Table A.1 – Summary of Exponents

Exponent	Type of Cooling System				
	OA	FA	NDFOA	DFOA	
x	0.5	0.5	0.5	1.0	Duct oil rise
y	0.8	0.9	0.9	1.0	Average oil rise
z	0.5	0.5	1.0	1.0	Top to bottom oil rise

The new value of the average bulk oil temperature is calculated from ΔT_{OAVG} Equation (A.7)

$$T_{OAVG,new} = T_{OAVG,old} + \Delta T_{OAVG} \quad \text{(A.8)}$$

The top- and bottom-oil temperature difference is given by:

$$\Delta T_{TO|BO} = (T_{TOR} - T_{BOR})\left(\frac{Q_{OLOST}}{P_{TR}+\Delta T}\right)^z \quad \text{(A.9)}$$

Where, $\Delta T_{TO|BO}$ is top and bottom oil temperature difference, T_{TOR} and T_{BOR} is top-oil and bottom-oil temperature, and z is exponent of top-oil to bottom-oil rise in radiator.

The top-oil and bottom-oil temperature difference gives the update to TO and T_{BO} as:

$$TO = T_{OAVG} + \Delta T_{TO|BO}/2. \quad \text{(A.10)}$$

$T_{BO} = T_{OAVG} - \Delta T_{TO|BO}/2.$ (A.11)

When the calculation completes the new value of all temperatures, the calculation loops back to starting point. It reiterates by time step of (Δt) until it reaches the end of the load cycle. The steady-state temperatures rise can be calculated from the following equations.

$$\Delta T_{TO} = \left[\frac{\Delta T_{TOR}+\Delta T_{BOR}}{2}\right](P_T)^y + \left[\frac{\Delta T_{TOR}-\Delta T_{BOR}}{2}\right](P_T)^Z \quad \text{(A.12)}$$

$$\Delta T_{BO} = \left[\frac{\Delta T_{TOR}+\Delta T_{BOR}}{2}\right](P_T)^y - \left[\frac{\Delta T_{TOR}-\Delta T_{BOR}}{2}\right](P_T)^Z \quad \text{(A.13)}$$

For OA, FA and NDFOA cooling: $\Delta T_{TDOR|BOR} = \Delta T_{TDOR} - \Delta T_{BOR}$

For NDFOA cooling: $\Delta T_{TDOR|BOR} = \Delta T_{WR} - \Delta T_{BOR}$

For all cooling type: $\Delta T_{TDO|BO} = \Delta T_{TDOR|bor}\, K^{2x}$ (A.12)

For OA, FA, and NDFOA cooling,

$$\Delta T_W = \left[\Delta T_{WR} - \Delta T_{BOR} - \frac{\Delta T_{TOR|BOR}}{2}\right]K^{1.6} + \Delta T_{BO} + \frac{\Delta T_{TDO|BO}}{2} \quad \text{(A.14)}$$

$$\Delta T_{HS} = \left[\Delta T_{HSR} - \Delta T_{BOR} - \Delta T_{TDOR|BOR}\right]K^{1.6} + \Delta T_{BO} + \Delta T_{TDO|BO} \quad \text{(A.15)}$$

For DFOA cooling,

$$\Delta T_W = \left[\Delta T_{WR} - \Delta T_{BOR} - \frac{\Delta T_{TOR|BOR}}{2}\right]K^{2.0} + \Delta T_{BO} + \frac{\Delta T_{TDO|BO}}{2} \quad \text{(A.16)}$$

$$\Delta T_{HS} = \left[\Delta T_{HSR} - \Delta T_{BOR} - \Delta T_{TDOR|BOR}\right]K^{2.0} + \Delta T_{BO} + \Delta T_{TDO|BO} \qquad \text{(A.17)}$$

This model requires a big number of data of the transformer and other models like IEEE Clause 7. However, it provides more informative results. For this thesis, this model was used because the purpose of this project is to know since the beginning all transformers parameters. It yields more accurate winding losses and hotspot calculations.

To calculate equivalent aging per unit factor, the Arrehenius reaction rate theory is used considering the hottest-spot temperature of the model.

$$EQ_{aging} = 9.8.\,10^{-18} e^{\left[\frac{15000}{HS+273}\right]} \qquad \text{(A.18)}$$